

Electronic Conduction at Grain Boundaries in Silicon:
Theory and Computer Aided Analysis

by

G.C. McGonigal

A thesis
presented to the University of Manitoba
in partial fulfillment of the
requirements for the degree of
Master of Science

Winnipeg, Manitoba, 1983

ELECTRONIC CONDUCTION AT GRAIN BOUNDARIES IN SILICON:
THEORY AND COMPUTER AIDED ANALYSIS

BY

GORDON C. McGONIGAL

A thesis submitted to the Faculty of Graduate Studies of
the University of Manitoba in partial fulfillment of the requirements
of the degree of

MASTER OF SCIENCE

© 1983

Permission has been granted to the LIBRARY OF THE UNIVER-
SITY OF MANITOBA to lend or sell copies of this thesis, to
the NATIONAL LIBRARY OF CANADA to microfilm this
thesis and to lend or sell copies of the film, and UNIVERSITY
MICROFILMS to publish an abstract of this thesis.

The author reserves other publication rights, and neither the
thesis nor extensive extracts from it may be printed or other-
wise reproduced without the author's written permission.

ABSTRACT

An experimental investigation of electronic conduction across isolated grain boundaries in large grain polycrystalline silicon is reported. A microcomputer-based automated data acquisition and processing (ADAP) system was designed and constructed to facilitate the measurements. An emission/diffusion conduction model has been developed to include the rates of carrier supply and collection at the grain boundary. Interface-state densities of approximately $1.0 \times 10^{12} \text{ eV}^{-1} \text{ cm}^{-2}$ have been measured. Activation energy measurements of the potential barrier suggest that a spatially-nonuniform distribution of charge exists over the plane of most grain boundaries. Documentation of the ADAP system, and of several algorithms employed in data reduction are included in the Appendices.

ACKNOWLEDGMENTS

I wish to extend my sincerest thanks to Professor H.C. Card for his guidance throughout the course of this work. Discussions with the other members of the Materials and Devices Research Group, especially Doug Thomson, Bob McLeod, Peter Hsieh, Lex De Groot, and Professor K.C. Kao are gratefully acknowledged. I would also like to thank Doug Thomson for his assistance with the experimental portions of this work.

LIST OF FIGURES

Figure 1.1: Electron energy-band diagrams for grain boundary with diffusion potential V_{do} . (a) $V=0$; (b) $V>0$.

Figure 1.2: Diffusion potential V_{do} vs. bulk doping concentration N_A for several uniform interface-state densities N_{is} .

Figure 2.1: Voltage developed across the forward- and reverse-biased sides of a grain boundary as a function of applied voltage. $V_{dr} = V_a + V_{df}$.

Figure 2.2: Maximum electric field at the forward- and reverse-biased sides, E_{mf} and E_{mr} respectively, as a function of applied voltage.

Figure 2.3: Preexponential factor $v_d / (v_d + v_r)$ as a function of applied voltage.

Figure 2.4: Fermi-potential at the grain boundary as a function of applied voltage. $N_{is} = 1.0 \times 10^{11} \text{ eV}^{-1} \text{ cm}^{-2}$.

Figure 2.5: Energy-band diagram of an illuminated grain boundary. The states between the imrefs are partially filled.

Figure 2.6: Reduction of the potential barrier due to optical illumination. In this example $L = 300 \mu\text{m}$, $N_A = 10^{15} \text{ cm}^{-3}$, $N_A^A = N_D^D = 10^{14} \text{ eV}^{-1} \text{ cm}^{-2}$, $\sigma_N = 10^{-16} \text{ cm}^2$, $\sigma_C = 10^{-14} \text{ cm}^2$, and $T = 300 \text{ K}$.

Figure 3.1: Sample geometry. Cross-sectional area of all samples $= 3 \times 10^{-3} \text{ cm}^2$.

Figure 3.3: Dark characteristics of grain boundary sample B-10 at several measurement temperatures.

Figure 3.4: Dark characteristics of grain boundary sample B-12 at several measurement temperatures.

Figure 3.5: Characteristics of B-6 and B-10 under 5 mW cm^{-2} optical illumination.

Figure 3.6: Characteristic of B-10 under $20 \mu\text{W cm}^{-2}$ optical illumination.

Figure 3.7: Current oscillations observed (as a voltage developed across a 10 resistor) at high d.c. current densities. Grain boundary sample B-11. $V=15V$, $I=150mA$. Vert. scale: $500 \mu A/div$. Horz. scale: $1 ms/div$.

Figure 3.8: Connections between ECI and the grain boundary samples (GB) for automated measurements.

Figure 3.9: Log-current vs. log-voltage plot of a grain boundary characteristic as measured and plotted using the "GB" control program. Sample B-99.

Figure 3.10: Interface-state densities within the forbidden gap of silicon at a grain boundary obtained from the deconvolution of current-voltage characteristics. The plot was made by the program AUTODECON from data collected by GB. Sample B-99.

Figure 4.1: The dependence of (a) the activation energy and (b) the diffusion potential on temperature for B-10 and B-12. Dark conditions.

Figure 4.2: Thomson penny model of grain boundary for an orientational mismatch of approx. 20° showing the periodic nature of a particular defect structure. A variety of bonding disorder is suggested over one period.

Figure 4.3: The dependence of (a) the activation energy and (b) the diffusion potential on illumination intensity for B-10 and B-12. $T=300 K$.

CONTENTS

ABSTRACT	ii
ACKNOWLEDGMENTS	iii
LIST OF FIGURES	iv
<u>Chapter</u>	<u>page</u>
I. INTRODUCTION	1
II. CARRIER TRANSPORT AT GRAIN BOUNDARIES	7
The Emission/Diffusion Theory	8
The Effect of Interface States	11
Numerical Simulation	12
Electrooptical Effects	16
III. MEASUREMENTS ON ISOLATED SILICON GRAIN BOUNDARIES	22
Sample Preparation	22
Experimental Results	25
Current Oscillations	31
Automated Measurement of Grain Boundary Samples	33
Determination of the Interface State Density by	
Deconvolution	37
Grain Boundary Activation Energy	42
IV. DISCUSSION	45
Experimental Determination of the Potential	
Barrier	45
Nonuniformity of the Grain Boundary Diffusion	
Potential	47
V. CONCLUSIONS	52
REFERENCES	54

<u>Appendix</u>	<u>page</u>
A. PHOTO GB	56
B. GB	59
C. AUTODECON	65
D. ADAP USERS' GUIDE	70

Chapter I

INTRODUCTION

Recent applications of polycrystalline silicon in integrated circuit and solar cell devices [1,2] have sparked a renewed interest in the electronic characterization of these materials. With respect to solar cell applications, commercially available polycrystalline devices have shown energy conversion efficiencies comparable to those of single-crystal devices - but at a fraction of the cost.

Polycrystalline materials are constructed of grains of crystalline material that are randomly oriented with respect to one another. The interfaces between adjacent grains are called grain boundaries. Typical dimensions of the individual grains range from hundreds of angstroms to several millimeters depending upon the conditions of formation.

Usually polycrystalline semiconductors are modelled as volumes of crystalline material separated by grain boundaries. The properties of crystalline semiconductors are relatively well known and therefore the study of polycrystalline material should center upon a characterization of the grain boundary.

Most of the physical models of grain boundaries can be classified into one of two main subgroups: those that con-

struct an amorphous (i.e. non-crystalline) intermediate layer between the grains [3]; and those that ignore such a layer and assume the crystal structure preserved to within one or two atomic spacings of the boundary [4]. The amorphous layer model might be justified for certain exceptional conditions such as heavy doping segregation to the boundary but TEM photographs of germanium grain boundaries by Krivanek [5] and silicon grain boundaries by Cunningham and Ast [6] coupled with intuitive feelings of the melt-zone crystal formation process lead us - and the majority of our co-workers - to adopt the latter model.

The grain boundary defines the interface between two unaligned crystal lattices. It is a discontinuity to the periodicity of each lattice and therefore the energy-band structure of each is not preserved locally. Bonds of varying length are formed at the interface. These "distorted" bonds manifest themselves as a continuum of energy levels lying within the forbidden gap. Such energy levels are referred to as interface states. Their interaction with electrical carriers is analogous to that of states introduced through bulk impurity doping [7] with the exception that interface states are spatially confined to the grain boundary.

Interface states can be classified as being either donor- or acceptor-like. Donor-like states are neutral when occupied by an electron and positively charged when empty. Conversely, acceptor-like states are negative when filled and

neutral when empty. Under equilibrium conditions the states below the Fermi-level will be occupied, while the states above will be empty. If the number of empty donor-like states differs from that of filled acceptor-like states the grain boundary will hold a net charge. For polycrystalline silicon this charge is invariably positive for p-type doping and negative for n-type doping [4].

In order to maintain space-charge neutrality, a depletion region is formed on both sides of the grain boundary. The charge associated with the overall depletion region is equal in magnitude, but opposite in sign, to the net charge in the interface states.

We use the space-charge approximation [8] to see how this charge affects the energy bands in the vicinity of the grain boundary. Solving Poisson's equation we find the potential at the grain boundary $V(x)$ to be

$$V(x) = \frac{qN_A}{2\epsilon_s} x^2 \quad (1.1)$$

where q is the electronic charge, N_A is the bulk impurity doping (assuming p-type material), and ϵ_s is the silicon permittivity. Figure 1.1 shows the corresponding energy-band diagram, with V_{do} the equilibrium diffusion potential. If we assume the acceptor- and donor-like states to be uniformly distributed in energy within the energy gap and of density N_{is} ($\text{eV}^{-1}\text{cm}^{-2}$), we can generate the relationship between the diffusion potential and the interface-state density as shown as a function of N_A and N_{is} in Fig. 1.2 .

When an external voltage V_a is applied across a grain boundary as shown in Fig. 1.1 a portion of V_a will reduce the barrier on what is termed the forward-biased side of the boundary, while the remaining voltage increases the barrier on the reverse-biased side.

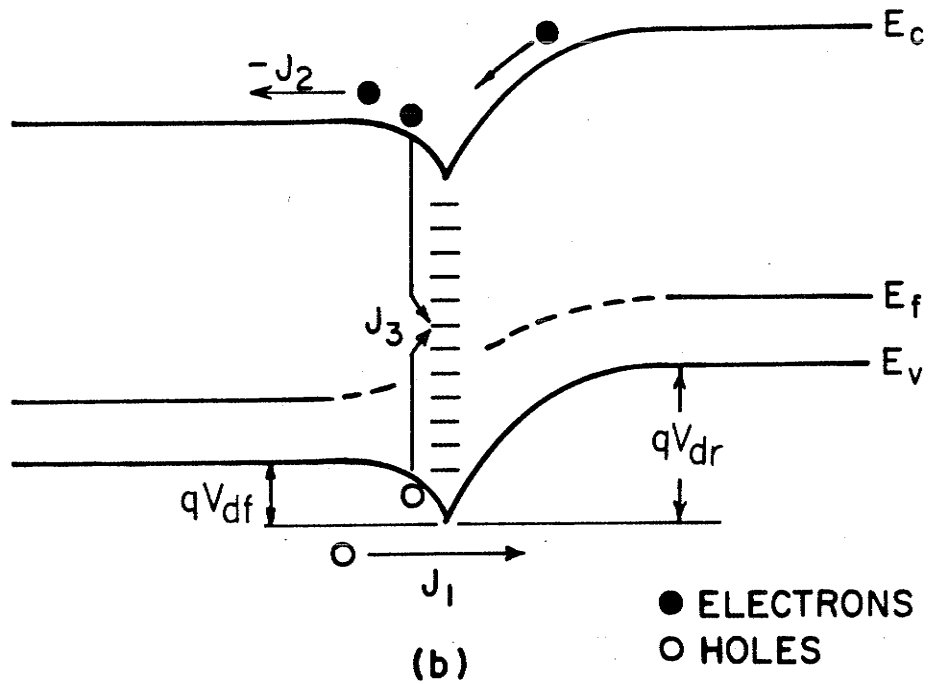
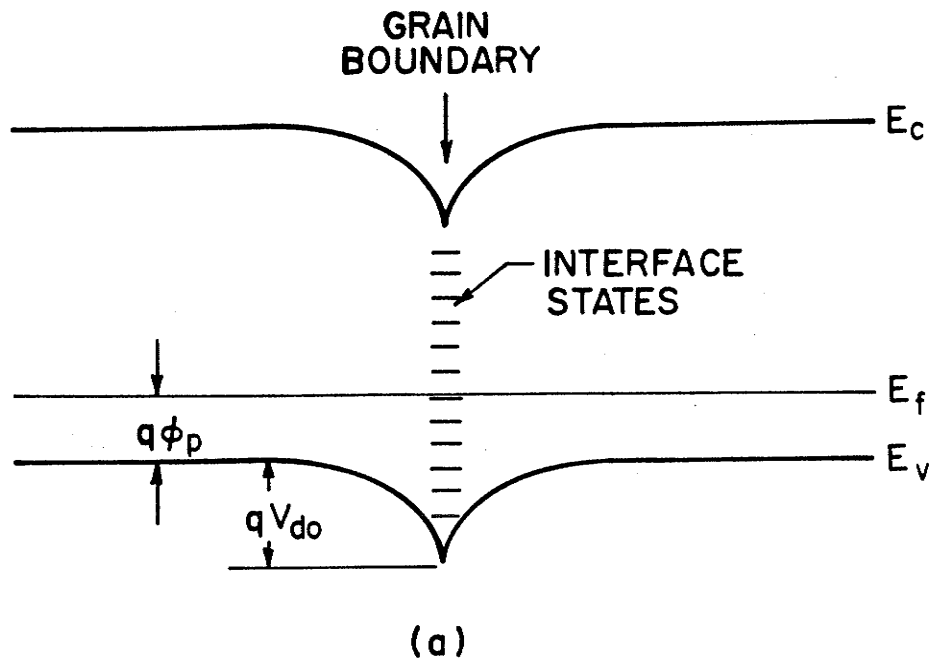


Figure 1.1: Electron energy-band diagrams for grain boundary with diffusion potential V_{do} . (a) $V=0$; (b) $V>0$.

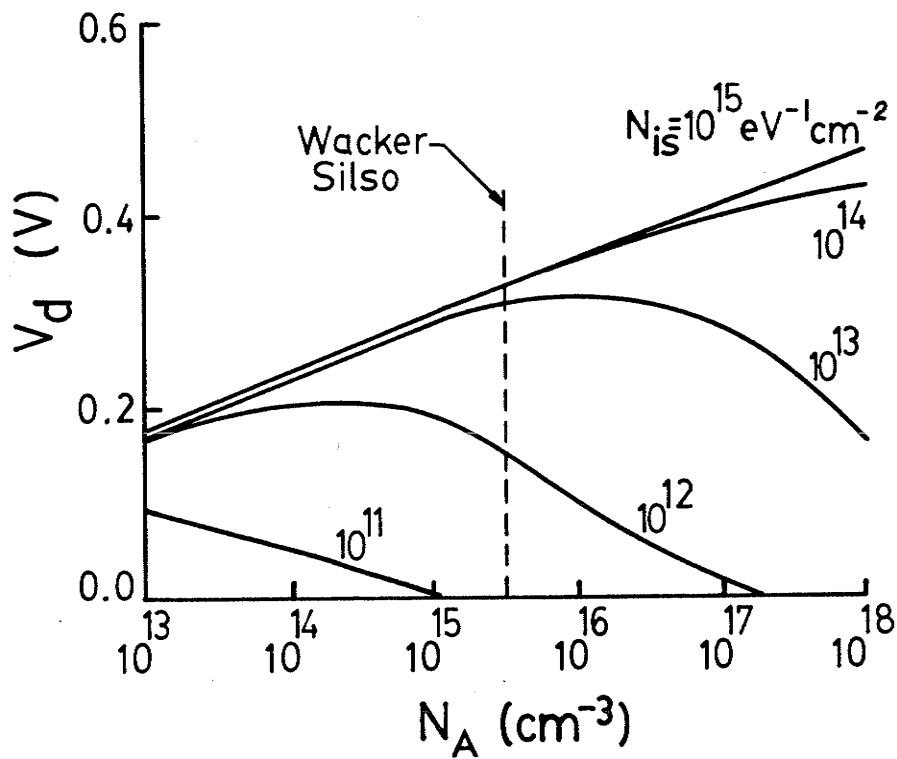


Figure 1.2: Diffusion potential V_{do} vs. bulk doping concentration N_A for several uniform interface-state densities N_{is} .

Chapter II

CARRIER TRANSPORT AT GRAIN BOUNDARIES

In this chapter we concentrate on developing an understanding of the mechanisms of carrier transport across (perpendicular to) a grain boundary. Here we isolate a grain boundary and ignore any interaction it may have with the other grain boundaries in the bulk polycrystalline material.

The steady-state current at a grain boundary consists of three distinct components. J_1 is the current due to transport of majority carriers over the potential barrier. J_2 is the component due to transport of minority carriers in the opposite direction. J_3 is the recombination current through the grain-boundary interface states. Figure 1.1 illustrates the three components. Under most conditions J_1 will dominate and the direct contribution of J_2 and J_3 to the total current can be ignored. These currents do however indirectly influence the magnitude of the majority-carrier current J_1 (as will be shown later).

2.1 THE EMISSION/DIFFUSION THEORY

The resemblance of the grain-boundary energy-band diagram to that of a pair of "back-to-back" Schottky-barrier contacts has lead many researchers [9-12] to adopt a current-voltage dependence modelled after the thermionic emission theory [13]. This is usually stated in the form

$$J = A^* T^2 \exp\left(\frac{-\phi_b}{V_T}\right) \left[\exp\left(\frac{V_a}{V_T}\right) - 1 \right] \quad (2.1)$$

where A^* is the modified Richardson constant $\approx 30 \text{ Acm}^{-2} \text{ K}^{-1}$ for p-type silicon, ϕ_b is the barrier height defined as the potential difference between the Fermi potential and the valence band edge at the grain boundary under zero bias, V_a is the forward voltage, and $V_T = kT/q$ is the thermal voltage.

The thermionic emission theory assumes there are a limited number of states capable of accepting a majority carrier on the metal side of the Schottky barrier. The reason is that there are very few available states in the metal with momentum parallel to the boundary to match that of the majority carriers from the semiconductor. This is because the energy at which the carriers are transferred is close to the valence band edge in the semiconductor but remote from the band edges in the metal.

Our physical model of the grain boundary is however devoid of any metal. Instead, silicon is both the emitting

and accepting material. The energy-momentum transfer restrictions are greatly reduced. Moreover the reverse-biased side of the barrier acts as an efficient collector of majority carriers. After a majority carrier crosses the grain boundary it is swept into the bulk material by the large electric field of the depletion region. These objections to the applicability of the thermionic-emission theory have led us to a more general theory based on a combined emission/diffusion transport mechanism [14].

We observe that the magnitude of the current across a grain boundary depends upon the rate at which carriers can be removed from the boundary as well as the rate at which they are supplied. We will use the term emission/diffusion to describe a carrier transport model that incorporates both of these processes.

The majority-carrier current as given by the emission/diffusion theory is

$$J_1 = qN_A \frac{v_d v_r}{v_d + v_r} \exp\left(\frac{-V_{df}}{V_T}\right) \left[1 - \exp\left(\frac{-V_a}{V_T}\right)\right] \quad (2.2)$$

where N_A is the bulk acceptor impurity doping, v_r is the grain boundary majority-carrier collection velocity, v_d is the diffusion velocity for majority carriers on the forward-biased side of the grain boundary, and V_{df} is the diffusion potential on the forward-biased side. Equation (2.2) is an

adaptation of the theory of carrier transport at grain boundaries proposed by Taylor, Odell, and Fan [15].

The diffusion velocity of majority carriers in the forward-biased depletion region v_d is

$$v_d = \mu E_{mf} \quad (2.3)$$

where μ is the majority-carrier mobility and E_{mf} is the maximum electric field. Similarly, the diffusion velocity away from the grain boundary on the reverse-biased side is given by

$$v_r = \mu E_{mr} \quad (2.4)$$

Note that v_d decreases as V_a increases. Thus $v_d < v_r$ which differs from the usual Schottky-barrier case. Using the depletion approximation

$$E_{mf} = \left(\frac{2qN_A}{\epsilon_s} (V_{df} - V_T) \right)^{1/2} \quad (2.5)$$

and

$$E_{mr} = \left(\frac{2qN_A}{\epsilon_s} (V_{dr} - V_T) \right)^{1/2} \quad (2.6)$$

where V_{dr} is the diffusion potential on the reverse-biased side and ϵ_s is the silicon permittivity.

2.2 THE EFFECT OF INTERFACE STATES

The amount of charge trapped in the grain-boundary interface states is not constant under all conditions. A change in the energy of the Fermi-level (due to a variation of temperature for example) will shift the distribution of interface states occupied by electrons. The net charge at the grain boundary is altered, resulting in a modification of the potential barrier V_{do} .

A similar effect occurs when the grain-boundary Fermi-level is disturbed by an applied voltage. In p-type material, the applied voltage will force the Fermi-level closer to the valence band edge, reducing the barrier height. This motion of the Fermi-level will however cause more interface states to empty, which tends to increase the barrier height. The "equilibrium" position of the Fermi-level will be determined by the interface-state density N_{is} . If N_{is} is small the barrier height can be reduced without adding significant charge to the grain boundary. If N_{is} is relatively large however, a small excursion of the Fermi-level will induce enough added charge to virtually maintain the barrier height. The Fermi-level is said to be "pinned" when this is the case. Equation (2.2) illustrates the role that the barrier height V_{df} plays in determining the current across the grain boundary. The interface-state distribution therefore indirectly contributes to the current-voltage characteristics.

The physics is somewhat complicated by "splitting" of the Fermi-level into separate electron and hole imrefs (quasi-Fermi-levels) under the nonequilibrium condition. Numerical calculations by Shaw (in [14]) have however revealed that the imrefs tend to intersect at the grain boundary. Knowing this we can still represent the carrier concentrations at the grain boundary with a single Fermi-level, although its exact energy under nonequilibrium conditions remains analytically uncertain.

2.3 NUMERICAL SIMULATION

A numerical simulation proved useful for visualizing certain aspects of the emission/diffusion carrier transport mechanism. The program, which used (2.2) as well as a consideration of the occupation of the interface states and the field dependence of the mobility, was implemented on an Apple II+ microcomputer (sec. 3.4). Parameter values were chosen to match the experimental samples measured later. For these calculations the impurity doping was $N_A = 3 \times 10^{15} \text{ cm}^{-3}$ with an equilibrium diffusion potential of $V_{do} = 0.28 \text{ V}$. The interface-state density N_{is} was chosen to be independent of energy and of magnitude $1.0 \times 10^{11} \text{ eV}^{-1} \text{ cm}^{-2}$.

Figure 2.1 details how the applied voltage is shared between the forward- and reverse-biased sides of the grain boundary. We observe that at low voltages each side of the boundary consumes half of the applied voltage. As the volt-

age is increased, more than half of the applied voltage is developed across the reverse-biased depletion region at the expense of the forward-biased depletion region.

The maximum electric field on each side of the grain boundary is shown in Fig. 2.2 as a function of applied voltage. We note that although the magnitude of the electric field is always less than the value corresponding to a scattering-limited velocity ($\approx 10^5 \text{ Vcm}^{-1}$), the carrier mobility cannot be considered to be independent of the electric field [8].

The preexponential term $v_d/(v_d+v_r)$ as a function of applied voltage is shown in Fig. 2.3. This has a very weak voltage dependence, changing from $1/2$ to approximately $1/3$ as V_a increases to one volt.

Finally we note the voltage dependence of the Fermi-potential at the grain boundary as shown in Fig. 2.4. With large N_{is} the Fermi-potential will be pinned at a fixed level but at the moderate density chosen here we see a shift towards the valence band with applied voltage. As previously noted, this will reduce the number of electrons trapped in the grain boundary interface states.

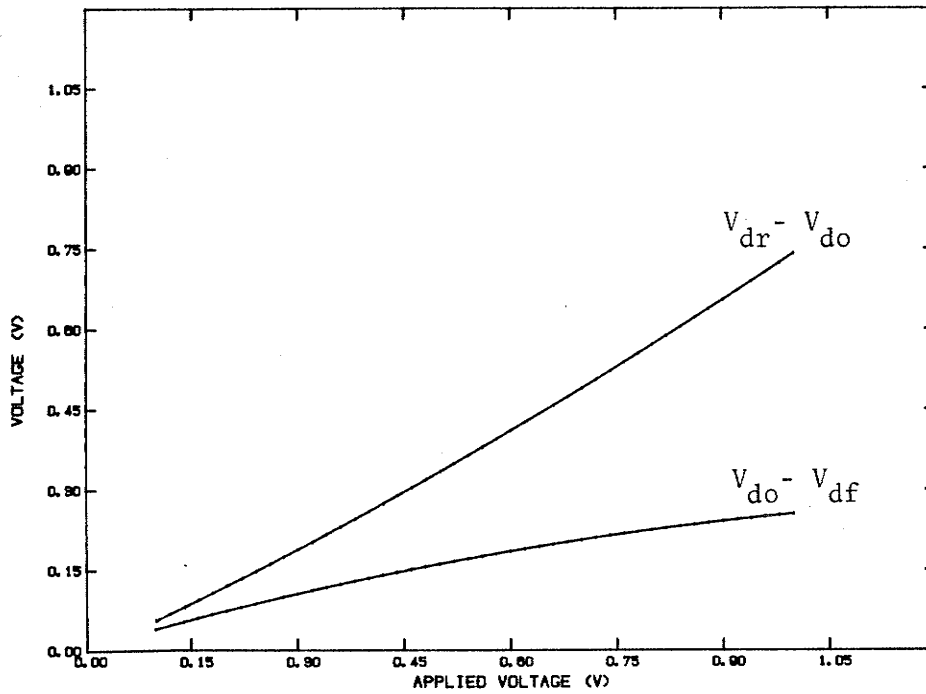


Figure 2.1: Voltage developed across the forward- and reverse-biased sides of a grain boundary as a function of applied voltage. $V_{dr} = V_a + V_{df}$.

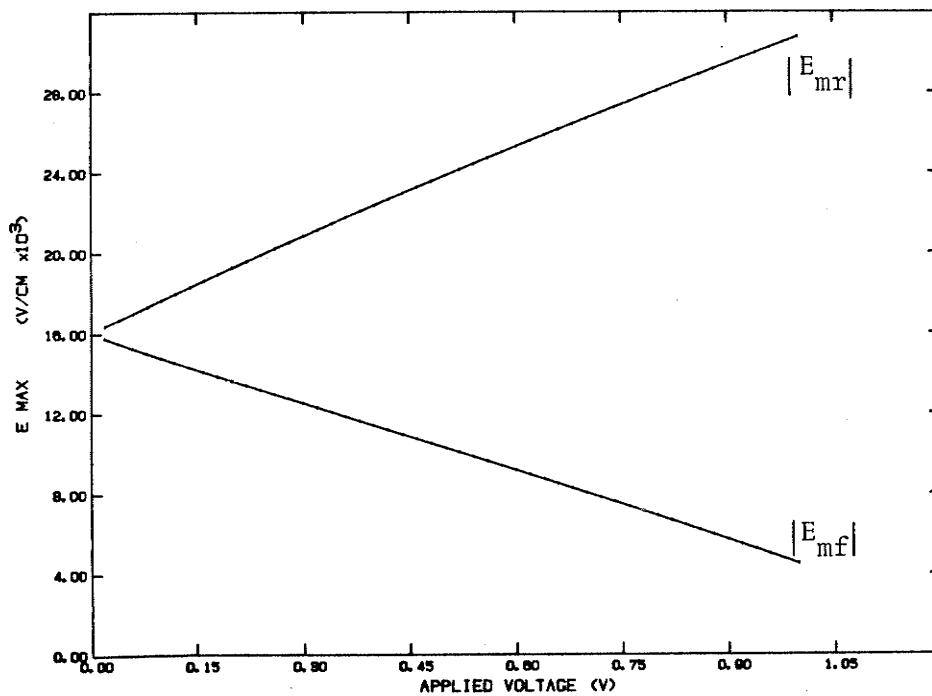


Figure 2.2: Maximum electric field at the forward- and reverse-biased sides, E_{mf} and E_{mr} respectively, as a function of applied voltage.

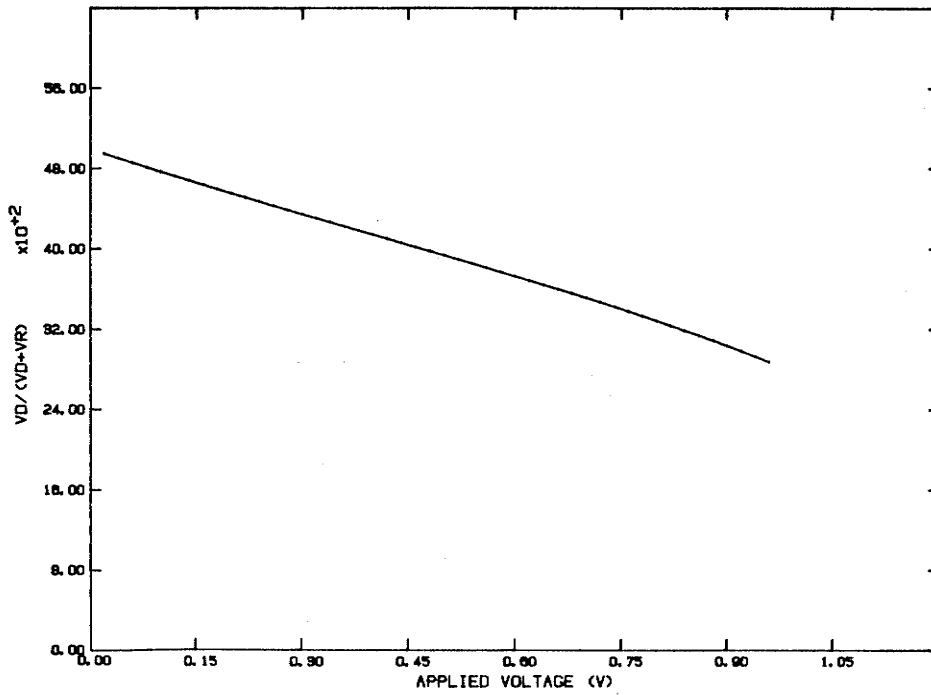


Figure 2.3: Preexponential factor $v_d/(v_d+v_r)$ as a function of applied voltage.

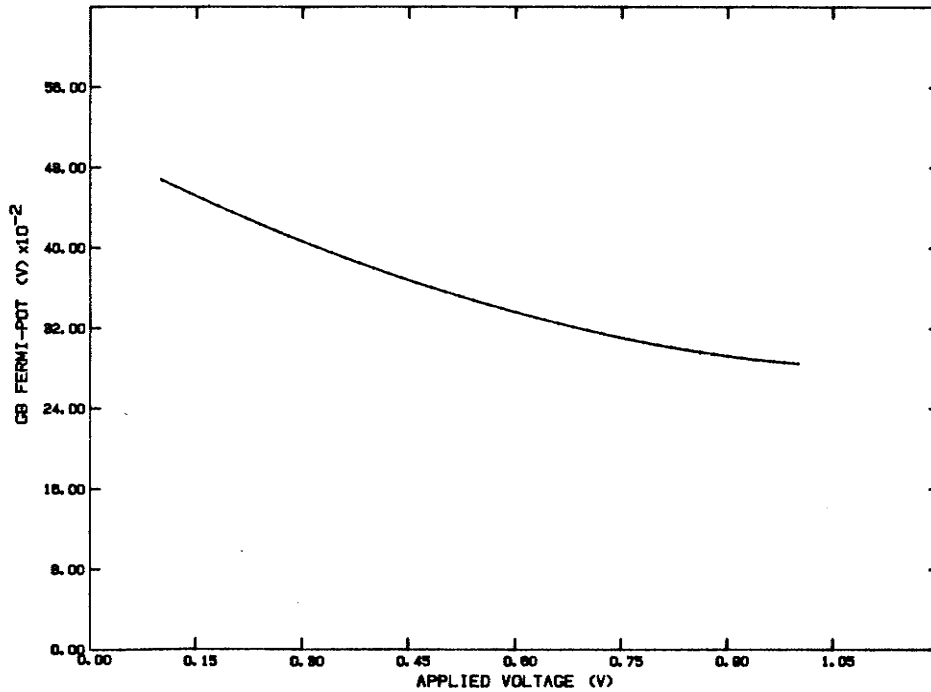


Figure 2.4: Fermi-potential at the grain boundary as a function of applied voltage. $N_{is} = 1.0 \times 10^{11} \text{ eV}^{-1} \text{ cm}^{-2}$.

2.4 ELECTROOPTICAL EFFECTS

The effects of minority carriers on the current transport at grain boundaries become important under conditions of optical illumination. We stress that minority carriers play an indirect role in determining the current by influencing the amount of charge trapped at the grain boundary. This determines the barrier height which in turn controls the majority-carrier current that dominates the total current.

The vicinity of the isolated grain boundary is illuminated such that there is a uniform volume photogeneration rate G_{ph} . If we assume that all minority carriers generated within a diffusion length L_n on either side of the grain boundary will be collected at the grain boundary due to the electric field of the depletion regions then for p-type material [16]

$$2L_n G_{ph} = \sigma_N n(0) v_{th} N_{is} \Delta E \quad (2.7)$$

where σ_N is the capture cross-section for neutral traps, v_{th} is the thermal velocity of electrons, N_{is} is the interface-state density which will be assumed to be independent of energy for this analysis, and ΔE is the energy difference of the imrefs. Note that the left-hand side of (2.7) is the total flux of generated minority carriers to the grain boundary. The majority-carrier concentration at the grain boundary $p(0)$ is

$$p(0) = N_V \exp\left(\frac{-\phi_p(0)}{V_T}\right) \quad (2.8)$$

where N_V is the effective density of states in the valence band, V_T is the thermal voltage kT/q , and $\phi_p(0)$ is the hole imref-potential at the grain boundary (relative to E_V).

$$\phi_p(0) = \phi_p(\text{bulk}) + V_d \quad (2.9)$$

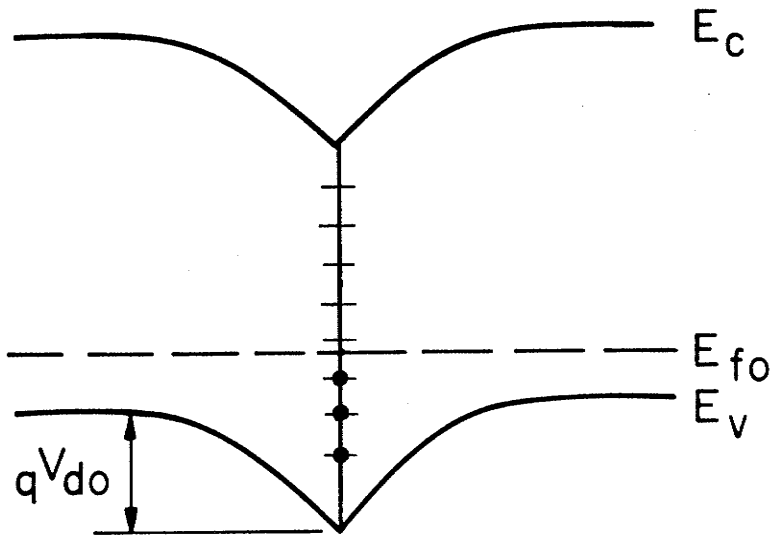
The minority-carrier concentration at the grain boundary $n(0)$ is

$$n(0) = N_C \exp\left(\frac{-\phi_n(0)}{V_T}\right) \quad (2.10)$$

The electron imref-potential $\phi_n(0)$ can be written as

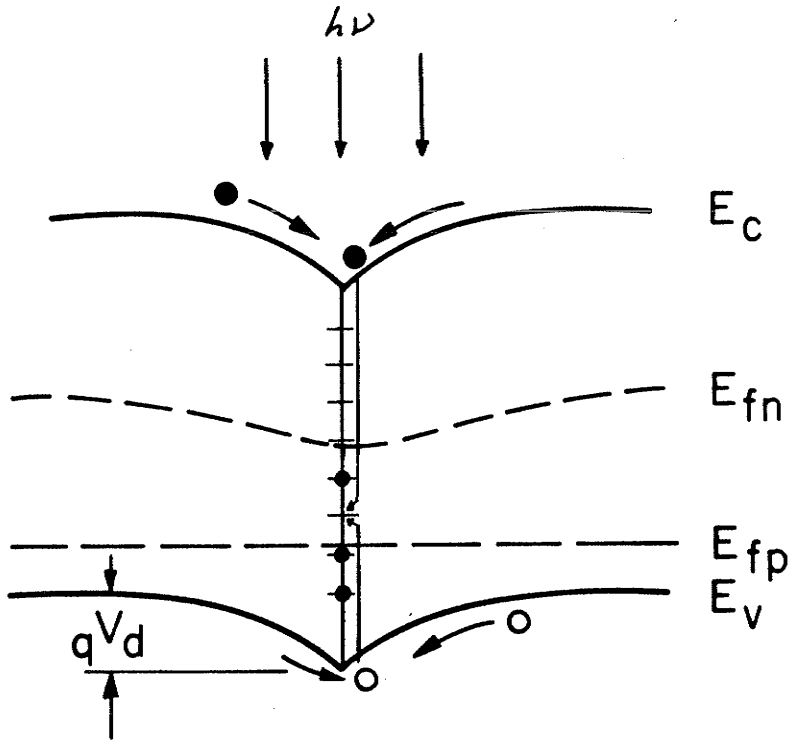
$$\phi_n(0) = \frac{E_g}{q} - \phi_p(0) - \frac{\Delta E}{q} \quad (2.11)$$

Figure 2.5 shows the energy-band structure near a uniformly-illuminated grain boundary in p-type silicon. Under illumination the energy states above the electron imref remain empty while those below the hole imref remain occupied. The occupation probability of states situated between the imrefs will depend on the relative electron and hole concentrations and their capture cross-sections at the grain boundary.



(a)

● Electrons
○ Holes



(b)

Figure 2.5: Energy-band diagram of an illuminated grain boundary. The states between the imrefs are partially filled.

The total charge at the grain boundary in the most general case is equated to the charge in the depletion regions as [16]

$$\begin{aligned}
 (8q N_A V_d)^{1/2} = & -q \left[\int_{E_{fn}(0)}^{E_C(0)} N_{is}^D(E) dE \right. \\
 & + \int_{E_{fp}(0)}^{E_{fn}(0)} \left\{ (1-f_D) N_{is}^D(E) - f_A N_{is}^A(E) \right\} dE \\
 & \left. - \int_{E_V(0)}^{E_{fp}(0)} N_{is}^A(E) dE \right] \quad (2.12)
 \end{aligned}$$

where N_A is the doping concentration in the bulk, $N_{is}^D(E)$ and $N_{is}^A(E)$ are the donor- and acceptor-like interface-state densities respectively, $E_{fn} = q\phi_n$, $E_{fp} = q\phi_p$, and f_A and f_D are the trap occupation functions equal to [16]

$$\begin{aligned}
 f_A &= \frac{\sigma_N n(0)}{\sigma_N n(0) + \sigma_C p(0)} \\
 f_D &= \frac{\sigma_C n(0)}{\sigma_C n(0) + \sigma_N p(0)}
 \end{aligned} \quad (2.13)$$

where we have assumed the neutral (σ_N) and coulombic (σ_C) capture cross-sections to have the same value for the donor- and acceptor-like states.

Assuming N_{is}^D and N_{is}^A are independent of energy (2.12) can be rearranged to give the barrier height V_d

$$V_d = \frac{q}{8\epsilon_s N_A} \left[-\phi_n N_{is}^D + \phi_p N_{is}^A - \Delta E \left\{ (1-f_D) N_{is}^D - f_A N_{is}^A \right\} \right]^2 \quad (2.14)$$

For computation we rewrite (2.7) as

$$\Delta E = \frac{2G_{ph} L_n}{\sigma_N v_{th} N_{is} n(0)} \quad (2.15)$$

where

$$N_{is} = N_{is}^A + N_{is}^D \quad (2.16)$$

A computer program that solves this set of equations for V_d as a function of the photogeneration rate G_{ph} has been written and is included here as Appendix A. Sample results are shown graphically in Fig. 2.6. We observe that the potential barrier V_d decreases with increasing separation of the imrefs ΔE . This implies that V_d decreases in proportion to the logarithm of the photogeneration rate of excess carriers. This effect may have serious implications for small-grain polycrystalline solar cell applications where the recombination lifetime of the excess carriers is important [17].

We note that optical illumination, by reducing the barrier height, effectively increases the conductivity of the barrier. This may eventually lead to the construction of polycrystalline optical sensors.

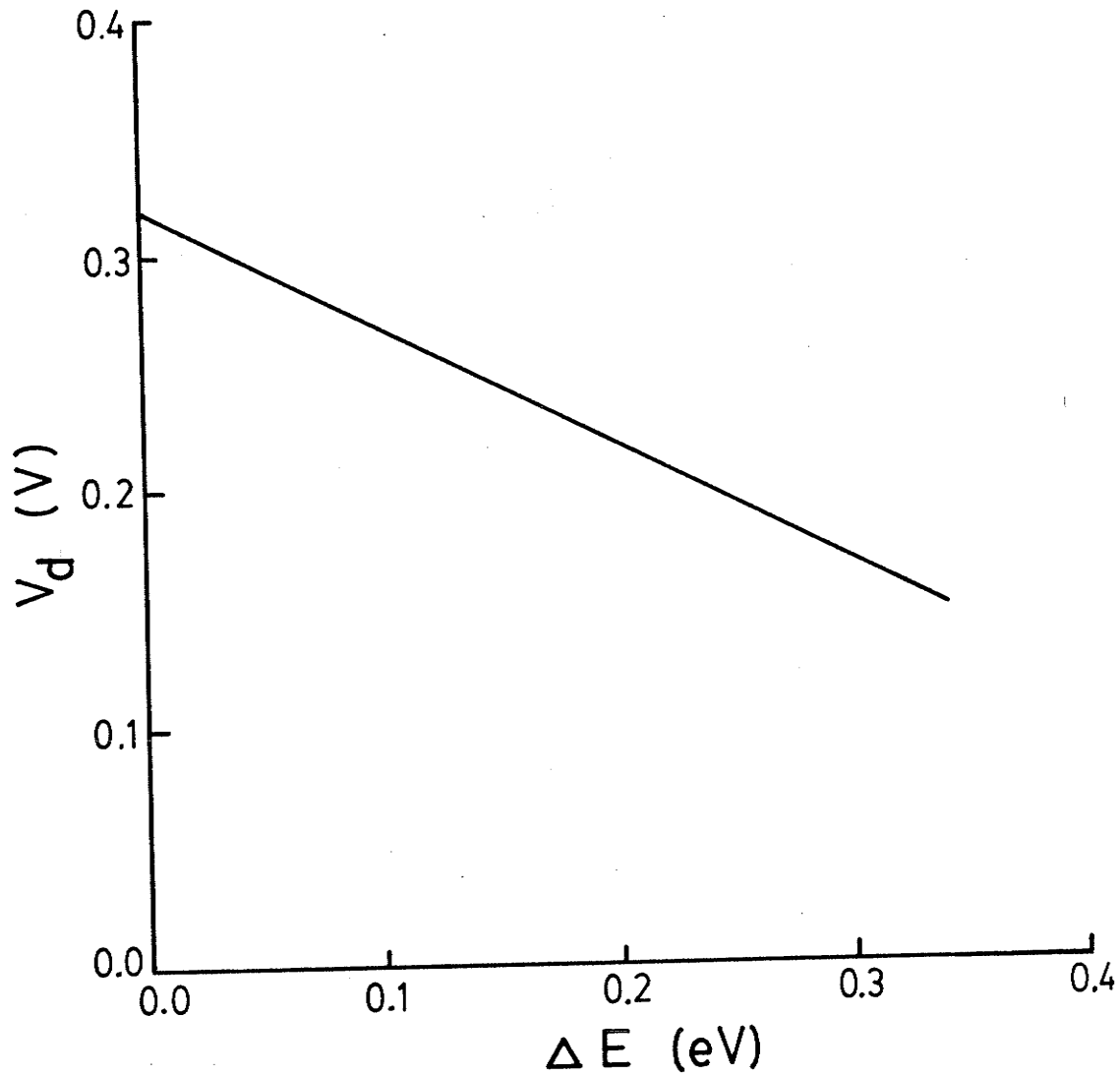


Figure 2.6: Reduction of the potential barrier due to optical illumination. In this example $L = 30 \mu\text{m}$, $N_A = 10^{15} \text{cm}^{-3}$, $N^A = N^D = 10^{14} \text{eV}^{-1} \text{cm}^{-2}$, $\sigma_N = 10^{-16} \text{cm}^2$, $\sigma_C = 10^{-14} \text{cm}^2$, and $T = 300 \text{K}$. is is

Chapter III

MEASUREMENTS ON ISOLATED SILICON GRAIN BOUNDARIES

3.1 SAMPLE PREPARATION

An experimental investigation of the electrical properties of grain boundaries in polycrystalline silicon under d.c. conditions was performed. Samples for this purpose were cut from 'Silso' solar-grade polycrystalline silicon obtained from Wacker Chemitronic Ltd. This material had a typical grain size of 1 mm. The p-type (boron) doping concentration N_A was approximately $3 \times 10^{15} \text{ cm}^{-3}$.

A diamond-edged wafering saw was used to cut the $100 \times 100 \times 0.4$ mm wafers into strips approximately 20×1 mm. These strips were then etched in 3:1:1 HNO_3 (79%): HF (49%): glacial acetic acid for approximately three minutes under gentle agitation to ensure uniformity. This etching served to eliminate the saw damage [18] as well as to highlight the individual grain boundaries [19]. After etching the cross-sectional area was slightly reduced to $3 \times 10^{-3} \text{ cm}^2$.

An optical microscope revealed which grain boundaries would be suitable for study. We selected boundaries that were planar throughout the cross-sectional extent of the sample strips and were somewhat remote from adjacent bounda-

ries, i.e. those most similar to our theoretical model. One suitable grain boundary from each of the strips was masked by a thin wire prior to the vacuum deposition of aluminum contacts. A four-probe configuration was created by mechanically removing thin strips of the aluminum film from either side of the grain boundary. The sample geometry is shown in Fig. 3.1. Ohmic behavior of the contacts was ensured by sintering at 600°C for 20 minutes in flowing nitrogen gas. The sample strips were mounted on test jigs made of printed-circuit-board by silver paste applied to the outer contacts. Aluminum wires were ultrasonically bonded to the inner contacts and brought out to contact pads on the jigs.

The four-probe configuration allows current to be injected and removed through the outer contacts while the voltage drop across the grain-boundary region can be accurately measured between the inner contacts with a high-impedance voltmeter.

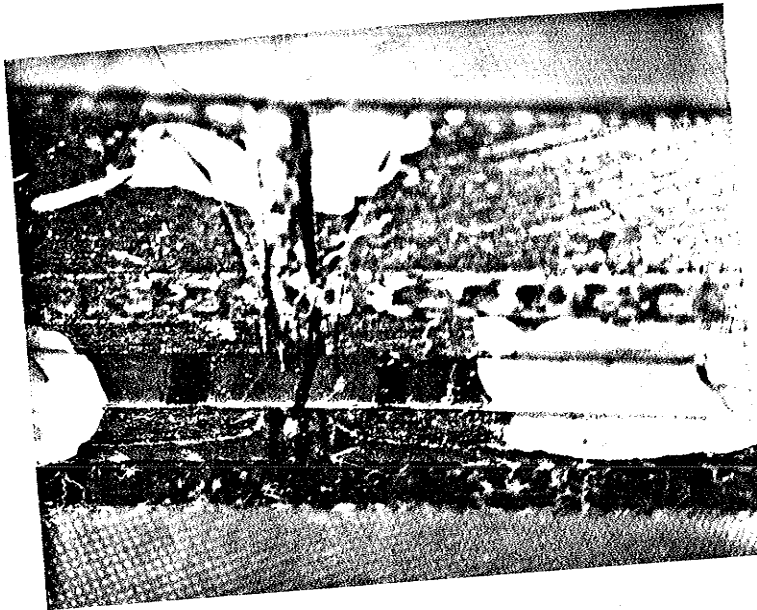
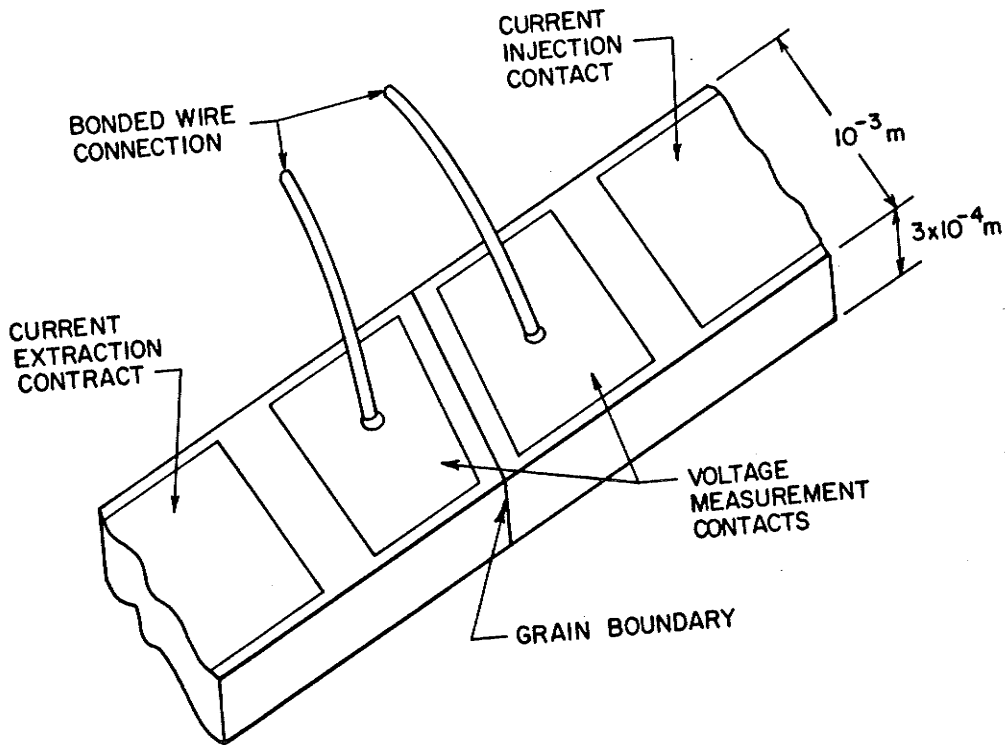


Figure 3.1: Sample geometry. Cross-sectional area of all samples = 3×10^{-3} cm².

3.2 EXPERIMENTAL RESULTS

A Keithly 610C electrometer and Tektronix DM 502 multimeter (for current and voltage functions respectively) were used to manually measure the current-voltage characteristics of the three sample grain boundaries shown in Figs. 3.2 - 3.4 . The differing current levels from sample to sample are attributed primarily to different magnitudes of the potential barrier V_{do} in the three samples.

The grain boundary samples were subjected to optical illumination from a Sylvania ELH projection lamp. An infrared filter eliminated all radiation with a wavelength of less than $1\mu\text{m}$. This ensured a relatively uniform illumination throughout the sample. Figures 3.5 and 3.6 show the effects of the illumination on the current-voltage characteristics of a low and high barrier grain boundary respectively.

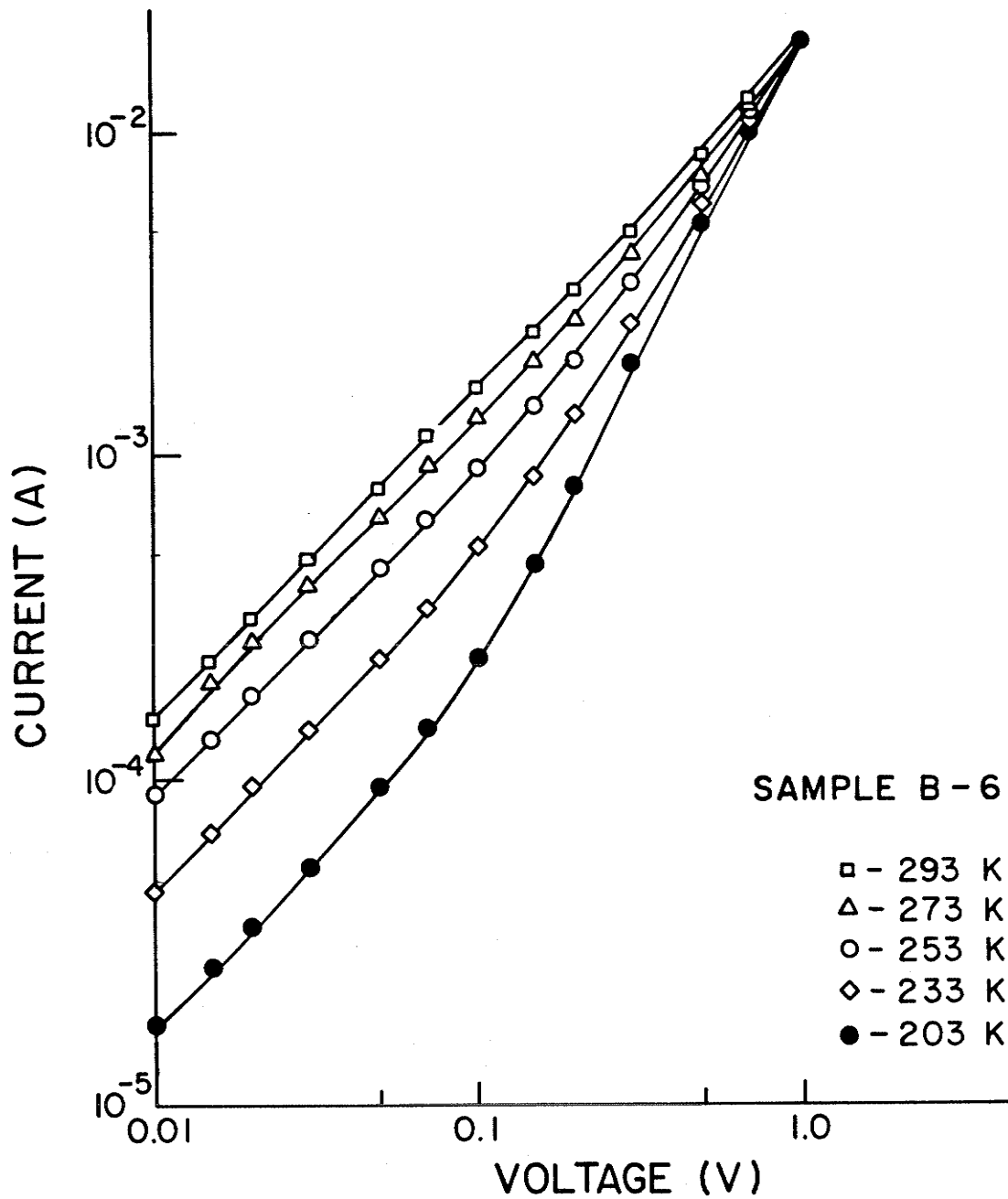


Figure 3.2: Dark characteristics of grain boundary sample B-6 at several measurement temperatures.

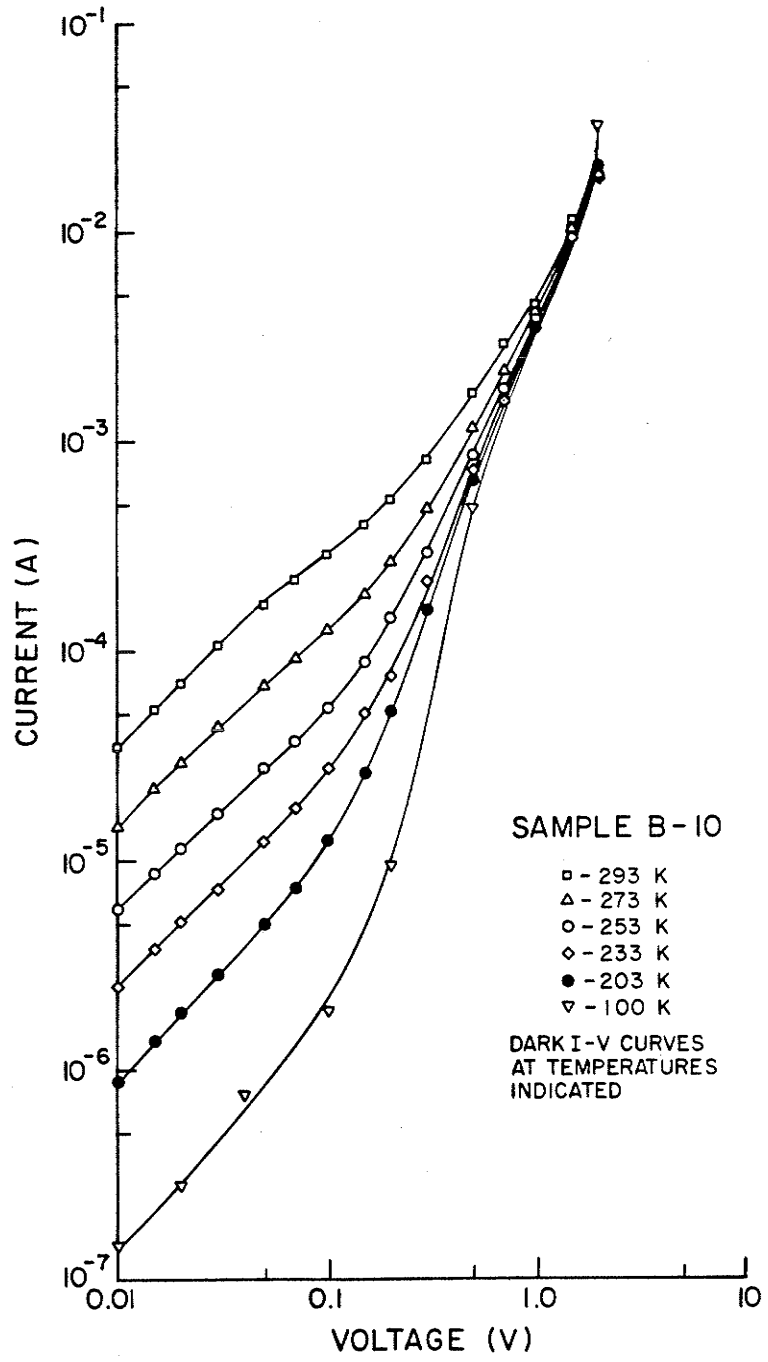


Figure 3.3: Dark characteristics of grain boundary sample B-10 at several measurement temperatures.

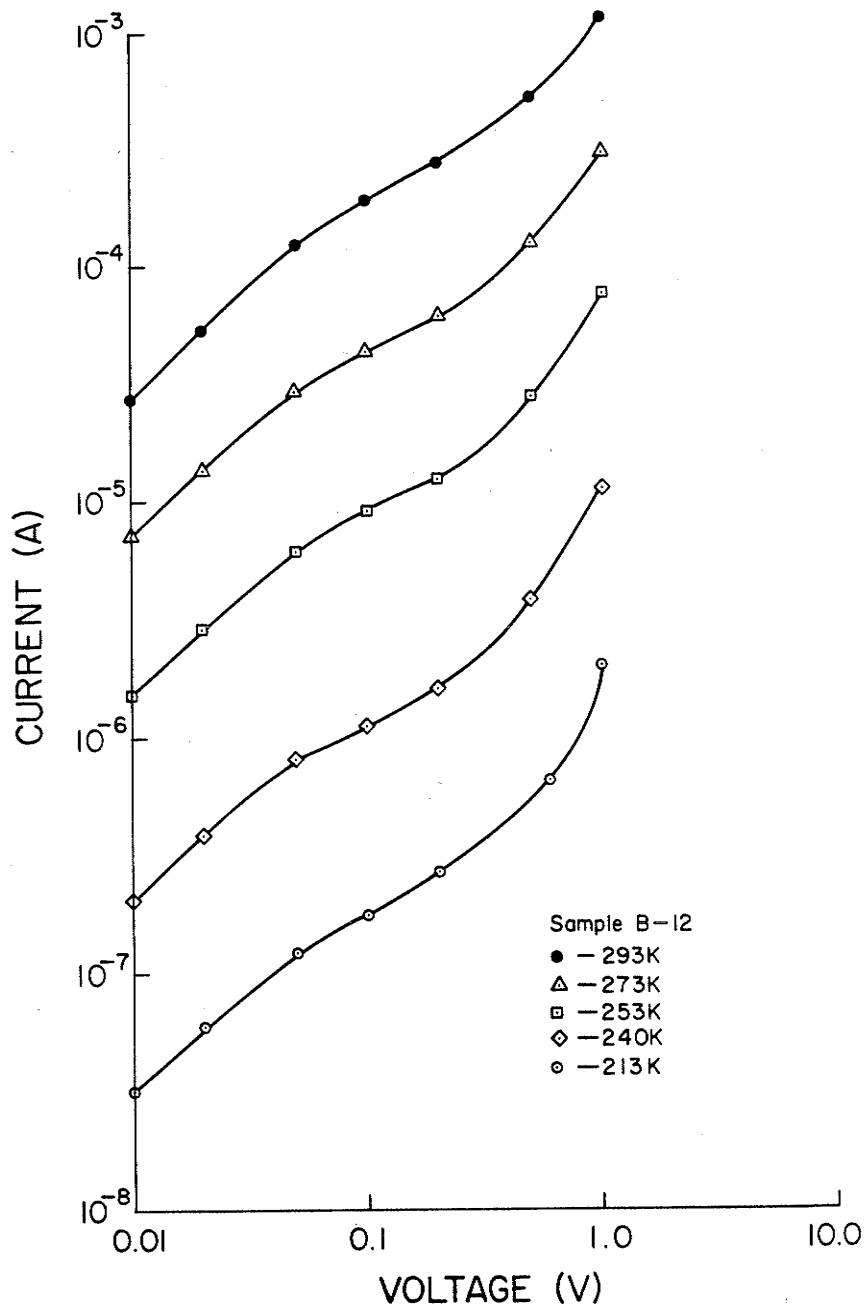


Figure 3.4: Dark characteristics of grain boundary sample B-12 at several measurement temperatures.

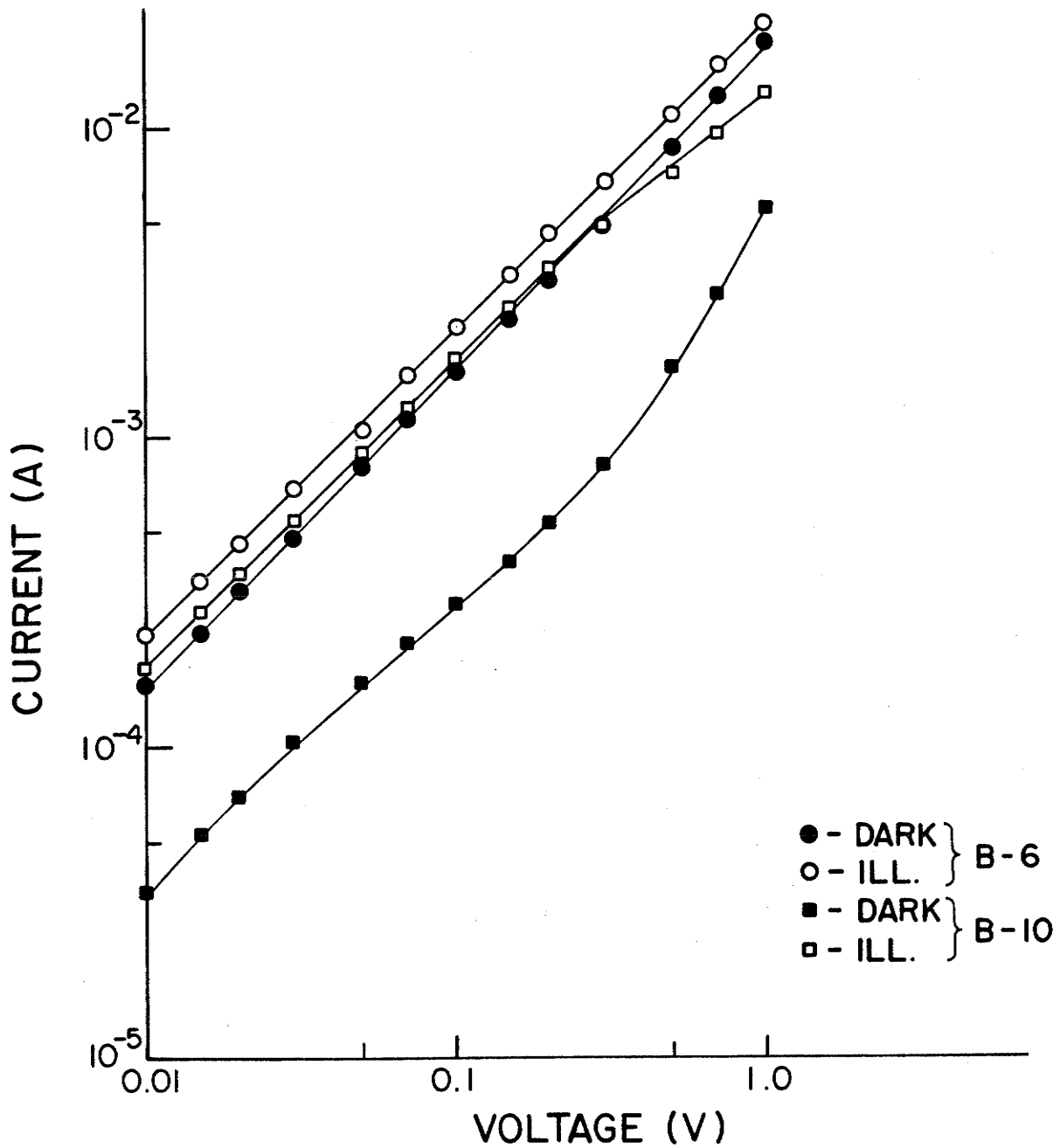


Figure 3.5: Characteristics of B-6 and B-10 under 5 mW cm^{-2} optical illumination.

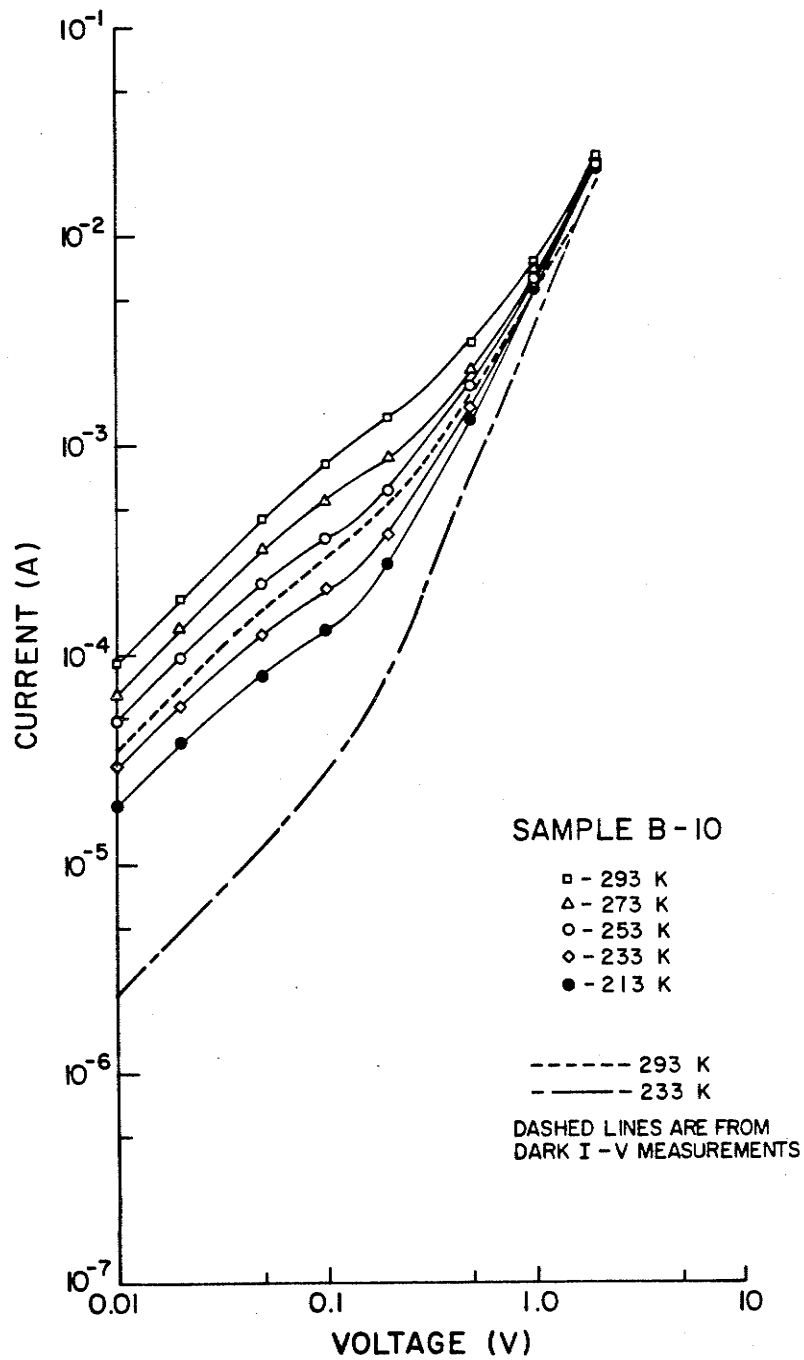


Figure 3.6: Characteristic of B-10 under $20 \mu\text{W cm}^{-2}$ optical illumination.

3.3 CURRENT OSCILLATIONS

Most grain boundary samples, when biased at a relatively high voltage, exhibited current oscillations such as those shown in Fig. 3.7. The magnitude of these oscillations was typically 1% of the d.c. current. Voltages in excess of 10V, resulting in current densities in the range 40-100 Acm^{-2} were required to induce these oscillations.

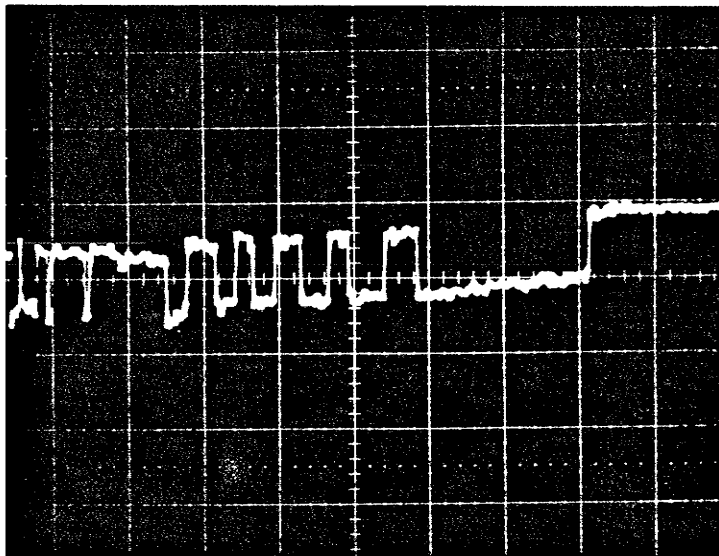


Figure 3.7: Current oscillations observed (as a voltage developed across a 10Ω resistor) at high d.c. current densities. Grain boundary sample B-11. $V=15\text{V}$, $I=150\text{mA}$. Vert. scale: $500\ \mu\text{A}/\text{div}$. Horz. scale: $1\ \text{ms}/\text{div}$.

Oscillations were not observed below this threshold level. Above the threshold, generally more and larger pulses were observed at higher current densities.

This experiment was originally intended to provide evidence of carrier multiplication processes at grain boundaries. Indeed, the observed oscillations are strikingly similar to those unambiguously arising from avalanche multiplication in p-n junctions [20]. It was however observed that the grain-boundary current oscillations could be thermally stimulated. That is, a sample, biased at a current below the threshold for oscillation, could be induced into oscillation by heating. The normal multiplication process is expected to be hindered by an increase in lattice temperature [8].

We now believe these oscillations to be due to electric-field-enhanced emission of carriers [21] from the localized interface states at the grain boundary. By this interpretation the large electric field on the reverse-biased side of the grain boundary lowers the coulombic potential well associated with the charged interface states, thus freeing a portion of the charge trapped at the grain boundary. The reduced grain boundary charge will result in a lower electric field and potential barrier. Field emission will cease temporarily until the charge is replenished, increasing the electric field. The current, being controlled by the potential barrier, exhibits rapid fluctuations in accordance with the modulation of the charge.

3.4 AUTOMATED MEASUREMENT OF GRAIN BOUNDARY SAMPLES

The direct current measurements of grain boundaries have been automated using an Automated Data Acquisition and Processing (ADAP) system. ADAP is an "in-house" data acquisition system specifically designed and constructed (as a part of this thesis project) for semiconductor material and device measurements. The system consists of an Apple II Plus microcomputer coupled to an Experiment Control Interface (ECI). ECI provides an 8-input channel, 12-bit analog-to-digital converter (A/D) and four 10-bit digital-to-analog (D/A) voltage outputs. Also incorporated is an ammeter in the form of a current-to-voltage converter with computer-controlled sensitivity. A detailed description of the ADAP and ECI systems can be found in the "ADAP User's Guide" included in this thesis as Appendix D.

The experimental setup is shown in Fig. 3.8. The four-probe measurement configuration used previously is replaced here by the two-probe method which is better suited for automated measurements. The Z output provides a bias voltage of up to one volt to the sample. The resulting current is passed through the current-to-voltage converter whose output is connected to input channel 6 for "reading" by the A/D.

An FTS Multi-Cool refrigeration unit provided temperature control from +20°C to -60°C. The sample temperature was monitored with a Fluke 2100A thermometer. The analog output voltage of the thermometer was amplified by a Keithley 610C (gain set to 100) and connected to the ECI input channel 4.

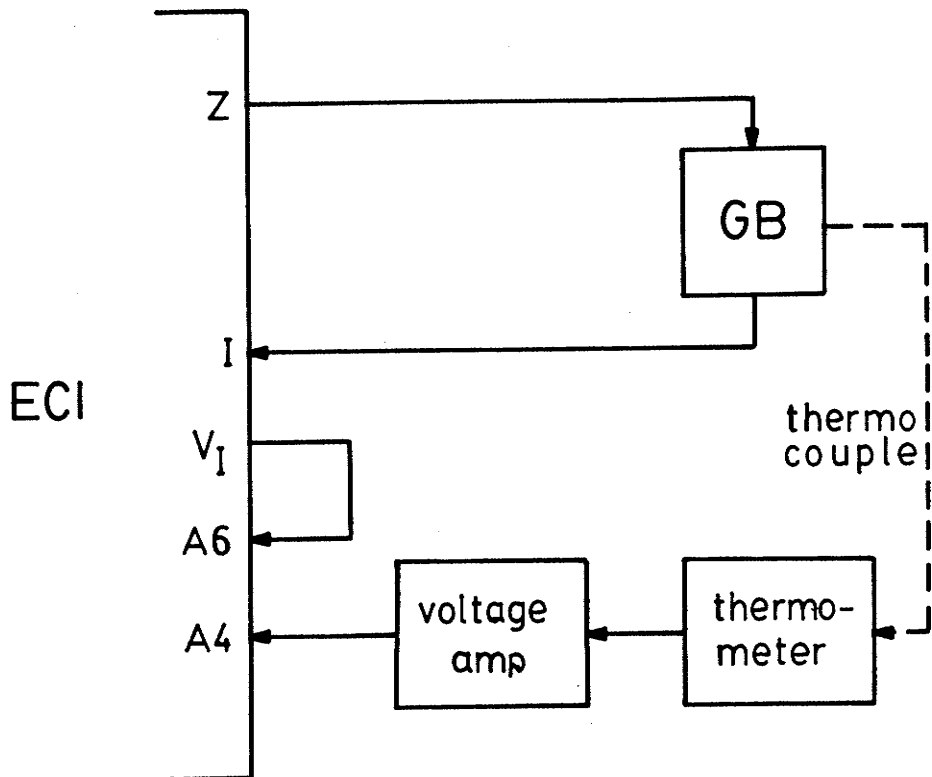


Figure 3.8: Connections between ECI and the grain boundary samples (GB) for automated measurements.

The current-voltage curves of a grain boundary were measured as a function of temperature by taping its jig to a thermal mass and placing it in the refrigeration unit at room temperature (+20°C). Cooling was then initiated and control of the experiment was handed to the ADAP system upon execution of the program "GB". This control program continuously monitored the sample temperature. At ten degree intervals (from +20° to -60°C) the bias voltage was swept through a series of levels from 0.020 to 0.500 volts and the respective currents recorded. These current values were en-

tered into a matrix (i.e. with temperature and voltage as coefficients) and stored on a floppy-disk for reduction by other programs. Appendix B is a listing of "GB".

Figure 3.9 shows a set of current-voltage characteristics that were collected and plotted on a log-log scale using "GB".

The computer facilitates these measurements in several ways. Most importantly, the experiment can run unattended for its two to three hour duration. Also, measurements at each temperature are completed in less than five seconds, thus ensuring isothermality. Clerical errors are eliminated by storing the data directly on floppy disk in a form suitable for subsequent processing. Graphical output in the convenient form of a log-current vs. log-voltage plot is immediately available.

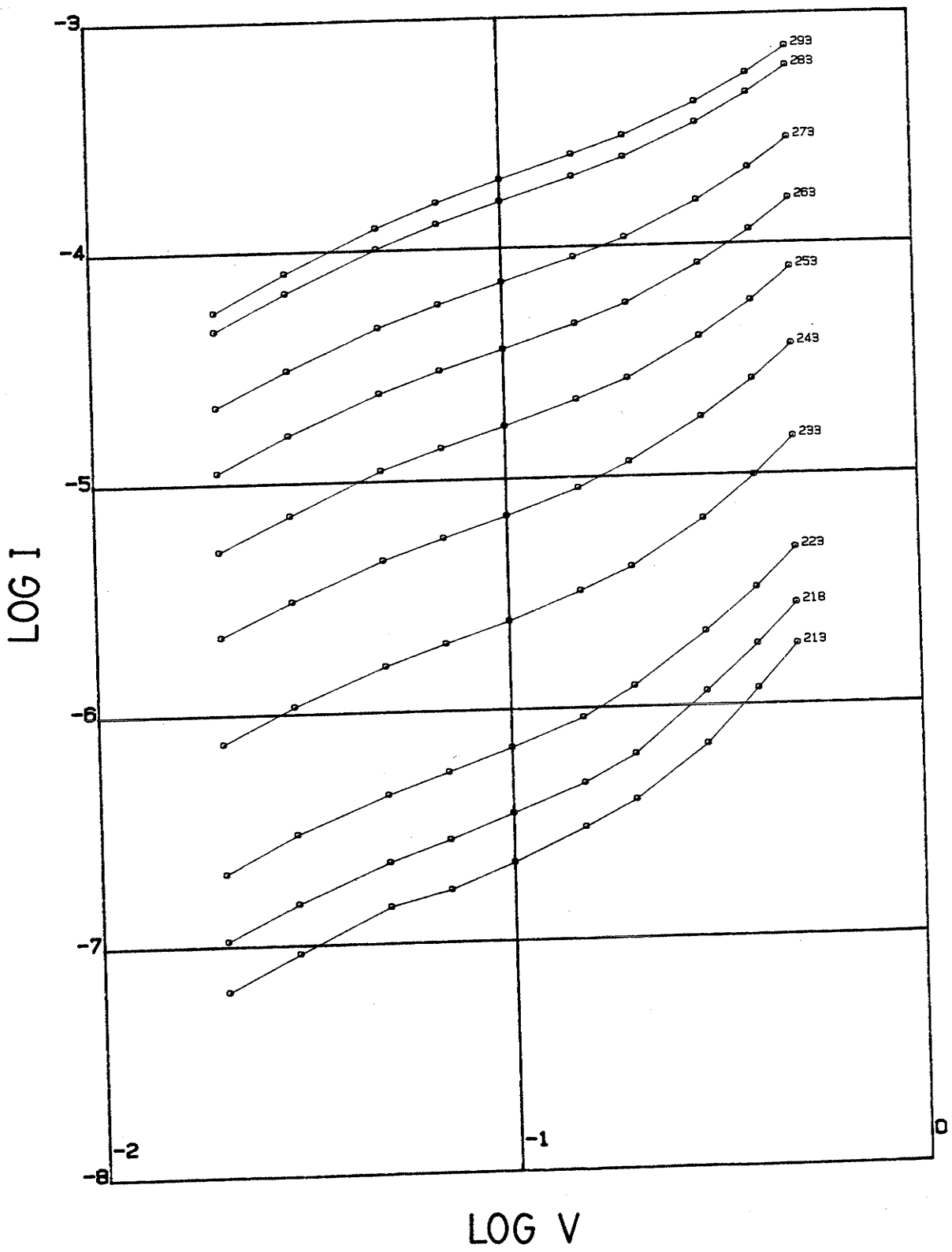


Figure 3.9: Log-current vs. log-voltage plot of a grain boundary characteristic as measured and plotted using the "GB" control program. Sample B-99.

3.5 DETERMINATION OF THE INTERFACE STATE DENSITY BY DECONVOLUTION

In sec. 2.2 we discussed the important role that the interface states play in determining the electrical conduction at grain boundaries. It is thus desirable to experimentally characterize the interface states of the samples previously described. A complete characterization would include the densities and capture cross-sections as a function of energy for both the acceptor- and donor-like states. The capture cross-sections are more relevant to transient and photo-response measurements and will not be dealt with in our present steady-state analysis. An iterative technique has been developed to provide an indication of the interface-state densities at grain boundaries from their current-voltage characteristics. This type of calculation has been dubbed "deconvolution" of the current-voltage characteristics [18].

We begin our formulation by assuming that the diffusion and recombination velocities at the grain boundary are approximately equal for the small applied voltages ($V_a < 1V$) we are considering. This assumption was justified by the results of the computer simulation (sec. 2.3) which revealed that $1/2 < v_d/(v_d + v_r) < 1/3$. Equation (2.2) is then

$$J \approx \frac{qN_A \mu E_{mf}}{2} \exp\left(\frac{-V_{df}}{V_T}\right) \left[1 - \exp\left(\frac{-V_a}{V_T}\right) \right] \quad (3.1)$$

We have used the electric field on the forward-biased side of the grain boundary E_{mf} because it has a slightly greater influence over the current than E_{mr} .

The difference between the diffusion potentials on the reverse- and forward-biased sides of the grain boundary V_{dr} and V_{df} respectively is equal to the applied voltage V_a and can be related to the electric field as

$$V_a = V_{dr} - V_{df} = \frac{\epsilon_s}{2qN_A} [E_{mr}^2 - E_{mf}^2] \quad (3.2)$$

The total charge trapped at the grain boundary Q_{GB} is

$$Q_{GB} = \epsilon_s (E_{mf} - E_{mr}) \quad (3.3)$$

From (3.2) and (3.3) we solve for the electric fields

$$E_{mf} = \frac{-V_a qN_A}{Q_{GB}} + \frac{Q_{GB}}{2\epsilon_s} = \left(\frac{2qN_A}{\epsilon_s} V_{df} \right)^{1/2} \quad (3.4)$$

$$E_{mr} = \frac{-V_a qN_A}{Q_{GB}} - \frac{Q_{GB}}{2\epsilon_s} = \left(\frac{2qN_A}{\epsilon_s} V_{dr} \right)^{1/2}$$

Solving for the diffusion potentials

$$V_{df} = \frac{\epsilon_s}{2qN_A} \left(\frac{-V_a qN_A}{Q_{GB}} + \frac{Q_{GB}}{2\epsilon_s} \right)^2 \quad (3.5)$$

$$V_{dr} = \frac{\epsilon_s}{2qN_A} \left(\frac{-V_a qN_A}{Q_{GB}} - \frac{Q_{GB}}{2\epsilon_s} \right)^2$$

We begin the iterative solution for the charge at the grain boundary (for a particular current-voltage pair) by choosing an initial value for the charge Q_{GB} . This value is used in (3.5) to establish a first estimate of the diffusion potentials at the grain boundary for the given applied voltage V_a . The resulting forward-biased diffusion potential V_{df} is used in (3.4) to calculate the corresponding electric field E_{mf} . The current equation (3.1) can now be solved for another value of V_{df} . An improved calculation of Q_{GB} follows from (3.4) and (3.3). The next iteration uses this Q_{GB} to calculate new diffusion potentials and so on. The iterations continue until Q_{GB} converges to a constant value.

When the applied voltage is increased, the Fermi-level at the grain boundary will shift closer to the valence-band edge in p-type material due to the reduction of the forward-biased diffusion potential. The concentration of holes (majority carriers) at the grain boundary $p(0)$ is expressed as [15]

$$p(0) = \frac{N_A}{E_{mr} - E_{mf}} \left\{ E_{mr} \exp\left(\frac{-V_{dr}}{V_T}\right) - E_{mf} \exp\left(\frac{-V_{df}}{V_T}\right) \right\} \quad (3.6)$$

which has a corresponding Fermi-level

$$E_f(0) = -qV_T \ln \left[\frac{p(0)}{N_V} \right] \quad (3.7)$$

where N_V is the effective density of states in the valence band. The values of E_{mf} , E_{mr} , V_{df} , and V_{dr} from the iterative solution are used to calculate $E_f(0)$ at each applied voltage.

Successive steps in applied voltage produce an incremental shift of the Fermi-level ΔE_f (as noted in sec. 2.3) and a corresponding alteration of the grain boundary charge ΔQ_{GB} . Provided that the interface states are in equilibrium with the majority-carrier Fermi-level we may write the interface-state density $N_{is}(E)$ as

$$N_{is}(E_f) = \frac{1}{q} \frac{\Delta Q_{GB}}{\Delta E_f} \quad (3.8)$$

The deconvolution of current-voltage characteristics measured at different temperatures are combined in Fig. 3.10 to show the experimentally determined relationship between the interface-state density and the electronic energy of these states. The upper energy limit that may be investigated is the sum of the bulk and zero-bias diffusion potentials. The lowest measureable energy is determined by several factors including pinning of the Fermi-level and the inevitable breakdown of our approximations under the large deviations from equilibrium required for probing close to the valence band.

It is interesting to note that the numerical simulation of sec. 2.3 has shown that at high voltages the emission approximation made by Seager [18] can lead to an underestimation of the interface-state density by a factor of two or three as compared to the emission/diffusion model employed here.

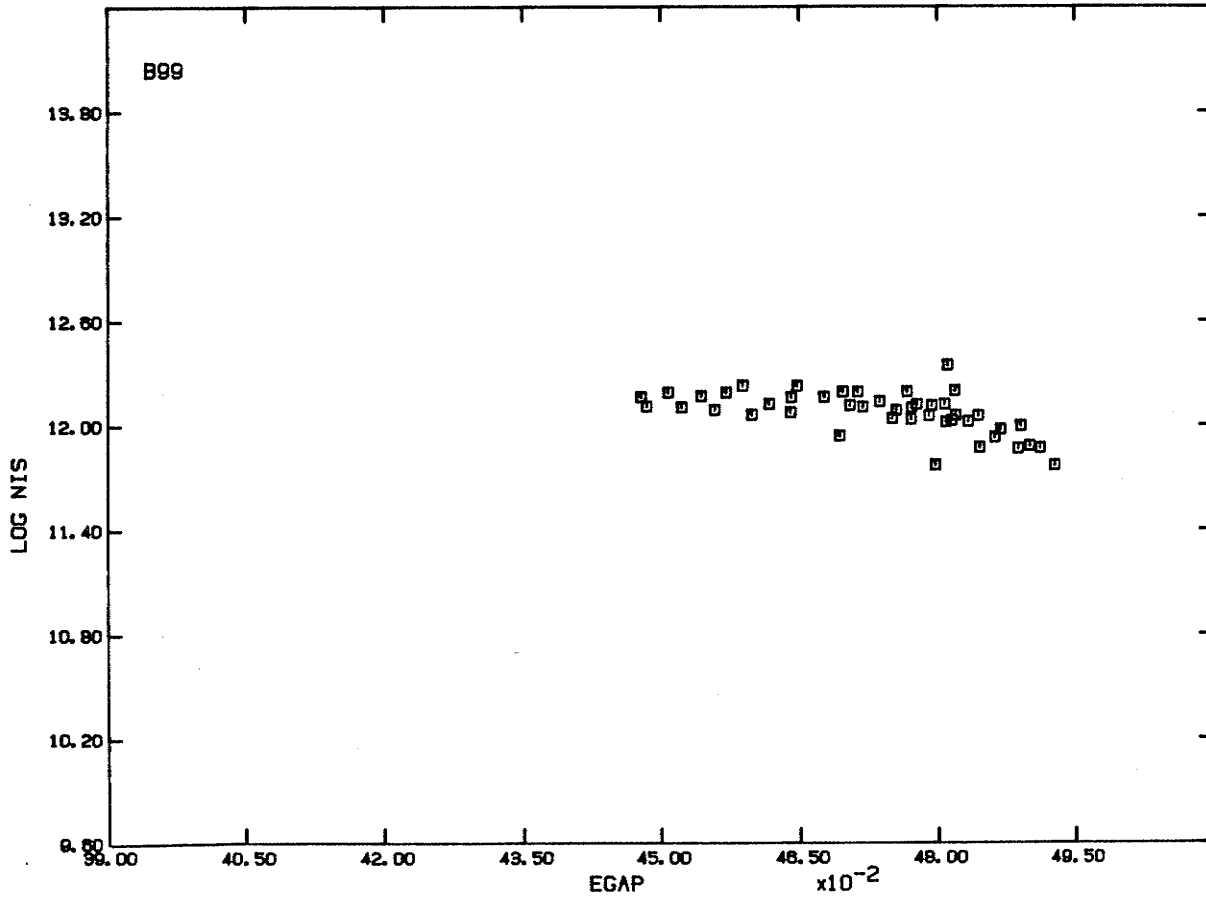


Figure 3.10: Interface-state densities within the forbidden gap of silicon at a grain boundary obtained from the deconvolution of current-voltage characteristics. The plot was made by the program AUTODECON from data collected by GB. Sample B-99.



3.6 GRAIN BOUNDARY ACTIVATION ENERGY

For $V_a \gg V_T$ the current equation (2.2) simplifies to

$$J \approx q \frac{v_d}{2} N_A \exp\left[\frac{-qV_{df}}{kT}\right] \quad (3.9)$$

and it follows that

$$\ln\left[\frac{J}{v_d}\right] = \ln\left[\frac{qN_A}{2}\right] - \frac{q}{k} V_{df} \left(\frac{1}{T}\right) \quad (3.10)$$

Taking the derivative of both sides of (3.10) with respect to $1/T$ we define an activation energy E_a as

$$\begin{aligned} E_a &= - \frac{d \ln(J/v_d)}{d(1/T)} = \frac{d\left[\frac{q}{k} V_{df}(1/T)\right]}{d(1/T)} \\ &= \frac{q}{k} \left(V_{df}(T) + \frac{1}{T} \frac{dV_{df}(T)}{d(1/T)} \right) = \frac{q}{k} \left(V_{df}(T) - T \frac{dV_{df}(T)}{dT} \right) \end{aligned} \quad (3.11)$$

Similarly for $V_a \ll V_T$

$$J \approx q^2 \frac{v_d N_A}{2} \frac{V_a}{kT} \exp\left(\frac{-qV_{do}}{kT}\right) \quad (3.12)$$

which results in the activation energy

$$E_a = \frac{d \ln(J \cdot T)}{d(1/T)} = \frac{q}{k} \left(V_{do}(T) - T \frac{dV_{do}(T)}{dT} \right) \quad (3.13)$$

The difference of activation energy measured at any two temperatures T_1 and T_2 will be

$$\begin{aligned}
 E_a(T_2) - E_a(T_1) &= \frac{q}{k} \left(V_{df}(T_2) - T_2 \frac{dV_{df}(T_2)}{dT} - V_{df}(T_1) + T_1 \frac{dV_{df}(T_1)}{dT} \right) \\
 &= \frac{q}{k} \left(V_{df}(T_2) - V_{df}(T_1) - \frac{dV_{df}}{dT} (T_2 - T_1) \right) = 0
 \end{aligned}
 \tag{3.14}$$

so that E_a is independent of temperature for grain boundaries that conform to our one-dimensional model, provided that $dV_{df}(T_1)/dT = dV_{df}(T_2)/dT$.

The diffusion potential is temperature dependent due to the temperature dependence of the bulk Fermi-potential given as

$$\phi_p = \frac{kT}{q} \ln(N_V/N_A)
 \tag{3.15}$$

As the temperature is decreased the Fermi-potential shifts closer to the valence band edge (p-type), increasing the charge trapped in the interface states. Thus $dV_{do}/dT < 0$. Quantitatively,

$$\frac{dV_{do}}{dT} = -\gamma \frac{d\phi_p}{dT} = -\gamma \frac{k}{q} \ln(N_V/N_A)
 \tag{3.16}$$

where we have neglected the weak temperature dependence of $\ln N_V$.

The parameter γ accounts for the increased charge at the grain boundary. If no interface states existed in the energy

range in question ($N_{is} = 0$) then $dV_{do}/dT = 0$ which leads to $\gamma = 0$. Conversely if N_{is} is relatively large $dV_{do}/dT = -d\phi_p/dT$, hence $\gamma = 1$.

To derive γ we recognize that at equilibrium

$$qN_{is} \frac{d(\phi_p + V_{do})}{dT} = \frac{dQ_{GB}}{dV_{do}} \cdot \frac{dV_{do}}{dT} \quad (3.17)$$

where $\phi_p + V_{do}$ is the Fermi-potential at the grain boundary. We then have

$$\frac{dV_{do}}{dT} = \frac{1}{\frac{1}{qN_{is}} \cdot \frac{dQ_{GB}}{dV_{do}} - 1} \cdot \frac{d\phi_p}{dT} \quad (3.18)$$

Comparing (3.18) and (3.16) we find γ to be

$$\gamma = \frac{1}{1 - \frac{1}{qN_{is}} \frac{dQ_{GB}}{dV_{do}}} \quad (3.19)$$

where

$$\frac{dQ_{GB}}{dV_{do}} = \left(\frac{2q\epsilon_s N_A}{V_{do}} \right)^{1/2} \quad (3.20)$$

provided that $V_{do} \gg V_T$. In general γ is a function of temperature; however, it can be considered constant provided N_{is} is relatively independent of energy (for the range of Fermi-level excursions to be considered).

Chapter IV

DISCUSSION

4.1 EXPERIMENTAL DETERMINATION OF THE POTENTIAL BARRIER

The potential barrier at a grain boundary V_{do} has been measured by several techniques. The first uses (3.12) and currents measured at low voltage to obtain V_{do} at near-equilibrium conditions. The second employs (3.13) to obtain V_{do} from the measured activation energies. This procedure requires an independent determination of the interface-state density which is acquired by deconvolution of the current-voltage characteristics (sec. 3.5). The results of these calculations for V_{do} as functions of measurement temperature are shown in Fig. 4.1 for several samples.

From Fig 4.1 it is evident that sample B-12 conforms, at least qualitatively, to the results predicted by (3.14) with $\gamma=1$. The marked decrease of E_a and V_{do} with decreasing temperature for sample B-10 is however incompatible with the present theory. Several possible causes of this effect will be discussed in the following section.

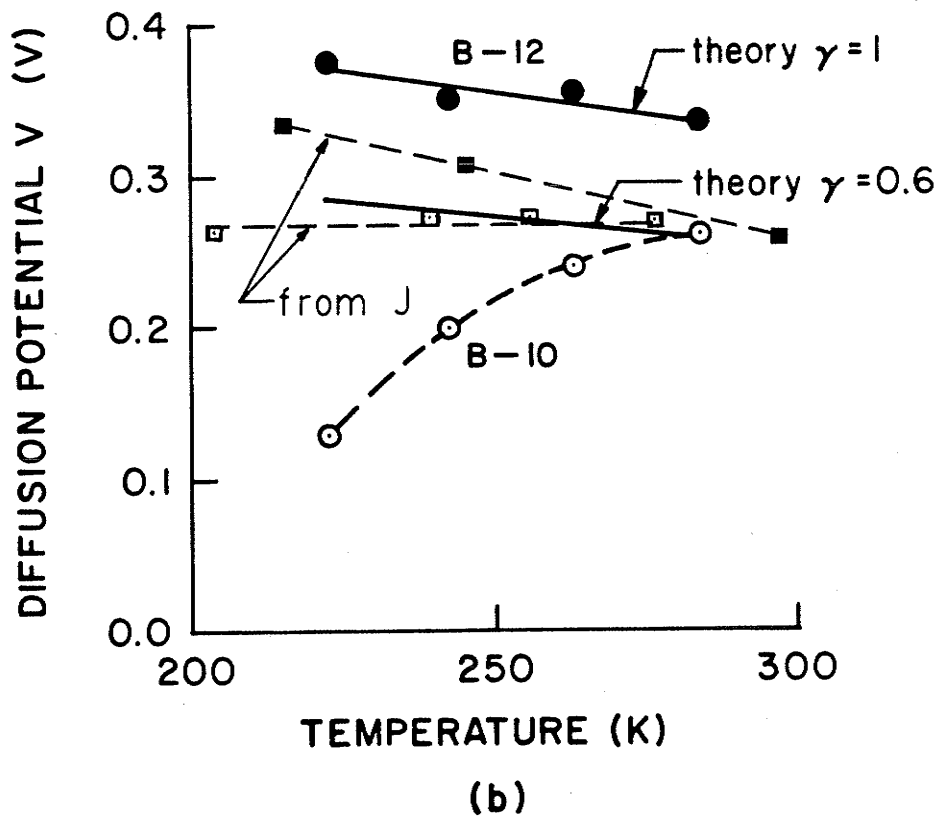
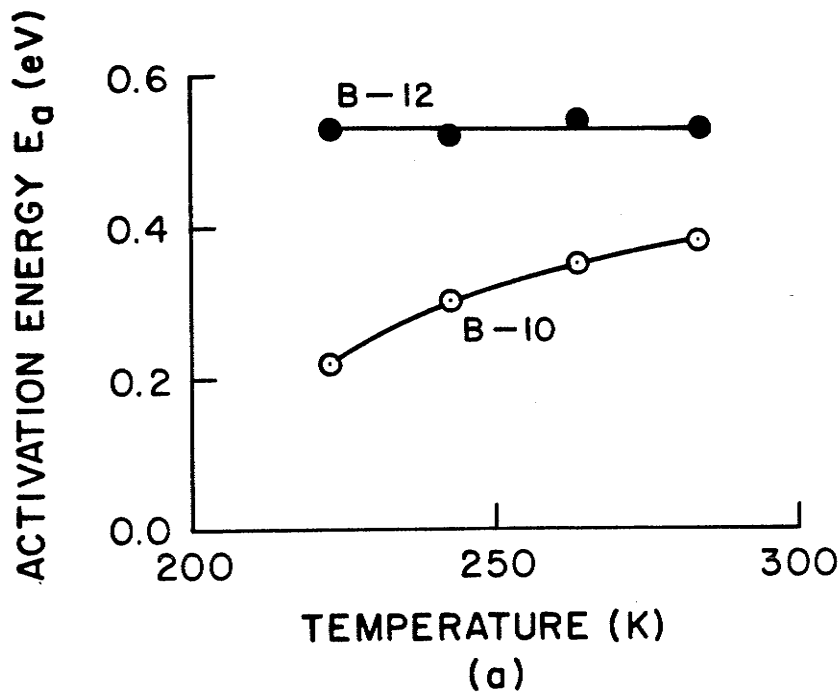


Figure 4.1: The dependence of (a) the activation energy and (b) the diffusion potential on temperature for B-10 and B-12. Dark conditions.

4.2 NONUNIFORMITY OF THE GRAIN BOUNDARY DIFFUSION POTENTIAL

So far we have assumed the grain boundary potential barrier to arise from a macroscopically uniform distribution of charge trapped in the interface states. There are however at least two reasons to suspect that most of our samples will have nonuniform potential barriers.

The material used for our experiments, Wacker "Silso" polycrystalline silicon, is cast in blocks with the boron doping incorporated in the melt. Upon cooling the boron atoms may cluster and be forced to the grain boundaries during recrystallization [22]. The impurity doping concentration could be considerably enhanced in the vicinity of the grain boundary resulting in a local reduction of the potential barrier.

The second possible source of the potential barrier nonuniformity is a consequence of the origin of the interface states. We have assumed that these states arise from the lattice mismatch between adjacent crystals. Figure 4.2 is a Thomson penny model (TPM) of the crystal lattices at the grain boundary. It is apparent that different mismatch angles will result in different bond energies across the boundary. A variation of the mismatch angle could alter the energies and densities of the interface states. This would lead to a localized variation of the grain boundary charge which would produce a nonuniform potential barrier.

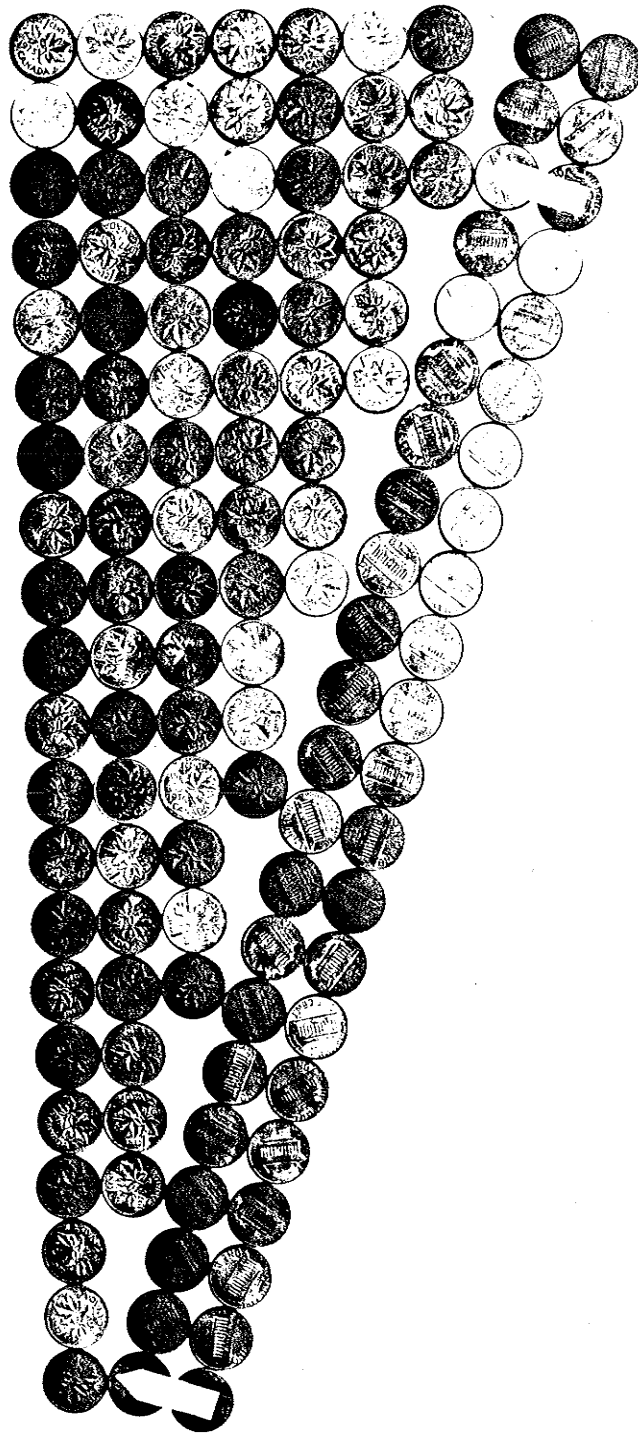


Figure 4.2: Thomson penny model of grain boundary for an orientational mismatch of approx. 20° showing the periodic nature of a particular defect structure. A variety of bonding disorder is suggested over one period.

We further suggest that the bonding defects at the grain boundary could be periodic in nature. Generally, large mismatch angles would produce bonding defects with periods of a few atomic spacings while low mismatch angles will generate longer periods. It is interesting to note that, by virtue of the periodic nature of the defect structure, a two-dimensional band conduction should be possible in the grain boundary plane.

Thomson [23] has hypothesized that the irregularities of the B-10 activation energies at low temperatures are a result of nonuniformities of the diffusion potential over the plane of the grain boundary. After assuming a truncated gaussian distribution of boundary potentials this approach produced qualitative agreement with the observed behavior of B-10. Quantitative agreement was not good, possibly because a gaussian distribution is unphysical for this problem. Also, many simplifications such as the neglect of spreading resistance (which could be significant, especially at low temperatures) were in effect. A Monte Carlo simulation of the grain boundary potentials may lead to a more favorable result. Experimental determination of the grain boundary potential distribution, possibly by scanning light spot techniques [24], would greatly enhance the usefulness of these numerical simulations.

The reduction of the potential barrier under illuminated conditions as described previously in sec. 2.3 has been ex-

perimentally verified (by Thomson in [14]). Low voltage activation energy measurements over a range of illumination intensities were used to construct the relation between the potential barrier and the intensity shown in Fig. 4.3 .

We wish to point out that sample B-12, which is thought to have a uniform potential barrier, conforms well to the predicted barrier reduction of 0.07 eV per decade of illumination. On the other hand, B-10 shows a significantly greater reaction to illumination. This again may be attributed to the nonuniform nature of its potential barrier.

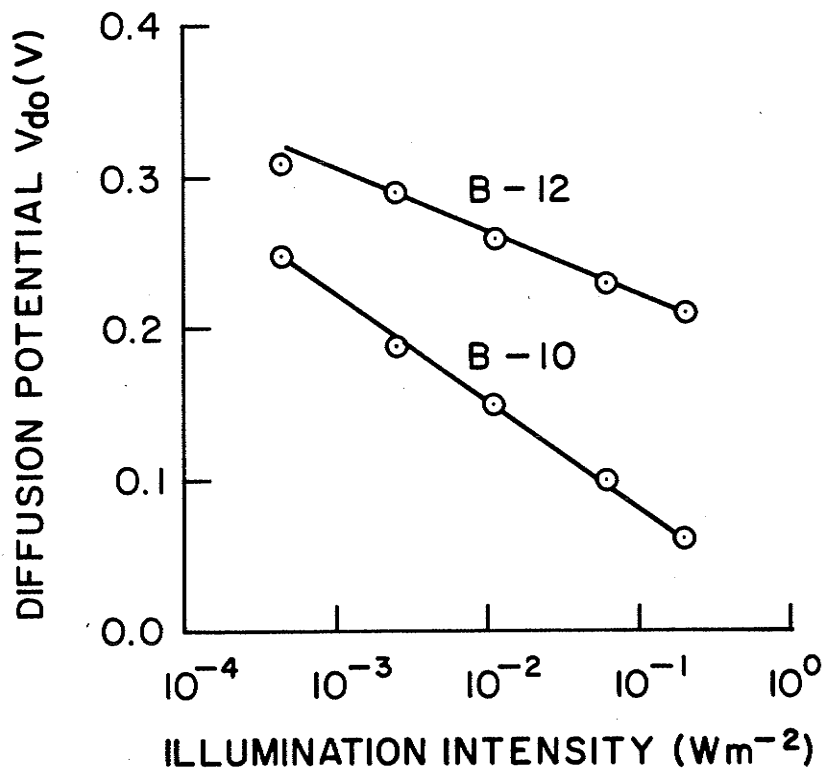
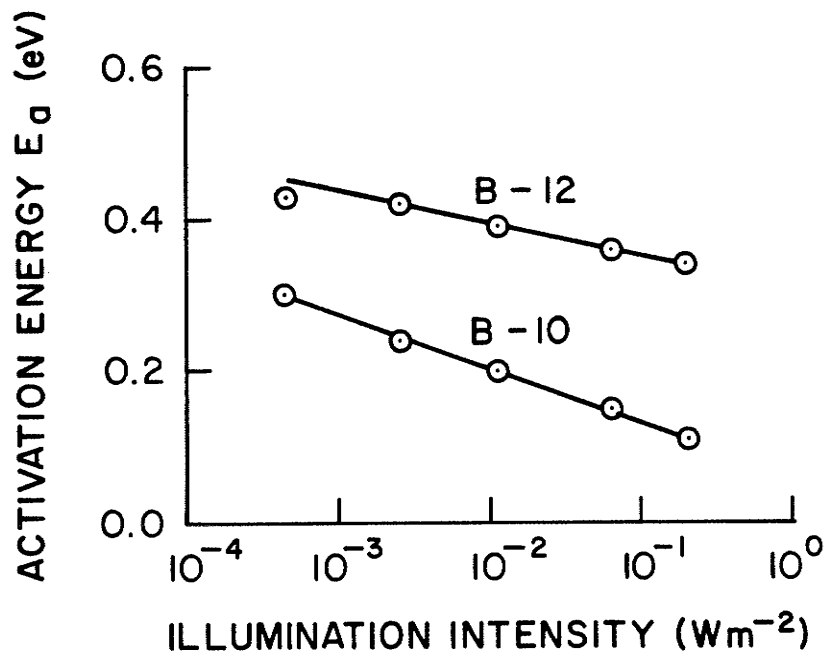


Figure 4.3: The dependence of (a) the activation energy and (b) the diffusion potential on illumination intensity for B-10 and B-12. $T=300$ K.

Chapter V

CONCLUSIONS

The majority-carrier current across silicon grain boundary potential barriers is controlled by an emission/diffusion transport mechanism. The diffusion velocity of majority carriers to the grain boundary is the current limiting factor.

The interface states at the grain boundary are found to play an important role in determining the electronic properties of polycrystalline silicon. Indeed, it is this fact that allows us to deconvolve the density of these states from current-voltage measurements of isolated grain boundaries. Interface-state densities of approximately 10^{12} $\text{eV}^{-1} \text{cm}^{-2}$ were measured. Under optical illumination, minority carriers interact with the interface states in such a way as to decrease the potential barrier to majority carriers.

Grain boundaries with a variety of diffusion potentials exist in Wacker 'Silso' polycrystalline silicon. Activation energy measurements have shown irregularities that were attributed to the nonuniformity of the diffusion potential over the plane of the grain boundary. The special case of a spatially uniform boundary has also been observed.

A microcomputer has proven useful for automating the current-voltage measurements and deconvolving the interface-state densities of grain boundary samples.

The many applications of polycrystalline semiconductors necessitates a complete understanding of their electrical and electrooptical properties. The large number of processes involved will make this a challenging research endeavor for years to come.

REFERENCES

1. H.Yamanaka, T. Wada, O. Kudoh, and M. Sakamoto, "Polysilicon interconnection technology for IC devices," J. Electrochem. Soc., 126, pp. 1415-1418, (1979).
2. C.M. Wu, E.S. Yang, W. Hwang, and H.C. Card, "Grain boundary effects on the electrical behavior of Al-poly-Si Schottky barrier solar cells," IEEE Trans. Electron Dev., ED-27, pp.687-692, (1980).
3. M.M. Mandurah, K.C. Saraswat, and T.I. Kamins, "A Model for Conduction in Polycrystalline Silicon - Part I:Theory," IEEE Trans. Electron Dev., ED-28, pp. 1163-1171, (1981).
4. L.L. Kazmerski, Polycrystalline and Amorphous Thin Films and Devices, New York: Academic Press, 1980. chap. 3.
5. O.L. Krivanek, S. Isoda, and K. Kobayashi, "Lattice imaging of a grain boundary in crystalline germanium," Phil. Mag., 36, pp. 931-940, (1977).
6. B. Cunningham and D.G. Ast, "High Resolution Electron Microscopy," in Grain Boundaries in Semiconductors, ed. C. Seager, New York: North-Holland, pp. 21-26, (1982).
7. W. Shockley and W.T. Read, "Statistics of the Recombination of Holes and Electrons," Phys. Rev., 87, pp. 835-842, (1952).
8. S.M. Sze, Physics of Semiconductor Devices, 2nd ed., New York: Wiley-Interscience, 1981.
9. J.Y.W. Seto, "The electrical properties of polycrystalline silicon films", J. Appl. Phys., 46, pp. 5247-5254, (1975).
10. J. Martinez, and J. Piqueras, "On the Mobility of Polycrystalline Semiconductors", Solid State Electron., 23, pp. 297-303, (1980).
11. C.H. Seager and T.G. Castner, "Zero-bias resistance of grain boundaries in neutron-transmutation-doped polycrystalline silicon", J. Appl. Phys., 49, pp. 3879-3889, (1978).

12. C.H. Seager and G.E. Pike, "Grain boundary states and varistor behavior in silicon bicrystals", Appl. Phys. Lett., 35, pp. 709-711, (1979).
13. E.H. Rhoderick, Metal-Semiconductor Contacts, Oxford: Oxford Press, 1978.
14. G.C. McGonigal, D.J. Thomson, J.G. Shaw, and H.C. Card, "Electronic Transport at Grain Boundaries in Silicon," Phys. Rev. B, to be published.
15. W.E. Taylor, N.H. Odell, and H.Y. Fan, "Grain Boundary Barriers in Germanium," Phys. Rev., 88, pp. 867-875, (1952).
16. P. Panayotatos and H.C. Card, "Recombination Velocity at Grain Boundaries in Polycrystalline Si under Optical Illumination," IEEE Electron Dev. Lett., EDL-1, pp. 263-266, (1980).
17. L.L. Kazmerski, "The Effects of Grain Boundary and Interface Recombination on the Performance of Thin-film Solar Cells," Solid St. Electron., 21, pp. 1545-1550, (1978).
18. C.H. Seager, "The Electronic Properties of Semiconductor Grain Boundaries," in ref. 6, pp. 85-98.
19. D.J. Thomson, S.R. Mejia, and H.C. Card, "The Influence of Surface Preparation on Rectification in Aluminum-Polycrystalline Silicon Solar Cells," J. Power Sources, 7, pp. 191-194, (1982).
20. K.G. McKay, "Avalanche Breakdown in Silicon," Phys. Rev., 94, pp. 877-884, (1954).
21. J. Frenkel, "On pre-breakdown phenomena in insulator and electronic semiconductors," Phys. Rev., 54, pp. 647-648, (1938).
22. L.L. Kazmerski, P.J. Ireland, and T.F. Ciszek, "Evidence for the segregation of impurities to grain boundaries in multigrained silicon using Auger electron spectroscopy and secondary ion mass spectroscopy," Appl. Phys. Lett., 36, pp. 323-325, (1980).
23. D.J. Thomson and H.C. Card, "Effects of Interface-Potential Nonuniformities on Carrier Transport across Silicon Grain Boundaries," J. Appl. Phys., in press.
24. J. Martinez, A. Criado, and J. Piqueras, "Grain boundary potential determination in polycrystalline silicon by the scanning light spot technique," J. Appl. Phys., 52, pp. 1301-1305, (1981).

Appendix A

PHOTO GB

```

//PHOTOGB JOB ',,,,,,T=10,L=2,C=0',MCGON
// EXEC PASCCG,PARM.PASC='NOXREF,NOPXREF,NOWARNING'
//SYSIN DD *
PROGRAM PHOTO_GB(INPUT,OUTPUT); (* IBM PASCAL/VIS REL. 2 *)
(***** PHOTO_GB *****)
(*
(*          WRITTEN BY G.C. MCGONIGAL
(*
(*          MATERIALS & DEVICES RESEARCH LAB
(*          DEPT. OF ELECTRICAL ENGINEERING
(*          UNIVERSITY OF MANITOBA
(*          1981.
(*
(*****
(*
(*PHOTO_GB CALCULATES THE POTENTIAL BARRIER AT A ONE-DIMENSIONAL*
(*GRAIN BOUNDARY AS A FUNCTION OF A UNIFORM PHOTOGENERATION RATE*
(*THE CORRESP. IMREF SEP. AND CAPACITANCE IS ALSO GIVEN.
(*
(*ALL UNITS ARE CGS
(*
(*INPUT PARAMETERS ARE:
(*  TEMPERATURE (K)
(*  BULK IMPURITY DOPING CONCENTRATION
(*  MINORITY CARRIER DIFFUSION LENGTH (BULK)
(*  ACCEPTOR INTERFACE ST. DENSITY, DONOR INT. ST. DENS.
(*  NEUTRAL CAPTURE X-SECTION, COULOMBIC CAP. X-SECTION
(*
(*****
VAR DELTA_E,DELTA_E_STAR,V_T,V_D,V_D_STAR,V_TH,N_V,N_C,N_D,G_PH,
    PHI_N,PHI_P,PHI_N_GB,PHI_P_GB,F_A,F_D,T,P_O,N_O,N_IS,L_P,Q,M_E,
    CAPACITANCE,
    N_IS_A,N_IS_D,SIG_N,SIG_C,EPSILON_S,P_O_STAR,G_PRINT,INC:REAL;
(*)

(*)
BEGIN
READLN(T);          WRITELN( ' TEMPERATURE = ',T:6:1, ' K');
READLN(N_D);        WRITELN( ' ND = ',N_D:10, ' PER CM CUBED');
READLN(L_P);        WRITELN( ' MIN. CAR. DIFF. L. = ',L_P:10);
READLN(N_IS_A,N_IS_D);
READLN(SIG_N,SIG_C);
WRITE( ' N-IS_A = ',N_IS_A:10);
WRITELN( ' N_IS_D = ',N_IS_D:10, ' PER CM SQUARED');

```

```

WRITE( ' NEUTRAL CAP. X-SECTION = ',SIG_N:10);
WRITELN( ' COULOMB CAP. X-SECTION = ',SIG_C:10,' CM SQUARED');
WRITELN;WRITELN;
WRITELN( ' G_PH,V_D,DELTA_E,P_O,N_O,F_A,F_D,PHI_P,PHI_N,CAP');
WRITELN;
(*)
.... CALCULATE CONSTANTS ....
*)
Q := 1.6E-19; (* ELECTRONIC CHARGE *)
M_E := 9.1E-31; (* ELECTRONIC MASS *)
V_T := 8.67E-5 * T; (* K*T/Q *)
V_TH := SQRT(3.0*V_T*Q/M_E)*100.0; (* THERMAL VELOC. *)
N_V := 2.0E15 * SQRT(T * T * T); (* # OF VAL. STS. *)
N_C := 5.389E15 * SQRT( T*T*T ); (* # OF COND. STS.*)
PHI_N := LN(N_C/N_D) * V_T; (* BULK MAJ C.FER LVL *)
N_IS := N_IS_A + N_IS_D; (* TOTAL INTERF. STS. *)
EPSILON_S := 11.8*8.854E-14; (* DIEL. CONSTANT *)
(*)
.... DEFINE INITIAL CONDITIONS FOR ITERATIONS ....
*)
DELTA_E := 0.00; (* SEP. OF FERMI LVLS *)
V_D := 0.30; (* DIFFUSION POTENTIAL*)
V_D_STAR := V_D;
G_PH := 0.0; (* PHOTO-GENERATION *)
(*)
.... REPEAT CALC. FOR VALUES OF G_PH ....
*)
WHILE G_PH < 1.0E20 DO
  BEGIN
    (*)
    .... BEGIN MAJOR ITERATION FOR V_D ....
    *)
    REPEAT
      V_D := V_D+(V_D_STAR-V_D)*1.0E-2;
      PHI_N_GB := PHI_N + V_D; (* GB MAJ. CAR. FER. LVL *)
      N_O := N_C*EXP(-PHI_N_GB/V_T); (* GB MAJ. CAR. CONCENTR.*)
    (*)
    .... BEGIN MINOR ITERATION FOR P_O & DELTA_E ....
    *)
    REPEAT
      PHI_P_GB := 1.12-PHI_N_GB-DELTA_E;(*GB MIN. CAR. F. LVL.*)
      P_O := N_V*EXP(-PHI_P_GB/V_T); (* GB MIN. CAR. CONCENTR.*)
      DELTA_E_STAR := 2.0*G_PH*L_P/SIG_N/V_TH/N_IS/P_O;
      DELTA_E := DELTA_E-(DELTA_E-DELTA_E_STAR)*0.001;
      UNTIL ABS(DELTA_E-DELTA_E_STAR) <= 0.0001;
      F_A := SIG_N*N_O/(SIG_N*N_O+SIG_C*P_O);(* ACCEPTOR OCCUP.*)
      F_D := SIG_C*N_O/(SIG_C*N_O+SIG_N*P_O);(* DONOR OCCUPATION*)
      V_D_STAR := SQR(Q*(-PHI_N_GB*N_IS_D+PHI_P_GB*N_IS_A
        -DELTA_E*(1.0-F_D)*N_IS_D-F_A
        *N_IS_A)))/(8.0*Q*N_D*EPSILON_S);
      UNTIL ABS(V_D_STAR-V_D) <= 0.0100;
      CAPACITANCE := SQRT(Q*EPSILON_S*N_D/8.0/V_D);
      WRITELN(G_PH:10,V_D:11:4,DELTA_E:11:4,P_O:11,N_O:11,F_A:11:4,
        F_D:11:4,PHI_P_GB:11:4,PHI_N_GB:11:4,CAPACITANCE:11);
  END

```

```

(* ARBITRAR. INCREMENT G PH *)
G PH := G PH*26.0/(LN(G PH+1.0)/2.3+5.0)+1.0E13;
END;(*WHILE*)
END.
/** SAMPLE INPUT PARMS....
//GO.INPUT DD *
300.0          TEMP
1.0E15        DOPING
30.0E-4       DIFF LENGTH
7.0E12 7.0E12 N IS A N IS D
1.0E-16 1.0E-14 SIGMA_N SIGMA_C
/**

```

Appendix B

GB

```
(**S+*)
PROGRAM GB;

(*)
  ANALOG INPUTS:
    0-
    1-
    2-
    3-
    4- TEMP:FROM KEITHLEY(G=100) FROM FLUKE TEMPERATURE METER.
    5-
    6- CURRENT:VOLTAGE FROM I/V
    7-

  ANALOG OUTPUTS:
    X-
    Y-
    W-
    Z- SAMPLE BIAS

*)
USES TRANSCEND, ECIDAS, APPLESTUFF, TURTLEGRAPHICS;

TYPE MATRIX=ARRAY[1..10] OF ARRAY[1..10] OF REAL;

VAR ITV: MATRIX;
    MODECHAR, INCHAR: CHAR;
    TEMPCO, J, I: INTEGER;
    V, VTEMP, TEMP: ARRAY[1..10] OF REAL;
    TOTAL: REAL;
    PLOT: BOOLEAN;
    T07470, IVDATA, T: TEXT;

PROCEDURE LOGGRID(XDECNUM, XMINMAG, YDECNUM, YMINMAG: INTEGER);
  (* GENERATES A LOG-LOG GRID *)
  (* DECNUM=NO. OF DECADES
  MINMAG=SMALLEST DECADE TO BE DISP *)
  VAR I, XMAXMAG, YMAXMAG: INTEGER;
      ISTR: STRING[3];
  BEGIN
    XMAXMAG:=XMINMAG+XDECNUM;
    YMAXMAG:=YMINMAG+YDECNUM;
    REWRITE(T07470, '#8:');
    WRITE(T07470, ' IN; SC ', XMAXMAG, ', ', XMINMAG, ', ', YMINMAG, ', ', YMAXMAG, ';');
    WRITE(T07470, 'SP1;'); (* LEFT PEN *)
    WRITE(T07470, 'DIO.0,1.0;');
    FOR I:=XMINMAG TO XMAXMAG DO
```

```

BEGIN
WRITE (TO7470, 'PU', I, ', ', YMAXMAG, ', ');
WRITE (TO7470, 'PD', I, ', ', YMINMAG, ', ');
STR(I, ISTR);
WRITE (TO7470, 'PU;DT', CHR(3), ', ;LB', CHR(8), CHR(8), CHR(3), 'PU;LB', ISTR, CHR(3));
END;
FOR I:=YMINMAG TO YMAXMAG DO
BEGIN
WRITE (TO7470, 'PU', XMAXMAG, ', ', I, ', ');
WRITE (TO7470, 'PD', XMINMAG, ', ', I, ', ');
STR(I, ISTR);
WRITE (TO7470, 'PU;DIO.2,1.0;LB', CHR(11), CHR(3), 'DIO.0,1.0;LB', ISTR, CHR(3));
END;
WRITE (TO7470, 'SPO;'); (* STORE PEN *)
WRITE (TO7470, 'DI;');
END;

```

```

PROCEDURE LOGPLOT (X, Y: REAL; XDECNUM, XMINMAG, YDECNUM, YMINMAG: INTEGER;
CONPTS: BOOLEAN; CHARMARKER: CHAR);
(* PLOTS POINTS ON THE LOG PLOT *)
(* DECNUM, MINMAG SAME AS FOR LOGGRID
X, Y=CO-ORDS. OF POINT TO BE PLOTTED
CONPTS=TRUE DRAWS A LINE TO NEXT PT.
CHARMARKER=CHAR TO BE PRINTED *)
BEGIN
WRITE (TO7470, 'SP2;SM', CHARMARKER, ', ');
IF CONPTS=TRUE THEN
WRITE (TO7470, 'PD;') (*PEN DOWN*)
ELSE
WRITE (TO7470, 'PU;') (*PEN UP*)
WRITE (TO7470, 'PA', LOG(X):5:3, ', ', LOG(Y):5:3, ', SM;');
END;

```

```

PROCEDURE LAYOUT;
(* DRAWS ELECTRICAL CONNECTIONS *)
VAR C: CHAR;
BEGIN
INITTURTLE;
PENCOLOR (NONE);
MOVETO (15, 180);
WSTRING ('ECI INSTRUMENT CONNECTIONS FOR GB');
MOVETO (40, 0);
PENCOLOR (WHITE);
MOVETO (40, 200);
MOVETO (40, 160);
MOVETO (190, 160);
MOVETO (190, 100);
MOVETO (40, 100);
MOVETO (40, 75);
MOVETO (60, 75);
MOVETO (60, 55);
MOVETO (40, 55);
MOVETO (40, 30);
MOVETO (220, 30);

VIEWPORT (160, 220, 110, 150);
FILLSCREEN (WHITE);

VIEWPORT (80, 140, 10, 50);
FILLSCREEN (WHITE);

VIEWPORT (180, 240, 10, 50);
FILLSCREEN (WHITE);

```



```

BEGIN
TOTAL:=0.0;
FOR I:=1 TO 100 DO
  BEGIN
  SAMPLE(6,IVOLTS);
  TOTAL:=TOTAL+IVOLTS;
  END;
  IVOLTS:=TOTAL/100.0;
  IVALUE:=-IVOLTS/PWROFTEN(RANGE+1);
  END;
ITV[TEMPCO,J]:=IVALUE;(*SAVE I*)
WRITE(' ');
WRITELN(V[J]:5:3,' ',IVALUE);
END;
ANALOGOUT(0.0,Z);(*ZERO OUTPUT*)
END;

```

```

PROCEDURE CASED;
(* USES THE TEMPERATURES PREVIOUSLY
  ENTERED IN THE TEMP.TEXT FILE
  AS MEASUREMENT TEMPS. *)
VAR TVOLTS:REAL;
BEGIN
RESET(T,'TEMP.TEXT');
FOR I:=1 TO 10 DO READLN(T,TEMP[I],VTEMP[I]);
WRITELN;
FOR I:=1 TO 10 DO WRITELN(' T(I:2,')= ',TEMP[I]:3:1,'K');
WRITELN('HIT <RET> TO INITIATE EXPERIMENT');
REPEAT UNTIL KEYPRESS;
READ(KEYBOARD,INCHAR);
WRITELN('NEXT T=',TEMP[I]:5:1);
TEMPCO:=1;
WHILE TEMPCO < 11 DO (*FOR 10 TEMPS*)
  BEGIN
  REPEAT (*WAIT UNTIL SPECIFIED TEMP*)
    TOTAL:=0.0;
    FOR I:=1 TO 10 DO (*AVE. 10 SAMPLES*)
      BEGIN
      SAMPLE(4,TVOLTS);
      TOTAL:=TOTAL+TVOLTS;
      END;
    TVOLTS:=TOTAL/10.0;
  UNTIL TVOLTS > VTEMP[TEMPCO];
  COLLECT;(*SWEEP THROUGH VOLTAGE STEPS*)
  TEMPCO:=TEMPCO+1;(*NEXT TEMP*)
  WRITELN;
  WRITELN('***** EXPERIMENT IN PROGRESS *****');
  FOR I:=1 TO 5 DO WRITELN;
  FOR I:=1 TO 14 DO WRITE(' ');
  IF TEMPCO<11 THEN WRITE('NEXT T=',TEMP[TEMPCO]:5:1);
  FOR I:=1 TO 27 DO WRITE(' ');
  END;
END;

```

```

PROCEDURE CASEN;
(* USED FOR CALIBRATING A NEW SET OF TEMPERATURE POINTS.
  TEN TEMPS MUST BE ENTERED.
  MAIN FCN IS TO ASSOCIATE A VOLTAGE FROM
  THE TEMP-METER WITH THE MEASURED TEMP..
  THE VOLTAGE-TEMP PAIRS (10) ARE ENTERED IN TEMP.TEXT *)
VAR TVOLTS:REAL;
BEGIN
WRITELN(CHR(12));
WRITELN('MANUAL TEMP INPUT MODE...');
WRITELN;

```

```

WRITELN('ENTER TEMP (K) TO INITIATE SAMPLING');
WRITELN('ENTER 0 TO EXIT. # OF T-PTS IS 10.');
```

```

WRITELN;
TEMPCO:=1;
WHILE TEMPCO<11 DO
  BEGIN
    WRITE('T(',TEMPCO:2,')=');
    READLN(TEMP[TEMPCO]);
    TOTAL:=0.0;
    FOR I:=1 TO 10 DO (* AVE SIGNAL FROM TEMP-METER*)
      BEGIN
        SAMPLE(4,TVOLTS);
        TOTAL:=TOTAL+TVOLTS;
      END;
    VTEMP[TEMPCO]:=TOTAL/10.0;
    COLLECT;(*SWEEP VOLTAGE STEPS*)
    IF TEMP[TEMPCO]=0.0 THEN TEMPCO:=11;
    WRITELN;
    WRITELN('***** EXPERIMENT IN PROGRESS *****');
    TEMPCO:=TEMPCO+1;(* NEXT TEMP *)
  END;
IF TEMPCO=11 THEN WRITELN('LAST TEMP PT.');
```

```

REWRITE(T,'TEMP.TEXT');
```

```

FOR I:=1 TO 10 DO WRITELN(T,TEMP[I]:5:1,VTEMP[I]:6);
CLOSE(T,LOCK);(*SAVE TEMPS*)
END;
```

```

PROCEDURE WRITEDATA;
(* GENERATES A TABLE OF CURRENTS FROM THE ITV MATRIX*)
VAR YMINMAG,YDECNUM:INTEGER;
    CONPTS:BOOLEAN;
BEGIN
  IF (MODECHAR='O') OR (MODECHAR='N') THEN
    BEGIN
      REWRITE(IVDATA,'ITV.TEXT');
```

```

      FOR TEMPCO:=1 TO 10 DO
        FOR J:=1 TO 10 DO
          WRITELN(IVDATA,ITV[TEMPCO,J]);
        CLOSE(IVDATA,LOCK);
      END;
  IF MODECHAR='P' THEN
    BEGIN
      RESET(T,'TEMP.TEXT');
```

```

      FOR I:=1 TO 10 DO READLN(T,TEMP[I],VTEMP[I]);
    END;
  RESET(IVDATA,'ITV.TEXT');
```

```

  FOR TEMPCO:=1 TO 10 DO
    FOR J:=1 TO 10 DO
      READLN(IVDATA,ITV[TEMPCO,J]);
    WRITELN;
    WRITE(' ');
    FOR TEMPCO:=1 TO 5 DO
      BEGIN
        WRITE(TEMP[TEMPCO]:5:1);
        WRITE(' ');
      END;WRITELN;
    FOR J:=1 TO 10 DO
      BEGIN
        WRITE(V[J]:5:2,' ');
        FOR TEMPCO:=1 TO 5 DO WRITE(ITV[TEMPCO,J]:13);
        WRITE(' ',V[J]:5:2);
        WRITELN;
      END;
    WRITE(' ');
    FOR TEMPCO:=6 TO 10 DO
      BEGIN
```

```

WRITE(TEMP[TEMPCO]:5:1);
WRITE(' ');
END;WRITELN;
FOR J:=1 TO 10 DO
BEGIN
WRITE(V[J]:5:2,' ');
FOR TEMPCO:=6 TO 10 DO WRITE(ITV[TEMPCO,J]:13);
WRITE(' ',V[J]:5:2);
WRITELN;
END;
IF PLOT THEN(* GEN LOGI-LOGV PLOT ON 7470 FROM ITV*)
BEGIN
YMINMAG:=TRUNC(LOG(ITV[10,1]))-1;
YDECNUM:=TRUNC(LOG(ITV[1,10]))-YMINMAG;
LOGGRID(YDECNUM,YMINMAG,2,-2);
WRITE(T07470,'D10.0,I10.0,S10.11,0.17;');
FOR TEMPCO:=1 TO 10 DO
BEGIN
CONPTS:=FALSE;
FOR J:=1 TO 10 DO
BEGIN
LOGPLOT(ITV[TEMPCO,J],V[J],YDECNUM,YMINMAG,2,-2,CONPTS,CHR(111));
CONPTS:=TRUE;
END;
WRITE(T07470,'PU;LB',ROUND(TEMP[TEMPCO]:4,CHR(3)));
END;
WRITE(T07470,'SFO;');
END;
END;

BEGIN (*MAIN*)
V[1]:=0.02; (* SPECIFY VOLTAGE STEPS *)
V[2]:=0.03;
V[3]:=0.05;
V[4]:=0.07;
V[5]:=0.10;
V[6]:=0.15;
V[7]:=0.20;
V[8]:=0.30;
V[9]:=0.40;
V[10]:=0.50;
WRITE('NEW OR OLD TEMP PTS OR PRESENT DATA? * ');
(* N=CALIB OF NEW TEMP PTS
D=PREVIOUSLY CALIB TEMPS FOUND IN TEMP.TEXT
P=WRITE DATA PRESENTLY IN ITV.TEXT *)
REPEAT UNTIL KEYPRESS;
READ(MODECHAR);WRITELN;
WRITE('PLOT? (Y/N) * '); (*LOGI-LOGV ON 7470A*)
REPEAT UNTIL KEYPRESS;
READ(INCHAR);
IF INCHAR='Y' THEN PLOT:=TRUE ELSE PLOT:=FALSE;
IF (MODECHAR='N') OR (MODECHAR='D') THEN LAYOUT;
CASE MODECHAR OF
'D':CASED;
'N':CASEN;
END;
WRITEDATA;
END.

```

Appendix C

AUTODECON

```
(**S**)  
PROGRAM AUTODECON;  
  
(***** APPLE AUTODECON I.0 *****)  
  
(* BY G.C.MCGONIGAL/1982  
MATERIALS & DEVICES RESEARCH LAB  
DEPT. OF ELECTRICAL ENGINEERING  
UNIVERSITY OF MANITOBA.  
  
FUNCTION:  
DECONVOLVES THE INTERFACE-STATE DENSITY FROM  
I-V CHARACTERISTICS OF GB SAMPLES MEASURED  
BY THE PROGRAM 'GB'.  
  
DATA:  
1) FILE 'TEMP.TEXT' MUST BE PRESENT ON #4.  
2) EITHER 'ITV.TEXT' SHOULD BE PRESENT ON #4  
   OR  
   A TEXT FILE ON #5 MAY BE USED AS DATA.  
  
OUTPUT: ROUTED TO THE 7470A PLOTTER.  
*)  
  
USES TRANSCEND,APPLESTUFF,TURTLEGRAPHICS,PLOTAIDS,PLOTTERGRAPHICS,FENPLOTAIDS;  
  
CONST EPSILON0=8.854E-14;  
      EPSILONR=11.7;  
      Q=1.6E-19;  
      ND=3.0E15;  
      AREA=3.0E-3;  
  
VAR T,NC,QGBA,QGB1,MU,VT,EPSILONS,  
    VDF,VDR,QGB,I,DELTAQ,DELTAEF,EF,EF1,NIS,  
    XBOT,YBOT,XDIV,YDIV,  
    PHIN,V,J,JOE:REAL;  
    FILENAME,TLABEL,SAMPLENAME:STRING[20];  
    TDECON:ARRAY[1..10] OF BOOLEAN;  
    CONPTS:BOOLEAN;  
    TVAL,VAFP:ARRAY[1..10] OF REAL;  
    INCHAR:CHAR;  
    STEPMAX,VCO,TEMPCO,II:INTEGER;  
    TVALUES,IVDATA:TEXT;  
    ITV:ARRAY[1..10] OF REAL;  
    SYM:POINTMARKER;
```

```

PROCEDURE VOLTAGEDIV;
(* FORW & REV. DIFFUSION POTS *)
BEGIN
VDF:=EPSILONS/2.0/Q/ND*SQR(-V*Q*ND/QGB+QGB/2.0/EPSILONS);
VDR:=EPSILONS/2.0/Q/ND*SQR(QGB/2.0/EPSILONS+V*Q*ND/QGB);
END;

```

```

PROCEDURE SATCUR;
(* SATURATION CURRENT *)
BEGIN
JOE:=J/(1.0-EXP(-V/VT));
END;

```

```

PROCEDURE BARRIER;
(* BARRIER HEIGHT *)
VAR E1:REAL;
BEGIN
E1:=SQRT(2.0*Q*ND*VDF/EPSILONS);
VDF:=-VT*LN(2.0*JOE/(Q*ND*MU*E1));
END;

```

```

PROCEDURE CHARGE;
(* GRAIN BOUNDARY CHARGE *)
VAR E1,E2:REAL;
BEGIN
E1:=SQRT(2.0*Q*ND*VDF/EPSILONS);
E2:=-SQRT(2.0*Q*ND*VDR/EPSILONS);
QGB:=EPSILONS*(E1-E2);
END;

```

```

PROCEDURE WRITEHEADER;
BEGIN
VAPP[1]:=0.02;
VAPP[2]:=0.03;
VAPP[3]:=0.05;
VAPP[4]:=0.07;
VAPP[5]:=0.10;
VAPP[6]:=0.15;
VAPP[7]:=0.20;
VAPP[8]:=0.30;
VAPP[9]:=0.40;
VAPP[10]:=0.50;

WRITELN(CHR(12));
WRITELN;
WRITELN('          MDRL AUTODECON I.0  OCT/82');
WRITELN;
WRITELN('DATAFILE NAME ( ' '* ' ' FOR PRESENT)');
READLN(FILENAME);
IF POS('* ',FILENAME)=1 THEN
  (* FIRST CHAR='*' USE PRESENT ITV *)
  BEGIN
  FILENAME:=' ITV.TEXT';
  WRITE('SAMPLE ');
  READLN(SAMPLENAME);
  END
ELSE
  (* USE FILE FROM #5 FOR ITV *)
  BEGIN
  SAMPLENAME:=FILENAME;
  FILENAME:=CONCAT('#5:',FILENAME, '.TEXT');
  END;
WRITELN;

```

```

FOR II:=1 TO 10 DO
  BEGIN
  WRITE('          DECON T(',II:2,')=',TVAL[III]:4:1,'? (Y/N) ');
  REPEAT UNTIL KEYPRESS;
  READ(INCHAR);
  IF INCHAR='Y' THEN
    TDECON[III]=TRUE
  ELSE
    TDECON[III]=FALSE;
  WRITELN;
  END;
WRITELN('MAX VSTEPS=? ');(* # OF VOLTAGE STEPS TO BE DECONED*)
READLN(STEPMAX);
WRITELN(CHR(12));
WRITELN('DECON FOR: ');
FOR II:=1 TO 10 DO
  IF TDECON[III]=TRUE THEN WRITELN('          ',TVAL[III]:4:1);
HDRAWGRID(0.5,0.40,14.5,10.0,XBOT,YBOT,XDIV,YDIV,FALSE);
HAXISLABEL('          EGAP','LOG NIS');
HMOVETO(30.0,178.0);
HWSTRING(SAMPLENAME);
END;

PROCEDURE WRITEDATA;
(* GEN CURRENT TABLE FROM ITV *)
BEGIN
WRITELN;
WRITE('          ');
FOR TEMPCO:=1 TO 5 DO
  BEGIN
  WRITE(TVAL[TEMPCO]:5:1);
  WRITE('          ');
  END;WRITELN;
FOR II:=1 TO 10 DO
  BEGIN
  WRITE(VAPP[III]:5:2,' ');
  FOR TEMPCO:=1 TO 5 DO WRITE(ITV[TEMPCO,II]:13);
  WRITE(' ',VAPP[III]:5:2);
  WRITELN;
  END;
WRITE('          ');
FOR TEMPCO:=6 TO 10 DO
  BEGIN
  WRITE(TVAL[TEMPCO]:5:1);
  WRITE('          ');
  END;WRITELN;
FOR II:=1 TO 10 DO
  BEGIN
  WRITE(VAPP[III]:5:2,' ');
  FOR TEMPCO:=6 TO 10 DO WRITE(ITV[TEMPCO,II]:13);
  WRITE(' ',VAPP[III]:5:2);
  WRITELN;
  END;
END;

FUNCTION MUP(T:REAL):REAL;
(* HOLE MOBILITY(TEMP) -LOW FIELD *)
(* C.F. ARORA ET. AL. *)
VAR MU1,MU2,TN:REAL;
BEGIN
TN:=T/300.0;
MU1:=1.36E8*EXP(-2.23*LN(T));
MU2:=ND/2.35E17/EXP(2.4*LN(TN))*0.88*EXP(-0.146*LN(TN));
MUP:=54.3*EXP(-0.57*LN(TN))+MU1/(1.0+MU2);
END;

```

```

PROCEDURE GBFERMI;
(* GRAIN BOUNDARY FERMI-LEVEL *)
VAR NO,E1,E2:REAL;
BEGIN
E2:=-V*Q*ND/QGB-QGB/2.0/EPSILONS;
E1:=-V*Q*ND/QGB+QGB/2.0/EPSILONS;
NO:=ND/(E2-E1)*(E2*EXP(-VDR/VT)-E1*EXP(-VDF/VT));
EF:=-VT*LN(NO/NC);
END;

(* END SUBROUTINES *)

(* MAIN BEGINS HERE *)

BEGIN

RESET(TVALUES,'TEMP.TEXT');

FOR TEMPCO:=1 TO 10 DO
  READLN(TVALUES,TVAL[TEMPCO]);

WRITEHEADER;

RESET(IVDATA,FILENAME);

FOR TEMPCO:=1 TO 10 DO
  FOR VCO:=1 TO 10 DO
    READ(IVDATA,ITV[TEMPCO,VCO]);

WRITEDATA;

EPSILONS:=EPSILONR*EPSILOND;
TEMPCO:=1;
WHILE TEMPCO <= 10 DO
  BEGIN
  WRITE('TEMPCO=');
  IF TDECON[TEMPCO] THEN
    BEGIN
    WRITELN(TEMPCO);
    DELTAQ:=0.0;
    QGB1:=0.0;
    QGB:=0.0;
    CONPTS:=FALSE;

    I:=ITV[TEMPCO,1];
    V:=VAPP[1];
    T:=TVAL[TEMPCO];

    MU:=MUF(T);
    NC:=1.925E15*SQRT(T*T*T);
    VT:=8.67E-5*T;
    PHIN:=LN(NC/ND)*VT;
    J:=I/AREA;
    VDF:=0.1;
    VDR:=0.1;
    SATCUR;
    BARRIER;
    CHARGE;
    FOR VCO:=1 TO STEPMAX DO (* EACH VOLTAGE PT *)
      BEGIN
      V:=VAPP[VCO];
      I:=ITV[TEMPCO,VCO];
      J:=I/AREA;

```

```

REPEAT (* FOR BARRIER HEIGHT *)
  QGBA:=QGB;
  VOLTAGEDIV;
  SATCUR;
  BARRIER;
  CHARGE;
UNTIL ABS(QGBA-QGB) = 0.0;
GBFERMI; (* ENERGY OF FERMI-LEVEL AT BOUNDARY *)
IF QGB1 <> 0.0 THEN
  (* FIND SHIFT OF FERMI FROM PREVIOUS VALUE *)
  BEGIN
  DELTAEF:=EF-EF1;
  DELTAQ:=QGB-QGB1;
  NIS:=-DELTAQ/DELTAEF/Q; (*INTERFACE-STATE DENSITY*)
  WRITE('          >');
  WRITELN(DELTAEF/2.0+EF1:3:3,NIS);
  IF NIS >= 0.0 THEN SYM:=SQUARE ELSE SYM:=CROSS;
  HPLOTPOINT(DELTAEF/2.0+EF1,LOG(ABS(NIS)),XBOT,YBOT,XDIV,YDIV,CONPTS,SYM);
  END;
  EF1:=EF; (* SAVE THESE CONDITIONS *)
  QGB1:=QGB;
  WRITELN(V:2:2,I,QGB);
  END;
END;
TEMPCO:=TEMPCO+1; (* REPEAT FOR NEXT TEMP*)
END;
END.

```

Appendix D
ADAP USERS' GUIDE

ADAP
Automated Data Acquisition
&
Processing System
Users' Guide

by

G.C. McGonigal

Materials & Devices Research Laboratory
Department of Electrical Engineering
University of Manitoba

OVERVIEW

ADAP is a computer-controlled data acquisition and processing system specifically designed for materials and devices testing and experimentation. An Apple II+ microcomputer provides the computing power required for data collection, reduction, and display. Experiments are interfaced to the computer via an Experiment Control Interface (ECI). ECI was designed by the author to provide:

1. 12-bit A/D converter
2. 8 buffered voltage inputs
3. 4 10-bit D/A converters
4. counter/timer
5. current-to-voltage converter
6. several digital inputs and outputs.

ACKNOWLEDGMENTS

The author wishes to acknowledge John Shaw, Robert Allen and Bruce Klimpke for their helpful suggestions concerning this project.

CONTENTS

OVERVIEW	ii
ACKNOWLEDGMENTS	iii
	<u>page</u>
1. SYSTEM COMPONENTS	1.1
Apple II+ Microcomputer	1.2
Programming	1.2
SSC Serial Interface	1.2
HP7470A Pen-plotter	1.3
Printer	1.3
Experiment Control Interface	1.4
2. ADAP SOFTWARE	2.1
Apple II Pascal 1.1	2.1
System Library	2.2
ECI Unit	2.3
PLOTAIDS Unit	2.6
PLOTTERGRAPHICS Unit	2.8
PENPLOTAIDS Unit	2.10
Compiling and Running Large Programs	2.11
Unit Summary	2.12
ECI	2.12
PLOTAIDS	2.13
PLOTTERGRAPHICS	2.14
PENPLOTAIDS	2.15
3. ECI HARDWARE	3.1
Apple Bus Buffering and Address Decoding	3.1
Memory Map	3.3
I/O Lines	3.4
A0 - A3	3.4
A4 - A7	3.4
D0 - D3	3.6
I	3.6
S1, S2	3.8
V _i	3.8
X, Y, W, Z	3.8
Analog-to-Digital Conversion	3.10
Programmable Timer Module (PTM)	3.12
Power Supply	3.13

REFERENCES REFER.1

Appendix page

A. ADAP SYSTEM LIBRARY UNITS A.1

LIST OF FIGURES

<u>Figure</u>	<u>page</u>
1 Schematic diagram of the ADAP system.	1.1
2 Bus buffering and address decoding	3.2
3 A0-A3 amplifier wiring connections.	3.5
4 A4-A7 amplifier wiring connections.	3.5
5 D-output wiring diagram.	3.6
6 Current-to-voltage converter wiring details.	3.7
7 D/A converter wiring	3.9
8 A/D section wiring.	3.11
9 PTM wiring connections.	3.12
10 ±15V power supply wiring details.	3.13

1

SYSTEM COMPONENTS

This section is intended to introduce the user to the ADAP system. Figure 1 is a schematic diagram of this system.

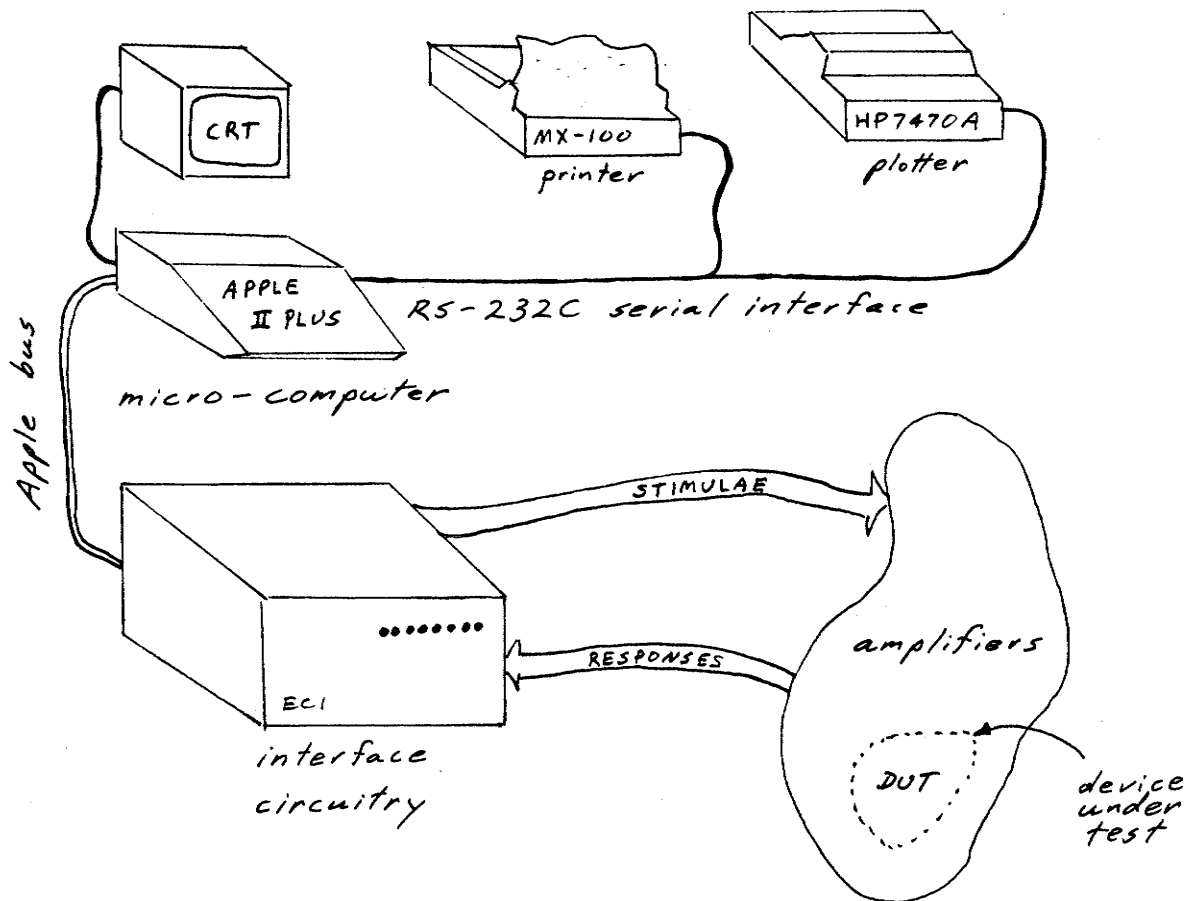


Figure 1: Schematic diagram of the ADAP system.

1.1 APPLE II+ MICROCOMPUTER

The heart of ADAP is an Apple II+ microcomputer outfitted with 64k RAM, two Apple 5-1/4 in. disk-drives and an NEC green-phosphor television monitor.

1.2 PROGRAMMING

A working knowledge of the (UCSD) Pascal computer language is required to program ADAP. This manual assumes that the user is familiar with Pascal. The user is referred to the Apple II Pascal manuals [1,2] for a detailed description of this language and operating system.

The ADAP software resides on four floppy-disks labeled 'ADAP1', 'ADAP2', 'ADAP3', and 'ADAP4'. ADAP1 and ADAP2 contain the Apple II Pascal 1.1 compiler, editor, and operating system. ADAP3 contains the source and code files that have been added to the system library for use by the ADAP system. ADAP4 contains many example programs that have been written for the ADAP system. ADAP1 includes the system library which contains the subroutines written specifically for ADAP. These subroutines are written in Pascal and are intended to simplify the implementation of ADAP programs. Included in the system library are programs for controlling ECI and plotting results on the Apple TV screen or HP7470A pen-plotter.

The ECI subroutines are especially important for they perform the machine-level tasks required to control the individual devices in the ECI interface. The use of these subroutines allows the user to access the various devices by simple names and pass parameters in convenient units (e.g. volts instead of their binary equivalent).

A complete description of the ADAP software is given in chapter 2.

1.3 SSC SERIAL INTERFACE

An Apple SSC RS-232C interface card provides serial communication to various peripherals. The SSC resides in card-slot 2 on the Apple bus. The Communications Mode of operation is used with all peripherals including plotters, printers, and links to other computers. The SSC appears as volume #8 to the Pascal operating system and is also referred to as REMIN and REMOUT. It is suggested that the data rate be set to 1200 baud. Detailed information on the SSC may be obtained from the "Super Serial Card, Installation and Operating Manual" [3].

1.4 HP7470A PEN-PLOTTER

Hard-copy of graphical results is obtained from the Hewlett-Packard 7470A pen-plotter. This plotter features two pens and an addressable resolution of 0.025mm (0.001 in.). Communication with the plotter is made through the SSC. The plotter is connected to the SSC on the Apple via an RS-232 cable. The dip-switch on the plotter beside the RS-232 connector should be configured as 00011101.

Commands are sent to the plotter in HP Graphics Language (HPGL) format. These instructions are of a high-level nature and include commands for automatic scaling, straight-line pen movements from A to B, and the printing of ASCII character strings. Details of the HPGL may be obtained from the "HP7470A Interfacing and Programming Manual" [4].

A Pascal UNIT of subroutines called PENPLOT AIDS is included in the ADAP system library. PENPLOT AIDS enables the user to obtain graphical hard-copy without a knowledge of the HPGL. Included are programs capable of drawing and appropriately scaling graphs as well as plotting points at the desired values. Also in the system library is a UNIT called PLOTTERGRAPHICS which is similar to TURTLEGRAPHICS. PLOTTERGRAPHICS provides many of the subroutines for drawing with the pen-plotter that TURTLEGRAPHICS provides for drawing on the Apple screen. A detailed description of these UNITS is found in chapter 2.

With PENPLOT AIDS and PLOTTERGRAPHICS the user is able to generate plots of usable quality. If further embellishments to the plots are required the user is referred to the 7470A manual mentioned above to take full advantage of its features.

1.5 PRINTER

Programs and numerical results may be transferred to a line printer such as the Epson MX-100 via the serial interface. Programs may be printed as they are compiled by adding the compiler directive (*\$L #8:*) to the top of the program. Disk files may be printed using the filer's T)RANSFER command with the destination specified as #8:. During program execution numerical results may be written to a TEXT file associated with #8: (see Pascal manual for syntax).

Note that the printer and plotter cannot be on-line simultaneously as they both require the SSC port.

1.6 EXPERIMENT CONTROL INTERFACE

The Experiment Control Interface (ECI) provides the interface between the user's experiment and the Apple computer.

ECI was designed to monitor the analog outputs of instruments as well as provide voltage stimulae to their analog inputs. Direct connection to a device under test should be undertaken only with extreme caution. ECI is a peripheral board housed in its own cabinet external to the Apple and is connected to card-slot 3 of the Apple bus via ribbon cable. ECI provides:

1. 12-bit A/D converter
2. 8 buffered voltage inputs
3. 4 10-bit D/A converters
4. counter/timer
5. current-to-voltage converter
6. several digital inputs and outputs.

Full details of the ECI hardware are given in chapter 3.

ADAP SOFTWARE

This chapter endeavours to present detailed documentation of the existing ADAP software as well as provide information regarding the more subtle aspects of the Apple Pascal system that the user may find useful.

2.1 APPLE II PASCAL 1.1

Apple II Pascal 1.1 was chosen as the programming language for ADAP because of its logical structure, flexibility, and readability. Apple Pascal closely follows the syntax of UCSD Pascal. This manual will assume the user has a working knowledge of this language. The particulars of Apple II Pascal may be obtained from the manuals [1,2].

The Apple Pascal provides the following facilities:

1. Pascal Compiler. Generates code for execution from a Pascal source file.
2. Editor. This is a full-screen editor used to create the Pascal source files.
3. Filer. This facility handles the bookkeeping for the files on the floppy-disks.
4. Assembler. Used to create assembly language subroutines that may be linked into a Pascal host file for execution. The assembler is required only when using the system at the machine-code level and is therefore not normally needed for ADAP programs.
5. Linker. The linker is used for adding assembly language subroutines to host Pascal programs and adding Pascal UNITS to the system library. The linker is not usually invoked by the ADAP user.

2.2 SYSTEM LIBRARY

The system library resides in the file SYSTEM.LIBRARY. This file contains the subroutines written for ADAP as well as many subroutines used by the Pascal system which are also available to the user. These subroutines take the form of Pascal PROCEDURES and FUNCTIONS. Groups of related subroutines are grouped into packages called UNITS. UNITS are accessed from the system library by the USES declaration which is required before the subroutines may be called.

Apple Pascal provides several useful units. The user may wish to refer to the Pascal manuals regarding all of these units but two are worth mentioning here. The user should be aware of the TRANSCEND unit which contains the basic transcendental functions such as LOG and SIN. The other important unit is TURTLEGRAPHICS. This unit comprises of the subroutines required to implement the UCSD Turtle Graphics language of graphics commands. These commands are useful for constructing output on the Apple's screen.

Several units written specifically for ADAP have been added to the system library. Their names and functions are as follows:

1. ECI performs the machine-level tasks required to control the individual devices in the ECI interface. These subroutines allow the user to access the various devices by simple names and pass parameters in convenient units (e.g. volts instead of their binary equivalent). A complete description of the ECI unit follows.
2. PLOTAIDS provides subroutines for drawing graphs on the Apple screen. Included is a subroutine to draw and scale a grid given its coordinate extrema. Another subroutine places markers at the desired values on the graph. A complete description of the PLOTAIDS unit follows.
3. PLOTTERGRAPHICS implements a version of UCSD Turtle Graphics that will drive the pen-plotter rather than the TV screen. PLOTTERGRAPHICS may be used to embellish plots made by PENPLOTAIDS. A complete description of the PLOTTERGRAPHICS unit follows.
4. PENPLOTAIDS is a slightly modified version of PLOTAIDS that is used to draw graphical output on the pen-plotter. A complete description of the PENPLOTAIDS unit follows.

ECI Unit

The ECI unit is a group of subroutines used to access the various devices resident on the ECI board. These subroutines perform the required machine-level tasks, thus the user is not required to learn the addresses or protocols of the various integrated circuits employed.

Apple Pascal allows assembly language subroutines to be referenced with the same syntax as a Pascal subroutine. The assembled subroutines may either be made available directly to the user (e.g. I2V) or called by another Pascal subroutine which in turn is made available (e.g. ANALOGOUT is the available Pascal subroutine that calls the assembled subroutine DIG2AN, which is not available). In the latter case the Pascal subroutines present a more intelligible parameter list to the user (e.g. Z rather than a device address).

Programs that call ECI subroutines must reference ECIDAS in the USES declaration, e.g.

```
USES ECI;
```

A listing of the compiled ECI unit and its assembled subroutines is included in Appendix A.

A complete description of the subroutines available through ECI is now given. The user may wish to consult chapter 3 regarding the hardware aspects of the devices employed.

PROCEDURE I2V(SCALE:INTEGER)

The current-to-voltage converter sensitivity is controlled by I2V. The integer parameter SCALE specifies the current that is required to produce a full-scale voltage output. The desired SCALE is calculated from the magnitude of the desired value of current (in powers of ten) multiplied by -1. The following table lists the possible values of SCALE and their corresponding full-scale currents.

SCALE : Full-scale current (A)

2	10mA
3	1mA
4	0.1mA
5	0.01mA

FUNCTION ASSAMPLE(CHANNEL:INTEGER):INTEGER

ASSAMPLE is an assembly language subroutine that controls the analog-to-digital converter and the analog multiplexer. The operations performed by ASSAMPLE are as follows:

1. Set the analog multiplexer to the desired channel specified by the input parameter CHANNEL. This is an integer value that corresponds to the number of the input to be sampled, e.g. if CHANNEL=3 then the A3 input voltage will be routed to the analog-to-digital converter.
2. A "start of conversion" request is sent to the A/D.
3. Wait until "conversion complete" is received from the A/D.
4. Read the resulting conversion value. This value will be an integer in the range 0 to 4095. A value of 0 corresponds to an input voltage of -10.240 volts while 4095 represents 10.235 volts. Zero volts returns a value of 2047.
5. Return value and exit.

PROCEDURE SAMPLE(CHANNEL:INTEGER;VAR RRESULT:REAL)

This subroutine performs the same functions as ASSAMPLE except that the conversion result is returned as a real-numbered voltage in the range -10.240 to 10.235 volts. Note that SAMPLE is a procedure whereas ASSAMPLE is a function.

PROCEDURE DOUT(HIORLO,LINENUM:INTEGER)

The digital outputs labeled D0,D1,D2, and D3 are controlled with DOUT. The parameter HIORLO specifies the state that the output LINENUM will assume after execution, e.g. the call DOUT(1,2) will make D2 go high while DOUT(0,3) would put D3 low.

FUNCTION SINPUT(LINE:INTEGER):INTEGER

SINPUT returns the status of either the S1 or S2 input.

If a low-to-high transition has occurred on the S1 input then SINPUT(1)=1, else SINPUT(1)=0. If a high-to-low transition has occurred on the S2 input then SINPUT(2)=1, else SINPUT(2)=0.

PROCEDURE ANALOGOUT(VOUT:REAL;D2A:DEVICE)

The voltage on any one of the four analog-to-digital converters is set by a call to ANALOGOUT. This procedure assumes that the converters are wired for a voltage range of -10.240 to +10.220. The Z output is, however, wired for 1 V operation so that the actual output voltage will be 1/10 of that specified by VOUT.

A new variable type called DEVICE has been created for this procedure. The members of this type are {X,Y,W,Z} which refer to the voltage outputs on the ECI module. The parameter D2A specifies which device the voltage control signals will be sent to.

The voltage to be converted is specified by the VOUT parameter. VOUT is the real-valued voltage in volts that is to appear at the output specified by D2A. Any value of type REAL between -10.24 and +10.22 can be specified.

The 10-bit converters provide a conversion resolution of 0.020 volts. Values of VOUT are thus rounded to the nearest 0.020 volts before they are sent to the converter.

As an example we may wish to set output Y to +3.20 volts. The procedure call ANALOGOUT(3.20,Y) will accomplish this.

ANALOGOUT calls the assembled procedure DIG2AN to perform the machine-level operations.

PROCEDURE INITECIDAS

This parameter-less procedure must be called before most of the ECIDAS devices can be accessed. One call at the start of a program is usually sufficient.

The primary function of INITECIDAS is to configure the PIA to read the A/D and S inputs, and write to the I/V converter. It also configures the three stages of the Programmable Timer Module for counting in microseconds, milliseconds and seconds. S1 is set to become active on a low-to-high input transition while S2 is active after a high-to-low input transition (see chap. 3). The assembled subroutine INITPIA is called to perform the necessary byte manipulations.

INITECIDAS also sets the voltage outputs X,Y,W,Z to 0.0 volts and the digital outputs D0..D3 to logic 0.

FUNCTION TIME(SECTION:INTEGER):INTEGER

Timing functions are provided by a 6840 Programmable Timer Module (PTM). This device contains three 16-bit counters which may be programmed to perform a variety of duties. An invocation of INITECI will configure the three counters T1, T2, and T3 to count microseconds, milliseconds, and seconds respectively. The input parameter to this assembly language function is either 1, 2, or 3 in reference to the three timer sections.

PROCEDURE ZEROT

This parameter-less procedure resets the timing counters by activating the PTM's master reset.

PLOTAIDS Unit

The unit PLOTAIDS provides facilities for constructing 2-D graphical output on the Apple's monitor. Included in this unit is a self-scaling axis generator and a subroutine for placing markers at the desired coordinates.

PLOTAIDS employs the UCSD graphics language Turtle Graphics for controlling the monitor display. The TURTLEGRAPHICS unit in the system library must be referenced before PLOTAIDS in the Pascal USES declaration, e.g. USES TURTLEGRAPHICS, PLOTAIDS. Documentation of the Turtle Graphics language can be found in the Apple Pascal "Language Reference Manual" [1].

The available resolution is 192 vertical by 282 horizontal pixels.

A listing of the compiled PLOTAIDS unit is included in Appendix A.

We now present a detailed explanation of the PLOTAIDS subroutines.

```
DRAWGRID(XMAX,XMIN,YMAX,YMIN:REAL;
          VAR XBOTTOMLINE,YBOTTOMLINE,
          XDIVSIZE,YDIVSIZE:REAL;
          DOTTEDLINES:BOOLEAN)
```

This procedure draws and labels a two-dimensional coordinate system on the monitor.

The first four parameters, XMAX, XMIN, YMAX, and YMIN, specify the value extrema that are to be plotted. This is a four-quadrant axis generator so any values may be specified. If their range is known, these values may be set at compile time. Alternatively, during execution, the data to be plotted may be scanned to determine the range of values present.

The four parameters that DRAWGRID returns, XBOTTOMLINE, YBOTTOMLINE, XDIVSIZE, and YDIVSIZE, contain information concerning the axis scaling that has been selected. These values are required by the PLOTPOINT procedure and should not be altered.

If DOTTEDLINES=TRUE, a grid of dotted reference lines will be added to the plot.

Scaling values are shown along the bottom and left-hand side of the plot. An exponential factor may be indicated by the character "E". For example if "E-3" is displayed, all values should be multiplied by 0.001.

```
PLOTPOINT(XNUM, YNUM, XBOTTOMLINE, YBOTTOMLINE,
          XDIVSIZE, YDIVSIZE:REAL;
          CONNECTPOINTS:BOOLEAN; POINTSYMBOL:POINTMARKER)
```

This procedure places markers at the desired coordinates on a plot previously constructed by DRAWGRID.

DRAWGRID must be called before PLOTPOINT.

The parameters XNUM and YNUM specify the x and y coordinate values of the point to be plotted. These values should be within the range previously established by XMAX, XMIN, YMAX, YMIN of the DRAWGRID procedure.

The input parameters XBOTTOMLINE, YBOTTOMLINE, XDIVSIZE, and YDIVSIZE should be obtained from the DRAWGRID procedure's output parameters of the same name. In this way PLOTPOINT is able to obtain information about the axis scaling that DRAWGRID has established.

If CONNECTPOINTS=TRUE a line will be drawn from the preceding point to the point currently being plotted. If CONNECTPOINTS=FALSE no line will be drawn and only the marker will appear at the specified point. This has an analogy with a mechanical plotter in that CONNECTPOINTS=TRUE puts the pen down before moving to the specified point whereas CONNECTPOINTS=FALSE will lift the pen before moving.

POINTSYPMBOL specifies which marker is to be drawn at the data points. This parameter is of the special type POINTMARKER and may have the value POINT, CROSS, or SQUARE.

PLOTTERGRAPHICS Unit

PLOTTERGRAPHICS allows the user to control the Hewlett-Packard 7470A penplotter in much the same manner that TURTLEGRAPHICS controls the Apple monitor.

PLOTTERGRAPHICS supports eight of the TURTLEGRAPHICS subroutines. Their functions are analogous to those of TURTLEGRAPHICS. The similarities between the two graphics units requires that the user need only learn one graphics language in order to manipulate both the screen and the plotter. Their compatibility also allows graphics programs to be easily transferred from one medium to the other.

There are two main differences between PLOTTERGRAPHICS and TURTLEGRAPHICS:

1. All length and angular parameters in PLOTTERGRAPHICS are of type REAL (whereas they are type INTEGER in TURTLEGRAPHICS). This enables full utilization of the plotter's 25 micron addressable resolution.
2. The SCREENCOLOR type has been modified in accordance with the requirements of a two-pen plotter such as the HP 7470A. See the description of the HPENCOLOR procedure for details.

A listing of the compiled PLOTTERGRAPHICS unit is included in Appendix A.

We now present a detailed explanation of the PLOTTERGRAPHICS subroutines.

HINITTURTLE

Initialization routine for the PLOTTERGRAPHICS mode. Its main function is to create a file called PLOTTER and associate it with the serial-port file REMOUT. The label PLOTTER may not be redefined.

The 7470A plotter is initialized so that the x- and y-coordinate scaling resembles the Apple monitor, i.e. user units are 282 x 192. All pens are stored and the holder moves to position 0,0.

PROCEDURE HTURNTO(ANGLE:REAL)

Explicitly sets the angular orientation of the turtle. The parameter ANGLE is specified in degrees. Angle=0 points the turtle to the right.

PROCEDURE HTURN(ANGLE:REAL)

Adds the ANGLE value (counter-clockwise) to the current angle.

PROCEDURE HMOVETO(X,Y:REAL)

This procedure moves the pen to the absolute position (X,Y) in user units. The parameters are of type REAL to take full advantage of the plotter's resolution.

PROCEDURE HMOVE(DIST:REAL)

HMOVE moves the pen relative to its current position. This motion will be in the direction specified by the current angular variable (set by HTURN and HTURNTO) for a distance DIST specified in user units.

PROCEDURE HPENCOLOR(PENMODE:HSCREENCOLOR)

HPENCOLOR directs the pen configuration.

For this procedure a new TYPE has been created called HSCREENCOLOR.

1. HPENCOLOR(NO) Lifts the pen. If the pen is already up, no action results.
2. HPENCOLOR(YES) Puts the pen down.
3. HPENCOLOR(ONE) Loads the pen stored in the lefthand well of the 7470A. If the pen is already in use no action results.
4. HPENCOLOR(TWO) - Loads the pen stored in the right-hand pen well of the 7470A.
5. HPENCOLOR(AWAY) - Stores any pen that is currently in use.

Note that to change pens a HPENCOLOR(AWAY) call is not required.

HVIEWPORT(LEFT,RIGHT,BOTTOM,TOP:REAL)

The plotting "window" is set by the parameters of the HVIEWPORT procedure. Values outside of the window will not be plotted. A "pen-up" command is executed by the plotter when this boundary is reached.

PROCEDURE HWSTRING(S:STRING)

The character string S is printed horizontally, at the current pen position, starting with the lower lefthand corner of the first character. The string S may be of any length. The pen should be raised prior to a HWSTRING call or else it will be returned to the paper at the starting position of the next (nonexistent) character.

PENPLOT AIDS Unit

PENPLOT AIDS is useful for obtaining graphical output on the 7470A plotter. PENPLOT AIDS is analogous to PLOT AIDS in the same manner that PLOTTERGRAPHICS is analogous to TURTLEGRAPHICS. In fact, portions of PLOTTERGRAPHICS were created by changing the TURTLEGRAPHICS routines in PLOT AIDS to the PLOTTERGRAPHICS equivalent.

Included in this unit is a self-scaling axis generator and a subroutine for placing markers at the desired coordinates.

A listing of the compiled PENPLOT AIDS unit is included in Appendix A.

We now present a detailed explanation of the PENPLOT AIDS subroutines.

```

HDRAWGRID(XMAX,XMIN,YMAX,YMIN:REAL;
          VAR XBOTTOMLINE,YBOTTOMLINE,
          XDIVSIZE,YDIVSIZE:REAL;
          DOTTEDLINES:BOOLEAN)

```

This procedure draws and labels a two-dimensional coordinate system on the plotter.

The first four parameters, XMAX, XMIN, YMAX, and YMIN, specify the value extrema that are to be plotted. This is a four-quadrant axis generator so any values may be specified. If their range is known, these values may be set at compile time. Alternatively, during execution, the data to be plotted may be scanned to determine the range of values present.

The four parameters returned by HDRAWGRID, XBOTTOMLINE, YBOTTOMLINE, XDIVSIZE, and YDIVSIZE, contain information concerning the axis scaling that has been selected. These values are required by the HPLOTPOINT procedure and should not be altered.

If DOTTEDLINES=TRUE, a grid of reference lines will be added to the plot.

Scaling values are shown along the bottom and left-hand side of the plot.

```
H PLOTPOINT(XNUM, YNUM, XBOTTOMLINE, YBOTTOMLINE,
            XDIVSIZE, YDIVSIZE:REAL;
            CONNECTPOINTS:BOOLEAN; POINTSYMBOL:HPOINTMARKER)
```

This procedure places markers at the desired coordinates on a plot previously constructed by HDRAWGRID.

HDRAWGRID must be called before H PLOTPOINT.

The parameters XNUM and YNUM specify the x and y coordinate values of the point to be plotted. These values should be within the range previously established by XMAX, XMIN, YMAX, YMIN of the HDRAWGRID procedure.

The input parameters XBOTTOMLINE, YBOTTOMLINE, XDIVSIZE, and YDIVSIZE should be obtained from the HDRAWGRID procedure's output parameters of the same name. In this way H PLOTPOINT is able to obtain information about the axis scaling that HDRAWGRID has established.

If CONNECTPOINTS=TRUE a line will be drawn from the preceding point to the point currently being plotted. If CONNECTPOINTS=FALSE no line will be drawn and only the marker will appear at the specified point. This has an analogy with a mechanical plotter in that CONNECTPOINTS=TRUE puts the pen down before moving to the specified point whereas CONNECTPOINTS=FALSE will lift the pen before moving.

POINTSYMBOL specifies which marker is to be drawn at the data points. This parameter is of the special type HPOINTMARKER and may have the value HPOINT, HDOT, HCROSS, or HSQUARE. Note that the HDOT marker is not supported in PLOTAIDS.

2.3 COMPILING AND RUNNING LARGE PROGRAMS

Special considerations are required for running large programs. Unpredictable results will occur if the program is too large for the Apple's memory.

The Apple Pascal has a segmentation system which allows sections of the code to be loaded into the main memory from the floppy-disk only when they are needed. UNITS and PROCEDURE subroutines are eligible for this segmentation.

The user is referred to the discussion of the segment swapping (\$S+) and \$RESIDENT compiler directives in [1]. Also, [5] contains a discussion of other methods for handling large programs.

2.4 UNIT SUMMARY

ECI

DEFINED TYPES:

DEVICE=(X,Y,W,Z)

RESERVED VARIABLES:

TEM, COPY, RETAD, LINE

AVAILABLE SUBROUTINES:

PROCEDURE I2V(SCALE:INTEGER)

FUNCTION TIME(SECTION:INTEGER):INTEGER

FUNCTION SINPUT(LINE:INTEGER):INTEGER

PROCEDURE DOUT(HIORLO,LINENUM:INTEGER)

FUNCTION ASSAMPLE(CHANNEL:INTEGER):INTEGER

PROCEDURE ZEROT

PROCEDURE SAMPLE(CHANNEL:INTEGER; VAR RRESULT:REAL)

PROCEDURE ANALOGOUT(VOUT:REAL; D2A:DEVICE)

PROCEDURE INITECI

PLOTAIDS

DEFINED TYPES:

POINTMARKER=(POINT,CROSS,SQUARE)

VECTOR = ARRAY[0..7] OF REAL

AUXILIARY UNITS REQUIRED:

TRANSCEND, TURTLEGRAPHICS

AVAILABLE SUBROUTINES:

PROCEDURE PLOTPOINT(XNUM, YNUM, XBOTTOMLINE, YBOTTOMLINE,
XDIVSIZE, YDIVSIZE:REAL;
CONNECTPOINTS:BOOLEAN;
POINTS YMBOL:POINTMARKER)

PROCEDURE DRAWGRID(XMAX, XMIN, YMAX, YMIN:REAL;
VAR XBOTTOMLINE, YBOTTOMLINE,
XDIVSIZE, YDIVSIZE:REAL;
DOTTEDLINES:BOOLEAN)

PLOTTERGRAPHICS

DEFINED TYPES:

HSCREENCOLOR=(NO,YES,ONE,TWO,AWAY)

RESERVED VARIABLES:

PLOTTER

AUXILIARY UNITS REQUIRED:

TRANSCEND

AVAILABLE SUBROUTINES:

PROCEDURE HINITTURTLE

PROCEDURE HTURN(ANGLE:REAL)

PROCEDURE HTURNTO(ANGLE:REAL)

PROCEDURE HMOVE(DIST:REAL)

PROCEDURE HMOVETO(X,Y:REAL)

PROCEDURE HPENCOLOR(PENMODE:HSCREENCOLOR)

PROCEDURE HVIEWPORT(LEFT,RIGHT,BOTTOM,TOP:REAL)

PROCEDURE HWSTRING(S:STRING)

PENPLOT AIDS

DEFINED TYPES:

HPOINTMARKER=(HPOINT,HDOT,HCROSS,HSQUARE)

AUXILIARY UNITS REQUIRED:

TRANSCEND, PLOTTERGRAPHICS

AVAILABLE SUBROUTINES:

PROCEDURE HPOINT(XNUM, YNUM, XBOTTOMLINE, YBOTTOMLINE,
XDIVSIZE, YDIVSIZE:REAL;
CONNECTPOINTS:BOOLEAN;
POINTS YMBOL:POINTMARKER)

PROCEDURE HDRAWGRID(XMAX, XMIN, YMAX, YMIN:REAL;
VAR XBOTTOMLINE, YBOTTOMLINE,
XDIVSIZE, YDIVSIZE:REAL;
DOTTEDLINES:BOOLEAN)

PROCEDURE HAXISLABEL(XLABEL, YLABEL:STRING)

3

ECI HARDWARE

3.1 APPLE BUS BUFFERING AND ADDRESS DECODING

Communication between the Apple computer and the ECI peripheral occurs via the Apple bus. A 24-wire ribbon cable connects a card in the Apple bus card-slot 3 to the ECI board where three 74LS245's, one for each of the data, address, and control busses provide the necessary buffering. The IRQ line is not buffered.

The Apple bus provides an 'I/O SELECT' line which is active when the memory associated with the card slot is being addressed. This provides decoding to the card-slot level so that only the eight least-significant address lines are required by ECI.

From the A3, A4, and A5 address lines, eight lines are further decoded to select the eight devices on the ECI board. These are as follows:

Chip Select Line	Device
CS0	Z D/A
CS1	W D/A
CS2	Y D/A
CS3	X D/A
CS4	PIA
CS5	amux latch
CS6	PTM
CS7	D-out latch

Each device is allocated eight consecutive memory locations. The buffering and decoding details are shown in fig. 2 .

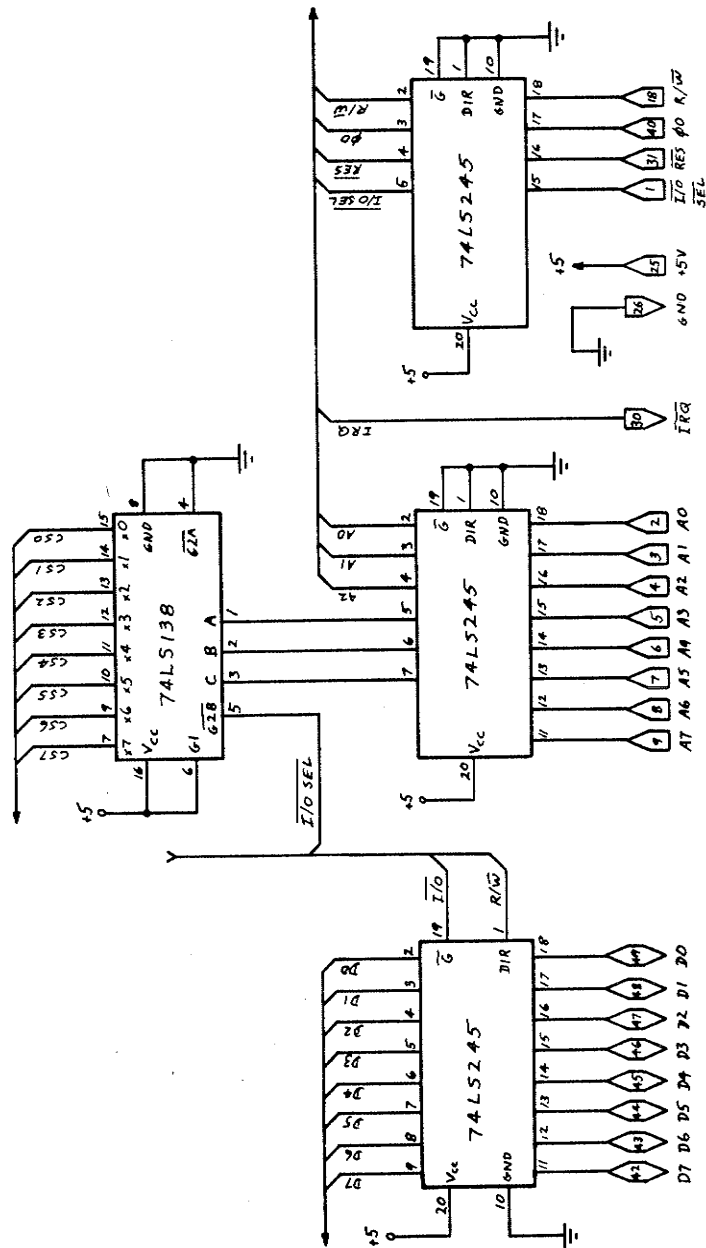


Figure 2: Bus buffering and address decoding

3.2 MEMORY MAP

The following is a compilation of the memory locations used by ECI. The ECI card resides in card-slot 3. The memory allocated for that slot is from C300 to C3FF.

LOCATION (hex)	REGISTER	DEVICE
C300	LSB	Z D/A
C301	MSB	
C308	LSB	W D/A
C309	MSB	
C310	LSB	Y D/A
C311	MSB	
C318	LSB	X D/A
C319	MSB	
C320	PRA	PIA
C321	CRA	
C322	PRB	
C323	CRB	
C328	latch	AMUX
C330	WCR1/3	PTM
C331	WCR2	
C332	read T1	
C333	write T1	
C334	read T2	
C335	write T2	
C336	read T3	
C337	write T3	
C338	latch	D-outputs

3.3 I/O LINES

The following is a list of the available ECI inputs and outputs, their functions, and electrical characteristics.

A0 - A3

These four input-pairs are connected to differential-input instrumentation amplifiers. Figure 3 is the amplifier circuit. The outputs are connected to the A/D converter's analog multiplexer for reading.

These devices are the National LH0037C. They have an input impedance of 300 M Ω . Common-mode rejection is greater than 100 dB.

Offset adjustment is via the 100K pot.

The gain of these amplifiers is normally unity, however a variable gain of up to 100 is available. This feature may be exercised by connecting a jumper between pins 7 and 8 on the amplifier's socket. Gain adjustment can now be made via the 10-turn pot which is accessible through the case.

A4 - A7

These four inputs are connected to single-ended amplifiers. Figure 4 is the amplifier circuit. The outputs are connected to the A/D converter's analog multiplexer for reading. These are non-inverting amplifiers constructed with the National LF356 op amp. This device has an input impedance of 1 G Ω .

Offset adjustment is via the 25K pot.

The gain of these amplifiers is normally unity, however a variable gain of up to 100 is available. Gain adjustment is via the 10-turn pot which is accessible through the case.

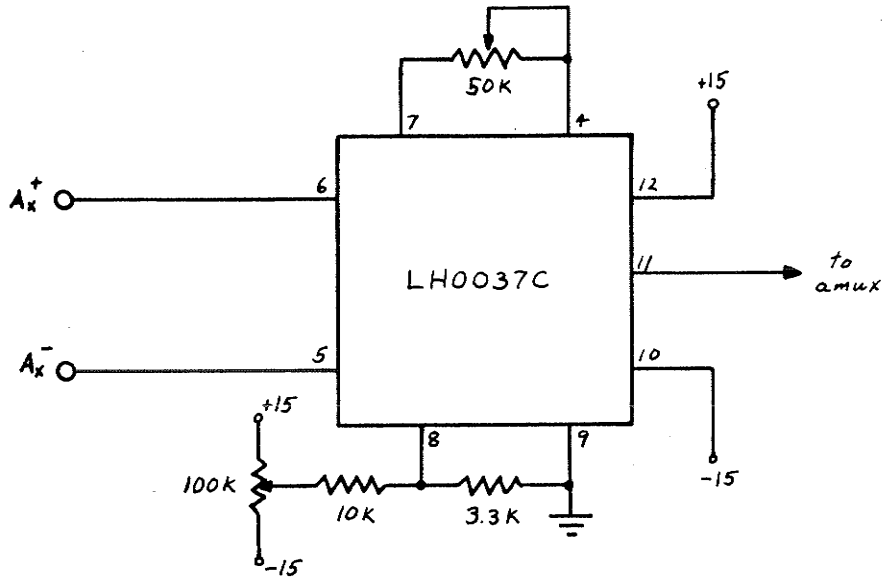


Figure 3: A0-A3 amplifier wiring connections.

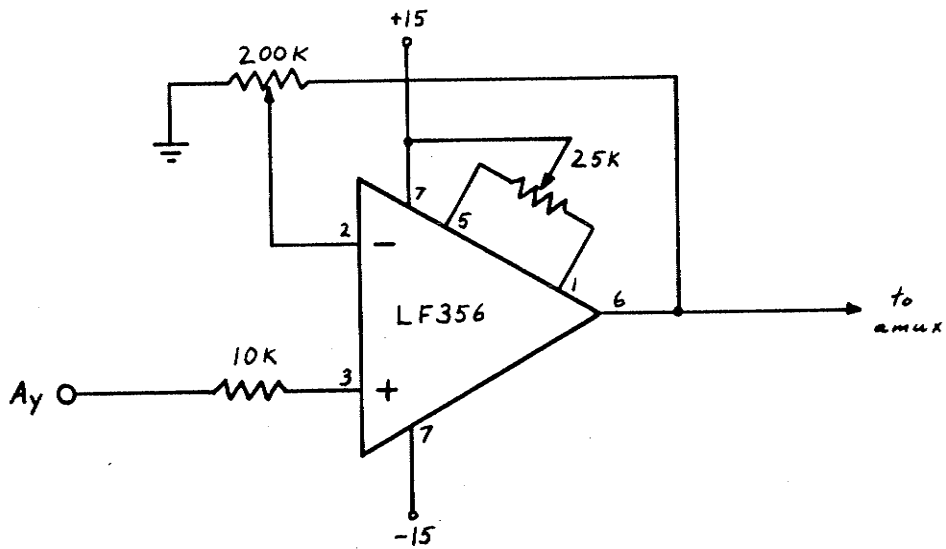


Figure 4: A4-A7 amplifier wiring connections.

D0 - D3

These are general-purpose 0-5 volt digital outputs. Their states are controlled independently with the DOUT Pascal procedure.

A 7417 provides open-collector buffering. These outputs may be wire-ORed. Figure 5 shows the wiring connections.

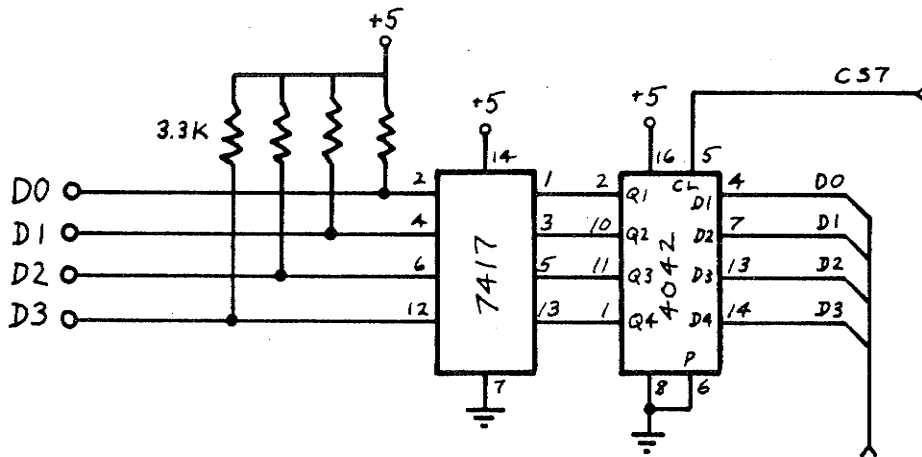


Figure 5: D-output wiring diagram.

I

This is the input for the selectable-sensitivity current-to-voltage converter.

The basic converter circuit consists of an op amp and a feedback resistor. The output voltage (see the V_1 output) is the negative of the input current multiplied by the resistance. In this particular circuit, a wide range of current magnitudes may be accurately measured because an analog multiplexer is used to select an appropriate resistance. Figure 6 shows the connection of the op amp, analog multiplexer, and measurement resistors.

The I input is at virtual ground.

The analog multiplexer channel is controlled via PB4, PB5, and PB6 on the 6821 PIA. These lines can be set with the I2V Pascal subroutine.

Four resistance values are currently supported (1K, 10K, 100K, 1M). If the 1K resistance is selected, a 10 mA current will produce a -10 V output. At the other extreme the 1 M resistance will respond to a one micro-amp input with a -1 V output. The minimum measureable current is determined by noise. If statistical averaging is employed, currents as low as 0.1 micro-amp are measureable. Four channels of the 8-input analog multiplexer are available for future use.

Output-offset adjust is provided by a 25K pot. Each of the measurement resistances have an associated pot for calibration to a known input.

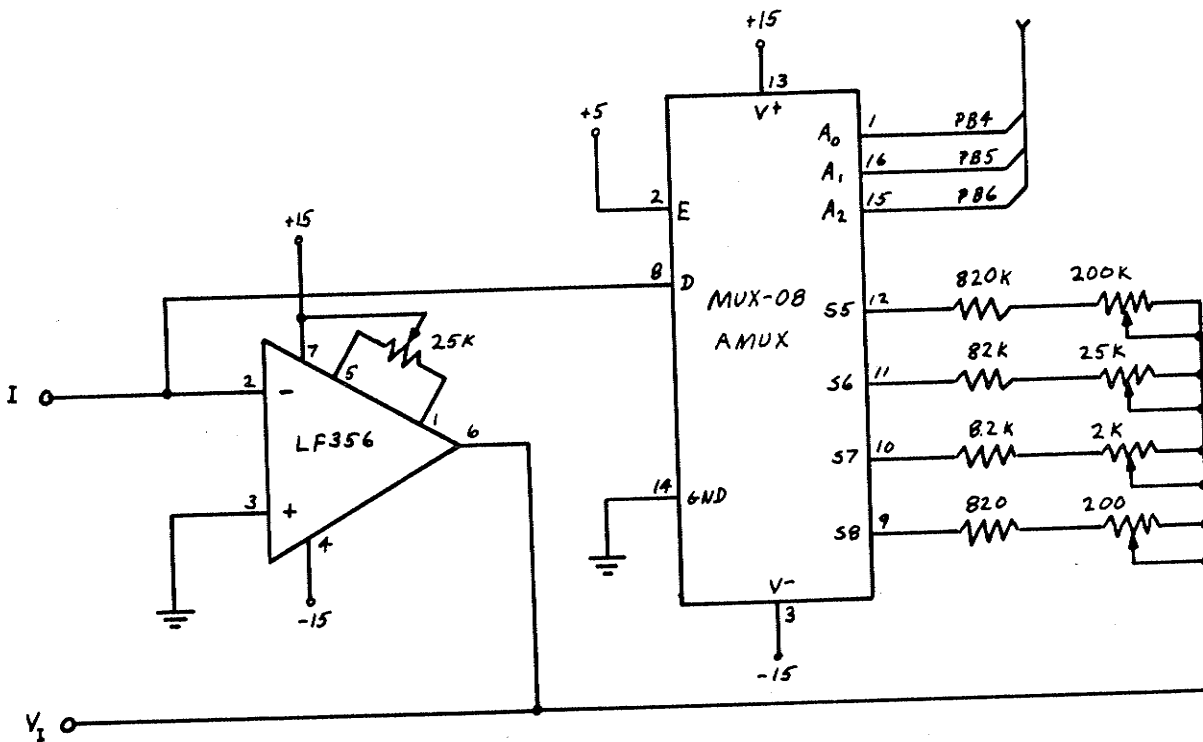


Figure 6: Current-to-voltage converter wiring details.

S1, S2

The S-inputs are general-purpose, edge-triggered digital inputs.

S1, and S2 are buffered by a 7414 Schmidt-trigger and connected to CB1 and CB2 on the 6821 PIA respectively. The status of either input may be examined with the Pascal subroutine SINPUT.

ECI is usually configured (with the INITECI procedure) so that S1 is active on a low-to-high (0-5 volt) transition and S2 is active after a high-to-low (5-0 volt) transition.

V_I

This is the output voltage of the current-to-voltage converter (see I).

Maximum output voltage is 10 volts. This output is usually connected to one of the A-inputs for reading by the A/D. Output-offset adjust is provided by a 25K pot. Each of the measurement resistances have an associated pot for calibration to a known input.

X, Y, W, Z

These four voltage outputs are each controlled by a 10-bit digital-to-analog converter (D/A).

The converter employed here is the microprocessor-compatible National DAC1006. The DAC1006 has 10-bit resolution and 10-bit accuracy.

Figure 7 is the complete wiring diagram for one of the outputs.

The output-voltage swing is determined by the feedback resistance of the final amplifier stage. A 10K resistance will produce a voltage swing from -10 to +10 volts. A 1K resistance will result in -1 to +1 volt.

The National LH0071 provides a reference voltage of 10.24 V. In this way each of the 1024 bits is approximately 20 mV over the 20.48 V output voltage range.

These outputs are controlled by the assembly-language program DIG2AN which is called by the Pascal procedure ANALOGOUT.

The Z output is equipped with pass transistors which allow this output to supply up to the power supply limit of 500 mA. All other outputs are restricted to less than 10 mA. The Z output, in standard configuration, has an output voltage swing of 1.024 volts. All other outputs have a 10.24 voltage range.

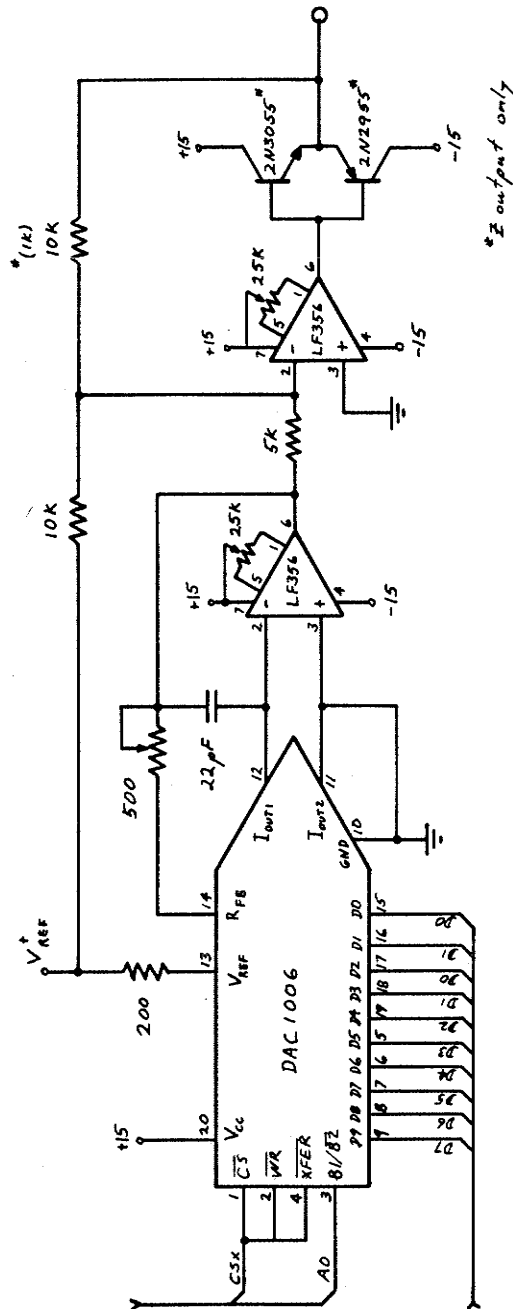


Figure 7: D/A converter wiring

3.4 ANALOG-TO-DIGITAL CONVERSION

The main function of the ECI system is to convert analog signals into a representative digital form. This is accomplished by the National ADC1211 12-bit, successive-approximation, analog-to-digital converter (A/D). An 8-channel analog multiplexer (PMI MUX-8) selects which of the A-inputs (0-7) will be routed to the input of the A/D prior to conversion initiation. The selected analog signal is preconditioned by a 1:2 voltage divider and connected through a buffer amp to the converter input.

Figure 8 is a wiring diagram of the A/D section.

A 10.24 V reference voltage is provided by a National LH0071. The converter is wired to accept bipolar inputs of one-half the reference voltage. Due to the voltage divider, the resulting input voltage range is -10.240 to +10.235 volts and each of the 4096 resolvable bits corresponds to 5 mV at the A-input (assuming unity gain).

A 140 kHz clock signal is generated by a 555 timer IC to drive the successive-approximation sequence.

The conversion time is approximately 100 microseconds.

The outputs from the 1211 are not tri-stated and therefore a Motorola 6821 Peripheral Interface Adapter (PIA) is required to provide the interface with the Apple bus. The A side of the PIA is connected to the eight least-significant bits of the A/D result while PB0-PB3 monitor the four most-significant bits. The PIA also serves as the source of the 'start conversion' pulse and monitors the 'end of conversion' line. Because the 1211 is a CMOS device, level-converters (MM74C901, MM74C906) are required to interface the digital signals.

The analog multiplexer is controlled by three outputs from an independent latch (4042). For diagnostic and cosmetic reasons, a string of LED's have been added to the front panel of the ECI case. These LED's show which input channel is currently routed to the A/D. This function is accomplished by driving the LED's from another analog multiplexer (4051) that is also receiving the control signals from the latch.

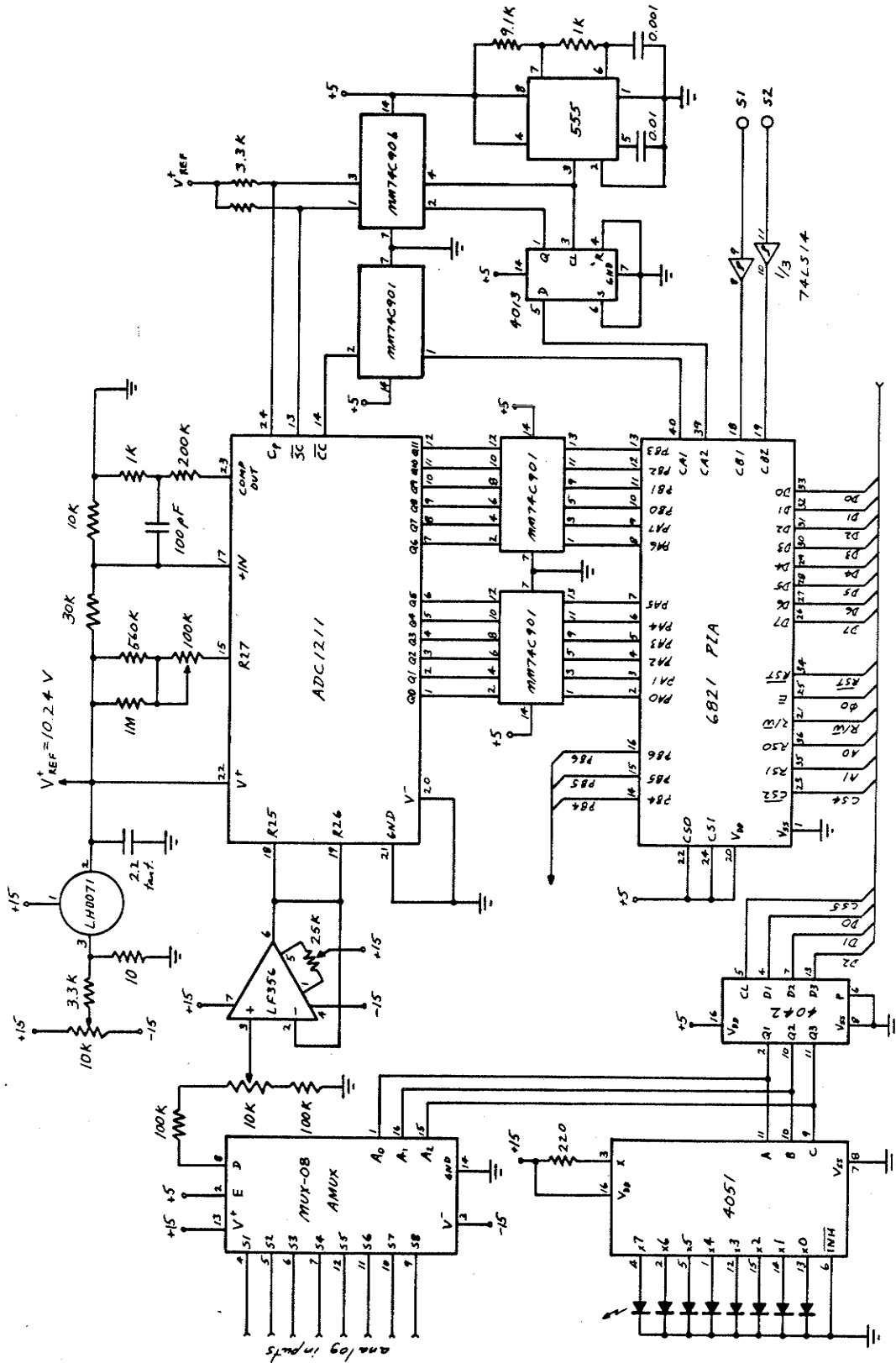


Figure 8: A/D section wiring.

3.5 PROGRAMMABLE TIMER MODULE (PTM)

The Motorola 6840 Programmable Timer Module (PTM) is capable of timing, event counting, frequency comparison, and astable- and monostable-pulse generation.

The PTM comprises three independent 16-bit counting registers. In the standard ECI configuration these registers are cascaded as shown in fig. 9. The output of register 1 is connected to the input clock of register 2. Similarly the output of register 2 is connected to the clock of register 3. The first register, and consequently all three, are clocked from the 1 MHz system clock. This allows the software (INITECI) to establish a system time-base for counting microseconds, milliseconds, and seconds.

The user may wish to rewire the timer and add his own assembly-language programs to utilize the timer in another mode. For example, a pulse generator may be required for a DLTS system [6]. In this case, one of the PTM's output lines could be brought out to one of the unused terminals on the ECI case. Another example might be an event counter for a shaft-encoder. In this case the external input would be connected to one of the timer's clock inputs.

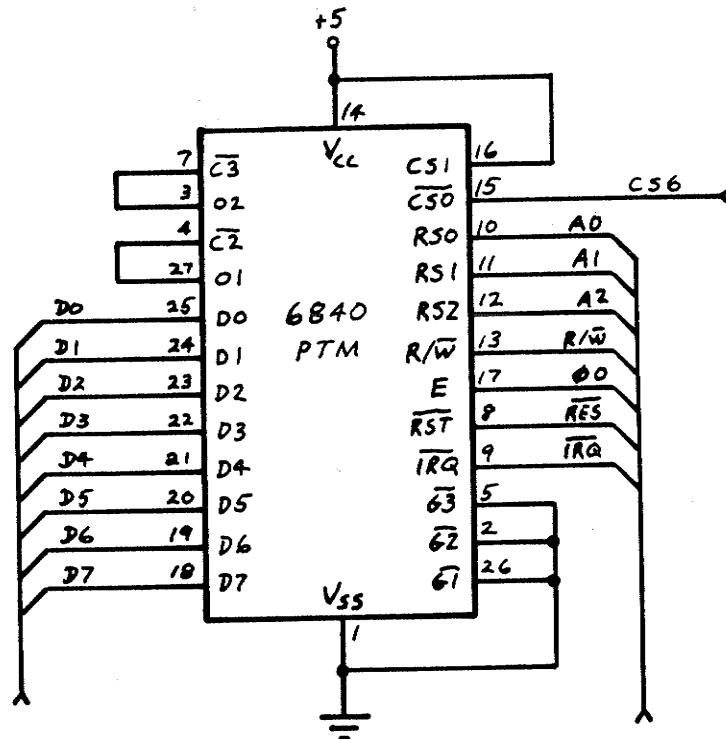


Figure 9: PTM wiring connections.

3.6 POWER SUPPLY

Power for ECI's analog devices is derived from a local $\pm 15V$ power supply. A Hammond 166 J28 transformer converts the line voltage to 28 V at 1 amp which is then rectified and regulated by a complementary pair of 15 V regulator ICs (LM78M15CP, LM79M15CP). Power for the 5V digital circuits is derived from the Apple bus. The power supply wiring is shown in fig. 10 .

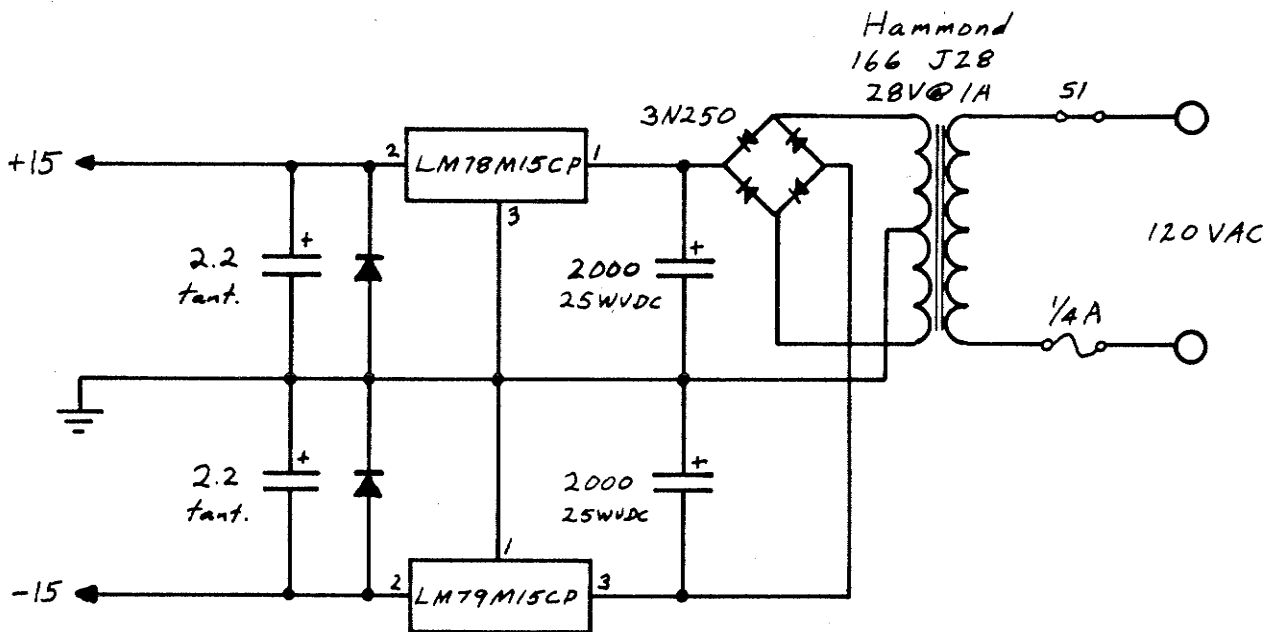


Figure 10: $\pm 15V$ power supply wiring details.

REFERENCES

1. "Apple Pascal Language Reference Manual," Apple Computer Inc., Cupertino, Calif., 1980.
2. "Apple Pascal Operating System Reference Manual," Apple Computer Inc., Cupertino, Calif., 1980.
3. "Super Serial Card, Installation and Operating Manual," Apple Computer Inc., Cupertino, Calif., 1981.
4. "HP 7470A Interfacing and Programming Manual," Hewlett-Packard, San Diego, Calif., 1982.
5. C. B. Grant and J. Butah, "Introduction to the UCSD p-System," Berkeley:Sybex, 1982.
6. D.V. Lang, "Deep-level transient spectroscopy: A new method to characterize traps in semiconductors," J. Appl. Phys., 45, pp. 3023-3032, (1974).

Appendix
ADAP SYSTEM LIBRARY UNITS

```

1 1 1:D 1 (*$L #8:*)
2 1 1:D 1 (*$S+*)
3 16 1:D 1 UNIT ECI;INTRINSIC CODE 16 DATA 31;
4 16 1:D 1
5 16 1:D 1 (***** ECI *****)
6 16 1:D 1 (*)
7 16 1:D 1 (*) WRITTEN BY G.C. MCGONIGAL (*)
8 16 1:D 1 (*)
9 16 1:D 1 (*) MATERIALS & DEVICES RESEARCH LABORATORY (*)
10 16 1:D 1 (*) DEPARTMENT OF ELECTRICAL ENGINEERING (*)
11 16 1:D 1 (*) UNIVERSITY OF MANITOBA (*)
12 16 1:D 1 (*)
13 16 1:D 1 (*) VER. 1.0/1982 (*)
14 16 1:D 1 (*)
15 16 1:D 1 (*****)
16 16 1:D 1 (*)
17 16 1:D 1 (*) ECI IS A UNIT OF PASCAL PROCEDURES DESIGNED TO SIMPLIFY (*)
18 16 1:D 1 (*) THE IMPLEMENTATION OF CONTROL PROGRAMS FOR THE "EXPERIMENT (*)
19 16 1:D 1 (*) CONTROL INTERFACE" (ECI). (*)
20 16 1:D 1 (*)
21 16 1:D 1 (*) RECOGNIZABLE FUNCTION NAMES AND "HIGH-LEVEL" PARAMETERS (*)
22 16 1:D 1 (*) ARE EMPLOYED TO "BUFFER" THE PROGRAMMER FROM THE MACHINE-LEVEL (*)
23 16 1:D 1 (*) PARTICULARS. (*)
24 16 1:D 1 (*)
25 16 1:D 1 (*) SUMMARY OF AVAILABLE PROCEDURES: (*)
26 16 1:D 1 (*) NAME: FUNCTION: (*)
27 16 1:D 1 (*)
28 16 1:D 1 (*) I2V SETS SENSITIVITY OF THE I TO V CONVERTER (*)
29 16 1:D 1 (*) TIME READS A COUNTER (*)
30 16 1:D 1 (*) SINFUT POLLS THE S1 OR S2 INPUT (*)
31 16 1:D 1 (*) DOUT CONTROLS THE D OUTPUTS (*)
32 16 1:D 1 (*) ASSAMPLE ASSEMBLED SAMPLING ROUTINE (*)
33 16 1:D 1 (*) ZEROT RESETS THE COUNTERS (*)
34 16 1:D 1 (*) SAMPLE RETURNS THE SAMPLED VOLTAGE (*)
35 16 1:D 1 (*) ANALOGOUT WRITES VOLTAGES TO THE DACS (*)
36 16 1:D 1 (*) INITECI SYSTEM INITIALIZATION ROUTINE (*)
37 16 1:D 1 (*)
38 16 1:D 1 (*****)
39 16 1:D 1
40 16 1:D 1
41 16 1:D 1 INTERFACE
42 16 1:D 1
43 16 1:D 1 TYPE DEVICE=(X,Y,W,Z);
44 16 1:D 1
45 16 1:D 1 VAR TEM,COPY,RETAD,LINE: INTEGER;
46 16 1:D 5
47 16 2:D 1 PROCEDURE I2V(SCALE: INTEGER);
48 16 2:D 2
49 16 3:D 3 FUNCTION TIME(SECTION: INTEGER): INTEGER;
50 16 3:D 4
51 16 4:D 3 FUNCTION SINFUT(LINE: INTEGER): INTEGER;
52 16 4:D 4
53 16 5:D 1 PROCEDURE DOUT(HIORLO,LINENUM: INTEGER);
54 16 5:D 3
55 16 6:D 3 FUNCTION ASSAMPLE(CHANNEL: INTEGER): INTEGER;
56 16 6:D 4
57 16 7:D 1 PROCEDURE ZEROT;
58 16 7:D 1
59 16 8:D 1 PROCEDURE SAMPLE(CHANNEL: INTEGER; VAR RRESULT: REAL);
60 16 8:D 3
61 16 9:D 1 PROCEDURE ANALOGOUT(VOUT: REAL; D2A: DEVICE);
62 16 9:D 4
63 16 10:D 1 PROCEDURE INITECI;
64 16 10:D 1

```

```

65 16 10:D 1
66 16 1:D 1 IMPLEMENTATION
67 16 1:D 5
68 16 2:D 1 PROCEDURE I2V;EXTERNAL;
69 16 2:D 2 (* CONTROLS THE RANGE SETTING OF THE CURRENT TO VOLTAGE CONVERTER.
70 16 2:D 2 THE PARM SCALE IS SET TO THE ABS OF THE MAGNITUDE OF THE DESIRED
71 16 2:D 2 FULL-RANGE CURRENT READING IN AMPS.
72 16 2:D 2 E.G. FOR FULL-SCALE (V=10 V) OF 1.0E-4 AMPS THEN SCALE=4. *)
73 16 2:D 2
74 16 2:D 2
75 16 3:D 3 FUNCTION TIME;EXTERNAL;
76 16 3:D 4 (* RETURNS THE CURRENT VALUE OF THE SPECIFIED COUNTER.
77 16 3:D 4 SECTION=1 COUNTS MICROSECONDS;
78 16 3:D 4 " 2 " MILLISECONDS, AND
79 16 3:D 4 " 3 " SECONDS. *)
80 16 3:D 4
81 16 3:D 4
82 16 4:D 3 FUNCTION SINPUT;EXTERNAL;
83 16 4:D 4 (* POLLS THE S1 OR S2 INPUT.
84 16 4:D 4 A '1' WILL BE RETURNED IF THE LINE IS ACTIVE (OTHERWISE '0').
85 16 4:D 4 S1 IS ACTIVE ON A LO TO HI TRANSITION.
86 16 4:D 4 S2 " " " " HI TO LO " *)
87 16 4:D 4
88 16 4:D 4
89 16 5:D 1 PROCEDURE DOUT;EXTERNAL;
90 16 5:D 3 (* CONTROLS THE DIGITAL OUTPUTS D0,D1,D2,D3.
91 16 5:D 3 LINENUM IS THE NUMBER OF THE LINE TO BE ACCESSED (0,1,2,OR 3).
92 16 5:D 3 HIORLO IS THE DESIRED STATE (1 OR 0). *)
93 16 5:D 3
94 16 5:D 3
95 16 6:D 3 FUNCTION ASSAMPLE;EXTERNAL;
96 16 6:D 4 (* ASSEMBLED PROC TO READ THE ADC.
97 16 6:D 4 CHANNEL SPECIFIES THE AMUX CHANNEL TO BE ACTIVATED DURING CONVERSION.
98 16 6:D 4 RESULT IS THE 12-BIT SIGNED INTEGER VALUE READ DIRECTLY FROM THE ADC.*)
99 16 6:D 4
100 16 6:D 4
101 16 11:D 1 PROCEDURE INITPIA;EXTERNAL;
102 16 11:D 1
103 16 11:D 1
104 16 12:D 1 PROCEDURE DIG2AN(VOUTI,CONVERTER:INTEGER);EXTERNAL;
105 16 12:D 3
106 16 12:D 3
107 16 7:D 1 PROCEDURE ZEROT;EXTERNAL;
108 16 7:D 1 (* RESETS THE TIMER'S COUNTERS *)
109 16 7:D 1
110 16 7:D 1
111 16 9:D 1 PROCEDURE ANALOGOUT;
112 16 9:D 4 (* CONTROLS THE DIGITAL TO ANALOG CONVERTERS.
113 16 9:D 4 VOUT=DESIRED OUTPUT VOLTAGE (REAL #(-10.240 TO +10.220)). THIS PROC
114 16 9:D 4 ROUNDS VOUT TO THE NEAREST VOLTAGE LIMITED BY THE CONVERTER
115 16 9:D 4 RESOLUTION WHICH IS 0.020 VOLTS
116 16 9:D 4 D2A=CONVERTER TO BE WRITTEN INTO. THIS IS A VAR OF TYPE DEVICE
117 16 9:D 4 WHICH IS ONE OF X,Y,W,Z.
118 16 9:D 4 E.G. PROCEDURE ANALOGOUT(-0.13,Y);
119 16 9:D 4 WOULD PRODUCE AN OUTPUT OF -0.140 VOLTS AT Y. *)
120 16 9:D 4
121 16 9:D 4 VAR VOUTI,CONVERTER:INTEGER;
122 16 9:D 6
123 16 9:0 0 BEGIN
124 16 9:1 0 VOUTI:=ROUND(VOUT/0.02+512.0);
125 16 9:1 23 IF D2A=Z THEN CONVERTER:=0;
126 16 9:1 31 IF D2A=W THEN CONVERTER:=8;
127 16 9:1 39 IF D2A=Y THEN CONVERTER:=16;
128 16 9:1 47 IF D2A=X THEN CONVERTER:=24;
129 16 9:1 55 DIG2AN(VDOUTI,CONVERTER);
130 16 9:0 59 END;
131 16 9:0 72
132 16 9:0 72
133 16 8:D 1 PROCEDURE SAMPLE;
134 16 8:D 3 (* SAME AS ASSAMPLE EXCEPT THAT THE RESULT IS RETURNED AS A REAL-VALUED
135 16 8:D 3 VOLTAGE (-10.24 TO +10.235). *)
136 16 8:D 3
137 16 8:D 3 VAR RESULT:INTEGER;
138 16 8:D 4
139 16 8:0 0 BEGIN
140 16 8:1 0 RRESULT:=(ASSAMPLE(CHANNEL)-2047)*0.005;
141 16 8:0 20 END;
142 16 8:0 32

```

```

143 16 8:0 32
144 16 10:D 1 PROCEDURE INITECI;
145 16 10:D 1 (* INITECI SHOULD BE CALLED BEFORE ANY OTHER ECI PROC TO ASSURE
146 16 10:D 1 THE SYSTEM IS PROPERLY CONFIGURED. INITECI ALSO INITIALIZES THE
147 16 10:D 1 VARIOUS DEVICES TO THE FOLLOWING:
148 16 10:D 1 X,Y,W,Z:=0.0 VOLTS
149 16 10:D 1 D0,D1,D2,D3:=LO;
150 16 10:D 1 S1=ACTIVE HI,S2=ACTIVE LO *)
151 16 10:D 1
152 16 10:0 0 BEGIN
153 16 10:0 0 (* SET-UP PIA *)
154 16 10:0 0 (* SET TIMER TO MICROSEC,MILLISEC,SECS *)
155 16 10:1 0 INITPIA;
156 16 10:1 2 (* ZERO X,Y,W,Z *)
157 16 10:1 2 ANALOGOUT(0.0,X);
158 16 10:1 11 ANALOGOUT(0.0,Y);
159 16 10:1 21 ANALOGOUT(0.0,W);
160 16 10:1 31 ANALOGOUT(0.0,Z);
161 16 10:1 41 (* SET D0..D3 LO *)
162 16 10:1 41 DOUT(0,0);
163 16 10:1 45 DOUT(0,1);
164 16 10:1 49 DOUT(0,2);
165 16 10:1 53 DOUT(0,3);
166 16 10:1 57 (* SET 12V TO LEAST-SENSITIVE RANGE *)
167 16 10:1 57 I2V(2);
168 16 10:0 60 END;
169 16 10:0 72
170 1 1:0 0 END.

```

```

0000:                                     .FUNC ASSAMPLE,1
Current memory available:                B132
0000:                                     .PUBLIC RETAD
0000:                                     ;THIS FUNC SELECTS THE INPUT CHANNEL
0000:                                     ;THRU THE AMUX (0..7),GENERATES A START
0000:                                     ;CONVERSION PULSE (SC),WAITS FOR END OF
0000:                                     ;CONVERSION, AND RETURNS THE 12-BIT
0000:                                     ;RESULT .
0000: C320      DRA      .EQU 0C320 ;PIA
0000: C321      CRA      .EQU 0C321
0000: C322      DRB      .EQU 0C322
0000: C323      CRB      .EQU 0C323
0000: C328      AMUX     .EQU 0C328 ;CHANNEL SELECT
0000: 68         PLA      ;SAVE RET ADR
0001: 8D 0000    STA RETAD
0004: 68         PLA
0005: 8D 0100    STA RETAD+1
0008: 68         PLA
0009: 68         PLA
000A: 68         PLA
000B: 68         PLA
000C: 68         PLA
000D: 8D 28C3    STA AMUX      ;SEL INPUT CHANNEL
0010: 68         PLA      ;DISCARD MSB
0011: A9 04      LDA #4
0013: 8D 23C3    STA CRB
0016: A9 36      LDA #36H      ;SC PULSE LO
0018: 8D 21C3    STA CRA
001B: EA         NOP      ;KEEP SC LO 1 CLOCK
001C: EA         NOP
001D: EA         NOP
001E: EA         NOP
001F: EA         NOP
0020: EA         NOP
0021: EA         NOP
0022: EA         NOP
0023: A9 3E      LDA #3E      ;SC PULSE HI
0025: 8D 21C3    STA CRA      ;CONVERSION BEGINS
0028: A9 80      LDA #80      ;WAIT FOR COMPLETION
002A: 2C 21C3    BIT CRA
002D: F0FB      BEQ #01
002F: A9 0F      LDA #0F      ;MASK 4 HI BITS
0031: 2D 22C3    AND DRB
0034: 48         PHA      ;STORE HI ORDER DATA
0035: AD 20C3    LDA DRA
0038: 48         PHA      ;STORE LO ORDER DATA
0039: AD 0100    LDA RETAD+1 ;PUSH RET ADR
003C: 48         PHA
003D: AD 0000    LDA RETAD
0040: 48         PHA
0041: 60         RTS      ;RETURN
0042:                                     .END

```

```

0000: .FUNC SINFUT,1
Current memory available: 8132
0000: .PRIVATE RETAD
0000: C323 CRB .EQU 0C323
0000: C322 DRB .EQU 0C322
0000: 68 PLA ;SAVE RETURN ADR
0001: 8D 0000 STA RETAD
0004: 68 PLA
0005: 8D 0100 STA RETAD+1
0008: 68 PLA
0009: 68 PLA
000A: 68 PLA
000B: 68 PLA
000C: 68 PLA
000D: C9 01 CMP #1 ;GET 1 OR 2 INPUT..
000F: F0** BEQ S1 ;..AND LEAVE 00 ON TOP
0011: C9 02 CMP #2 ;LOOK AT S1
0013: F0** BEQ S2 ;LOOK AT S2
0015: D0** BNE NONE ;LOOK AT NONE
000F* 06
0017: A9 80 S1 LDA #80 ;MASK CRB-7
0019: 4C **** JMP CNT
0013* 07
001C: A9 40 S2 LDA #40 ;MASK CRB-6
0014* 1E00
001E: 2C 23C3 CNT BIT CRB
0021: F0** BEQ LO
0023: A9 01 LDA #1 ;SINFUT=1
0025: 4C **** JMP EXIT
0021* 05
0028: A9 00 LO LDA #0 ;SINFUT=0
002A: 4C **** JMP EXIT
0015* 16
002D: A9 02 NONE LDA #2 ;SINFUT=2
002B* 2F00
0026* 2F00
002F: 4B EXIT PHA ;PUT SINFUT ON STACK
0030: AD 0100 LDA RETAD+1 ;RETURN
0033: 4B PHA
0034: AD 0000 LDA RETAD
0037: 4B PHA
0038: AD 22C3 LDA DRB ;CLEAR INPUT FLAGS
003B: 60 RTS
003C: .END

```

```

0000:          .PROC 12V,1
Current memory available:  B132
0000:          ;THIS PROC SELECTS THE ACTIVE CHANNEL
0000:          ;ON THE CURRENT/VOLTAGE CONVERTER. PIA
0000:          ;OUTPUTS PB4-PB6 ADR THE AMUX.
0000:          ;THE INPUT PARM "SCALE" IS AN INTEGER
0000:          ;VALUE THAT IS CALC BY TAKING THE ABS
0000:          ;VALUE OF THE MAGNITUDE OF THE DESIRED
0000:          ;CURRENT AT FULL-SCALE OUTPUT (10 VOLTS).
0000:          ;E.G. SCALE=4 WOULD LEAD TO A FULL
0000:          ;SCALE OUTPUT @ I=1.0E-4 AMFS.
0000:          .PRIVATE RETAD,SCALE
0000: C322      DRB      .EQU 0C322
0000: 68         PLA      ;SAVE RETURN ADR
0001: BD 0000    STA RETAD
0004: 68         PLA
0005: BD 0100    STA RETAD+1
0008: 68         PLA
0009: BD 0000    STA SCALE  ;SAVE SCALE FACTOR
000C: A9 0A     LDA #0A
000E: 18        CLC
000F: ED 0000    SEC SCALE  ;CALC AMUX CHANNEL
0012: 18        CLC
0013: 2A        ROL A    ;SHIFT BEFORE
0014: 2A        ROL A    ;WRITING TO PIA
0015: 2A        ROL A
0016: 2A        ROL A
0017: BD 0000    STA SCALE
001A: AD 22C3   LDA DRB    ;MAINTAIN DRB-7
001D: 29 80     AND #80
001F: OD 0000    ORA SCALE
0022: BD 22C3   STA DRB    ;WRITE TO PIA
0025: 68         PLA      ;CLEAN-UP STACK
0026: AD 0100    LDA RETAD+1 ;RETURN
0029: 4B        PHA
002A: AD 0000    LDA RETAD
002D: 4B        PHA
002E: 60        RTS
002F:          .END

```

```

0000:          .PROC INITPIA
Current memory available:  B132
0000:          ;CONFIGURES THE PIA AND PTM
0000:          ;FOR STANDARD ECI OPERATION.
0000: C320      DRA      .EQU 0C320 ;PIA
0000: C321      CRA      .EQU 0C321 ;
0000: C322      DRB      .EQU 0C322 ;
0000: C323      CRB      .EQU 0C323 ;
0000: C330      WCR13    .EQU 0C330 ;PTM
0000: C331      WCR2     .EQU 0C331 ;
0000: C332      RT1C    .EQU 0C332 ;
0000: C334      RT2C    .EQU 0C334 ;
0000: C336      RT3C    .EQU 0C336 ;
0000: A9 00     LDA #0    ;RESET CONTROL REGS.
0002: BD 21C3   STA CRA
0005: BD 23C3   STA CRB
0008: BD 20C3   STA DRA    ;SET A-SIDE TO INPUTS
000B: A9 3E     LDA #3E    ;CA1=IN,CA2=OUT&HI
000D: BD 21C3   STA CRA
0010: A9 F0     LDA #0F0   ;PB0..3=IN
0012: BD 22C3   STA DRB    ;PB4..7=OUT
0015: A9 06     LDA #6     ;CB1=ACTIVE (HI)
0017: BD 23C3   STA CRB    ;CB2=ACTIVE (LO)
001A: A9 03     LDA #3     ;START T1 COUNT @ 999
001C: BD 32C3   STA RT1C   ;
001F: A9 F9     LDA #0F9   ;
0021: BD 33C3   STA RT1C+1 ;
0024: A9 03     LDA #3     ;START T2 COUNT @ 999
0026: BD 34C3   STA RT2C   ;
0029: A9 F9     LDA #0F9   ;
002B: BD 35C3   STA RT2C+1 ;
002E: A9 7F     LDA #07F   ;START T3 COUNT @ 32K
0030: BD 36C3   STA RT3C   ;
0033: A9 FF     LDA #0FF   ;
0035: BD 37C3   STA RT3C+1 ;
0038: A9 00     LDA #0     ;INIT PTM CR
003A: BD 31C3   STA WCR2   ;POINT TO WCR13
003D: A9 10     LDA #10H   ;PUT T3 IN 16-BIT MODE
003F: BD 30C3   STA WCR13  ;& EXTERNAL CLOCK.
0042: A9 95     LDA #95H   ;PUT T2 IN 8-BIT MODE
0044: BD 31C3   STA WCR2   ;& EXTERNAL CLOCK.
0047: A9 96     LDA #96H   ;PUT T3 IN 8-BIT MODE
0049: BD 30C3   STA WCR13  ;INTERNAL 1.023 MHZ CLOCK.
004C: 60        RTS
004D:          .END

```

```

0000: .FUNC TIME,1
Current memory available: 8132
0000: ;THE TIMER WILL BE CONFIGURED BY INITECI
;TO COUNT MICROSECS,MILLISECS,AND SECS.
0000: ;THE INPUT PARM SELECTS WHICH WILL BE READ.
0000: ;PARM = 1 --> TIMER1 --> MICROSECS,
; 2 --> TIMER2 --> MILLISECS,
0000: ; 3 --> TIMER3 --> SECONDS.
;TIMER3 MAX=32767.
0000: .PRIVATE RETAD,MSB,LSB
0000: C330 WCR13 .EQU 0C330
0000: C331 WCR2 .EQU 0C331
0000: C332 RT1C .EQU 0C332
0000: C334 RT2C .EQU 0C334
0000: C336 RT3C .EQU 0C336
0000: 68 PLA ;SAVE RETURN ADR
0001: BD 0000 STA RETAD
0004: 68 PLA
0005: BD 0100 STA RETAD+1
0008: 68 PLA ;FIX STACK
0009: 68 PLA ;
000A: 68 PLA ;
000E: 68 PLA ;
000C: 68 PLA ;GET TIMER # TO BE READ
000D: C9 01 CMP #1 ;LOOK AT T1
000F: F0** BEQ T1
0011: C9 02 CMP #2 ;LOOK AT T2
0013: F0** BEQ T2 ;ELSE LOOK AT T3
0015: AD 36C3 LDA RT3C ;READ TIMER3
0018: BD 0000 STA MSB
001B: AD 37C3 LDA RT3C+1
001E: BD 0000 STA LSB
0021: A9 00 LDA #0 ;CONVERT T3 RESULT TO THE
0023: 18 CLC ; APPROPRIATE DATA
0024: ED 0000 SBC LSB ; FORMAT
0027: BD 0000 STA LSB ;
002A: A9 80 LDA #80 ;
002C: ED 0000 SBC MSB ;
002F: BD 0000 STA MSB ;
0032: 4C **** JMP OUT
0013* 20
0035: AD 34C3 T2 LDA RT2C ;READ TIMER2
0038: BD 0000 STA MSB
003B: AD 35C3 LDA RT2C+1
003E: 4C **** JMP OUT2
000F* 30
0041: AD 32C3 T1 LDA RT1C ;READ TIMER1
0044: BD 0000 STA MSB
0047: AD 33C3 LDA RT1C+1
004A:
003F* 4A00
004A: BD 0000 OUT2 STA LSB ;CONVERT T2 OR T1 RESULT
004D: AD 0000 LDA MSB ; TO THE APPROPRIATE
0050: F0** BEQ C0 ; DATA FORMAT.
0052: C9 02 CMP #2
0054: 30** BMI C1
0056: F0** BEQ C2
0058: A9 12 LDA #12.
005A: 4C **** JMP CNT
0056* 05
005D: A9 0C C2 LDA #12.
005F: 4C **** JMP CNT
0054* 0C
0062: A9 06 C1 LDA #6.
0064: 4C **** JMP CNT
0050* 15
0067: A9 00 C0 LDA #0
0065* 6900
0060* 6900
005E* 6900
0069: 18 CNT CLC
006A: 69 E7 ADC #0E7
006C: 38 SEC
006D: ED 0000 SBC LSB
0070: BD 0000 STA LSB
0073: A9 03 LDA #3
0075: ED 0000 SBC MSB
0078: BD 0000 STA MSB
0033* 7B00
007B: 68 OUT PLA ;STACK CLEAN-UP
007C: AD 0000 LDA MSB ;RETURN RESULT
007F: 48 PHA ;
0080: AD 0000 LDA LSB ;
0083: 48 PHA ;
0084: AD 0100 LDA RETAD+1 ;RETURN
0087: 48 PHA
008E: AD 0000 LDA RETAD
008E: 48 PHA
008C: 60 RTS
008D: .END

```

```

0000:                .PROC ZEROT
Current memory available: 8132
0000:                ;RESETS THE TIMER COUNTERS.
0000:                ;USES THE INTERNAL-RESET BIT (CR1-0).
0000:                .PRIVATE RETAD
0000: C330           WCR13 .EQU 0C330
0000: C331           WCR2  .EQU 0C331
0000: C332           RT1C  .EQU 0C332
0000: C334           RT2C  .EQU 0C334
0000: C336           RT3C  .EQU 0C336
0000: 68             PLA           ;SAVE RETURN ADR
0001: 8D 0000        STA RETAD
0004: 68             PLA
0005: 8D 0100        STA RETAD+1
0008: A9 97         LDA #97H       ;INTERNAL RESET
000A: 8D 30C3      STA WCR13
000D: A9 96         LDA #96H
000F: 8D 30C3      STA WCR13
0012: AD 0100        LDA RETAD+1 ;RETURN
0015: 48             PHA
0016: AD 0000        LDA RETAD
0019: 48             PHA
001A: 60             RTS
001B:                .END

```

```

0000:                .PROC DIG2AN ,2
Current memory available: 8132
0000:                ;CONTROLS THE D/A CONVERTERS.
0000:                ;CALLED BY ANALOGOUT IN ECI.
0000:                .PRIVATE RETAD,V,YTEMP,XTEMP
0000: C300           SLOT3 .EQU 0C300
0000: 8C 0000        STY YTEMP ;SAVE Y STATUS
0003: BE 0000        STX XTEMP ;SAVE X STATUS
0006: 68             PLA           ;SAVE RETURN ADR
0007: 8D 0000        STA RETAD
000A: 68             PLA
000B: 8D 0100        STA RETAD+1
000E: 68             PLA
000F: AA             TAX           ;GET D2A OFFSET
0010: 68             PLA
0011: 68             PLA
0012: AB             TAY           ;SAVE LO ORDER VOLTS
0013: 8D 0000        STA V
0016: 68             PLA
0017: 8D 0100        STA V+1
001A: 6E 0100        ROR V+1 ;PUT THE 8 M.S.BITS IN V
001D: 6E 0000        ROR V
0020: 6E 0100        ROR V+1
0023: 6E 0000        ROR V
0026: AD 0000        LDA V
0029: 9D 01C3      STA SLOT3+1,X;WRITE MSBS
002C: 98             TYA
002D: 9D 00C3      STA SLOT3,X ;WRITE L.S.BITS
0030: AD 0100        LDA RETAD+1 ;RETURN
0033: 48             PHA
0034: AD 0000        LDA RETAD
0037: 48             PHA
0038: AC 0000        LDY YTEMP ;RESTORE Y STATUS
003B: AE 0000        LDX XTEMP ;RESTORE X STATUS
003E: 60             RTS
003F:                .END

```

```

1 1 1:D 1 (*$L #8:*)
2 1 1:D 1 (*$S+*)
3 17 1:D 1 UNIT PLOTAIDS;INTRINSIC CODE 17;
4 17 1:D 1
5 17 1:D 1 (***** PLOTAIDS *****)
6 17 1:D 1 (*)
7 17 1:D 1 (*) WRITTEN BY G.C. MCGONIGAL (*)
8 17 1:D 1 (*)
9 17 1:D 1 (*) MATERIALS & DEVICES RESEARCH LAB (*)
10 17 1:D 1 (*) DEPT. OF ELECTRICAL ENGINEERING (*)
11 17 1:D 1 (*) UNIVERSITY OF MANITOBA (*)
12 17 1:D 1 (*)
13 17 1:D 1 (*) VER 1.0/1982 (*)
14 17 1:D 1 (*)
15 17 1:D 1 (*****)
16 17 1:D 1 (*)
17 17 1:D 1 (*) PLOTAIDS IS A PACKAGE OF PASCAL SUBROUTINES DESIGNED (*)
18 17 1:D 1 (*) TO REDUCE THE COMPLEXITY OF PROGRAMS THAT CONSTRUCT (*)
19 17 1:D 1 (*) GRAPHICAL DISPLAYS ON THE APPLE MONITOR. (*)
20 17 1:D 1 (*)
21 17 1:D 1 (*) PLOTAIDS IS ACCESSED FROM SYSTEM.LIBRARY BY THE DECL. (*)
22 17 1:D 1 (*) USES TRANSCEND,TURTLEGRAPHICS,PLOTAIDS; (*)
23 17 1:D 1 (*)
24 17 1:D 1 (*) SUMMARY OF PROC. PROVIDED: (*)
25 17 1:D 1 (*) NAME: TYPE/FUNCTION: (*)
26 17 1:D 1 (*)
27 17 1:D 1 (*) PLOTPOINT PROC WRITES A SYMBOL AT THE SPECIFIED PT. (*)
28 17 1:D 1 (*) DRAWGRID PROC GENERATES AND LABELS THE GRIDLINES (*)
29 17 1:D 1 (*)
30 17 1:D 1 (*****)
31 17 1:D 1
32 17 1:D 1 INTERFACE
33 17 1:D 1
34 29 1:D 1
35 29 2:D 3 FUNCTION SIN(X:REAL):REAL;
36 29 3:D 3 FUNCTION COS(X:REAL):REAL;
37 29 4:D 3 FUNCTION EXP(X:REAL):REAL;
38 29 5:D 3 FUNCTION ATAN(X:REAL):REAL;
39 29 6:D 3 FUNCTION LN(X:REAL):REAL;
40 29 7:D 3 FUNCTION LOG(X:REAL):REAL;
41 29 8:D 3 FUNCTION SQRT(X:REAL):REAL;
42 29 8:D 5
43 20 1:D 5
44 20 1:D 1 TYPE
45 20 1:D 1 SCREENCOLOR=(none,white,black,reverse,radar,
46 20 1:D 1 black1,green,violet,white1,black2,orange,blue,white2);
47 20 1:D 1
48 20 2:D 1
49 20 3:D 1 PROCEDURE INITTURTLE;
50 20 4:D 1 PROCEDURE TURN(ANGLE: INTEGER);
51 20 5:D 1 PROCEDURE TURNTO(ANGLE: INTEGER);
52 20 6:D 1 PROCEDURE MOVE(DIST: INTEGER);
53 20 7:D 1 PROCEDURE MOVETO(X,Y: INTEGER);
54 20 8:D 1 PROCEDURE PENCOLOR(PENMODE: SCREENCOLOR);
55 20 9:D 1 PROCEDURE TEXTMODE;
56 20 10:D 1 PROCEDURE GRAFMODE;
57 20 11:D 1 PROCEDURE FILLSCREEN(FILLCOLOR: SCREENCOLOR);
58 20 12:D 3 PROCEDURE VIEWPORT(LEFT,RIGHT,BOTTOM,TOP: INTEGER);
59 20 13:D 3 FUNCTION TURTLEX: INTEGER;
60 20 14:D 3 FUNCTION TURTLEY: INTEGER;
61 20 15:D 3 FUNCTION TURTLEANG: INTEGER;
62 20 16:D 1 FUNCTION SCREENBIT(X,Y: INTEGER): BOOLEAN;
63 20 16:D 2 PROCEDURE DRAWBLOCK(VAR SOURCE; ROWSIZE,XSKIP,YSKIP,WIDTH,HEIGHT,
64 20 17:D 1 XSCREEN,YSCREEN,MODE: INTEGER);
65 20 18:D 1 PROCEDURE WCHAR(CH: CHAR);
66 20 19:D 1 PROCEDURE WSTRING(S: STRING);
67 20 19:D 2 PROCEDURE CHARTYPE(MODE: INTEGER);
68 17 1:D 2
69 17 1:D 1 USES TRANSCEND,TURTLEGRAPHICS;
70 17 1:D 1
71 17 1:D 1 TYPE POINTMARKER= ( POINT,CROSS,SQUARE );
72 17 1:D 1 VECTOR= ARRAY[0..7] OF REAL;

```

```

73 17 1:D 1
74 17 2:D 1 PROCEDURE PLOTPOINT(XNUM, YNUM,
75 17 2:D 1 XBOTTOMLINE, YBOTTOMLINE, XDIVSIZE, YDIVSIZE:REAL;
76 17 2:D 13 CONNECTPOINTS:BOOLEAN; POINTSYMBOL:POINTMARKER);
77 17 2:D 15
78 17 3:D 1 PROCEDURE DRAWGRID(XMAX, XMIN, YMAX, YMIN:REAL;
79 17 3:D 9 VAR XBOTTOMLINE, YBOTTOMLINE,
80 17 3:D 9 XDIVSIZE, YDIVSIZE:REAL; DOTTEDLINES:BOOLEAN);
81 17 3:D 14
82 17 3:D 14
83 17 1:D 14 IMPLEMENTATION
84 17 1:D 1
85 17 4:D 3 FUNCTION EXPD(X:REAL):INTEGER;
86 17 4:D 5 (* RETURNS THE EXPONENTIAL PART OF X *)
87 17 4:0 0 BEGIN
88 17 4:1 0 IF X=0.0 THEN
89 17 4:2 14 EXPD:=0
90 17 4:1 14 ELSE
91 17 4:2 19 EXPD:=TRUNC(LOG(ABS(X))+100)-100;
92 17 4:0 38 END;
93 17 4:0 50
94 17 4:0 50
95 17 5:D 3 FUNCTION MANTISSA(X:REAL):REAL;
96 17 5:D 5 (* RETURNS THE MANTISSA OF X *)
97 17 5:0 0 BEGIN
98 17 5:1 0 MANTISSA:=X/EXP(EXPD(X)*2.30259);
99 17 5:0 30 END;
100 17 5:0 42
101 17 5:0 42
102 17 6:D 3 FUNCTION XNOR(A, B:BOOLEAN):BOOLEAN;
103 17 6:D 5 (* EXECUTES THE EXCLUSIVE NOR FCN ON (A, B) *)
104 17 6:0 0 BEGIN
105 17 6:1 0 XNOR:=(A AND B) OR ((NOT A) AND (NOT B));
106 17 6:0 11 END;
107 17 6:0 24
108 17 6:0 24
109 17 2:D 1 PROCEDURE PLOTPOINT;
110 17 2:D 15 (* WRITES A SYMBOL AT THE REAL # CO-ORD. (XNUM, YNUM)
111 17 2:D 15 XBOTTOMLINE, YBOTTOMLINE, XDIVSIZE, YDIVSIZE ARE REAL PARMS GENERATED
112 17 2:D 15 BY DRAWGRID. THE POINT WILL BE CONNECTED BY A STRAIGHT LINE TO THE
113 17 2:D 15 PREVIOUS POINT IF CONNECTPOINTS=TRUE. POINTSYMBOL IS OF TYPE
114 17 2:D 15 POINTMARKER (EITHER CROSS, SQUARE, OR POINT). *)
115 17 2:D 15
116 17 2:D 15 VAR C:INTEGER;
117 17 2:D 16
118 17 2:0 0 BEGIN
119 17 2:1 0 PENCOLOR(BLACK);
120 17 2:1 4 IF NOT CONNECTPOINTS THEN
121 17 2:2 8 PENCOLOR(NONE);
122 17 2:2 12 (* CALC POSITION ON SCREEN *)
123 17 2:1 12 MOVETO(ROUND(21+(XNUM-XBOTTOMLINE)/XDIVSIZE*32.0),
124 17 2:1 39 ROUND(9+(YNUM-YBOTTOMLINE)/YDIVSIZE*23.0));
125 17 2:1 68 IF POINTSYMBOL = CROSS THEN
126 17 2:2 73 BEGIN
127 17 2:3 73 TURNTO(0);
128 17 2:3 77 MOVE(1);
129 17 2:3 81 PENCOLOR(BLACK);
130 17 2:3 85 TURN(135);
131 17 2:3 91 MOVE(1);
132 17 2:3 95 TURN(90);
133 17 2:3 99 MOVE(1);
134 17 2:3 103 TURN(90);
135 17 2:3 107 MOVE(1);
136 17 2:3 111 TURN(135);
137 17 2:3 117 MOVE(1);
138 17 2:3 121 PENCOLOR(WHITE);
139 17 2:3 125 MOVE(0);
140 17 2:2 129 END;
141 17 2:1 129 IF POINTSYMBOL = SQUARE THEN
142 17 2:2 134 BEGIN
143 17 2:3 134 TURNTO(45);
144 17 2:3 138 MOVE(1);
145 17 2:3 142 TURNTO(180);
146 17 2:3 148 PENCOLOR(BLACK);

```

```

147 17 2:3 152 FOR C:= 1 TO 4 DO
148 17 2:4 163 BEGIN
149 17 2:5 163 MOVE(2);
150 17 2:5 167 TURN(90);
151 17 2:4 171 END;
152 17 2:3 178 TURNT0(225);
153 17 2:3 184 MOVE(1);
154 17 2:3 188 PENCOLOR(WHITE);
155 17 2:3 192 MOVE(0);
156 17 2:2 196 END;
157 17 2:1 196 IF POINTSYMBOL = POINT THEN
158 17 2:2 201 BEGIN
159 17 2:3 201 PENCOLOR(BLACK);
160 17 2:3 205 MOVE(0);
161 17 2:2 209 END;
162 17 2:1 209 PENCOLOR(NONE);
163 17 2:1 213 (* MOVE BACK TO PT. *)
164 17 2:1 213 MOVETO(ROUND(21+(XNUM-XBOTTOMLINE)/XDIVSIZE*32.0),
165 17 2:1 239 ROUND(9+(YNUM-YBOTTOMLINE)/YDIVSIZE*23.0));
166 17 2:1 268 PENCOLOR(BLACK);
167 17 2:0 272 END;
168 17 2:0 286
169 17 2:0 286
170 17 7:D 3 FUNCTION LABELODDS(VAR LINEVALUE:VECTOR):BOOLEAN;
171 17 7:D 4 (* USED BY DRAWGRID TO DETERMINE IF THE 4 ODD OR EVEN NUMBERED
172 17 7:D 4 GRIDLINES SHOULD BE LABELED *)
173 17 7:D 4
174 17 7:D 4 VAR I:INTEGER;
175 17 7:D 5
176 17 7:0 0 BEGIN
177 17 7:1 0 LABELODDS:=FALSE;
178 17 7:1 3
179 17 7:1 3 (* CHECK FOR WHOLE NUMBERS *)
180 17 7:1 3 IF ABS(ROUND(MANTISSA(LINEVALUE[I]))-MANTISSA(LINEVALUE[0]))
181 17 7:1 34 > 0.01 THEN
182 17 7:2 44 LABELODDS:=TRUE;
183 17 7:2 47
184 17 7:2 47 (* CHECK FOR 'ZERO' AXIS *)
185 17 7:1 47 FOR I:=0 TO 7 DO
186 17 7:2 58 BEGIN
187 17 7:3 58 IF ABS(LINEVALUE[I]/(LINEVALUE[7]-LINEVALUE[0])) < 0.01 THEN
188 17 7:4 98 LABELODDS:=ODD(I);
189 17 7:2 101 END;
190 17 7:0 108 END;
191 17 7:0 122
192 17 7:0 122
193 17 8:D 1 PROCEDURE LINEARAXIS(VAR LINEVALUE:VECTOR;MAX,MIN:REAL);
194 17 8:D 6
195 17 8:D 6 VAR I,RGBPTR: INTEGER;
196 17 8:D 8 DIVSIZE,RANGE,RGMANTISSA: REAL;
197 17 8:D 14 FULLRANGE:ARRAY[0..10] OF REAL;
198 17 8:D 36
199 17 8:0 0 BEGIN
200 17 8:0 0 (* SET-UP RANGE POSSIBILITIES *)
201 17 8:1 0 FULLRANGE[0]=1.2;
202 17 8:1 16 FULLRANGE[1]=1.6;
203 17 8:1 32 FULLRANGE[2]=2.0;
204 17 8:1 48 FULLRANGE[3]=2.4;
205 17 8:1 64 FULLRANGE[4]=3.2;
206 17 8:1 80 FULLRANGE[5]=4.0;
207 17 8:1 96 FULLRANGE[6]=4.8;
208 17 8:1 112 FULLRANGE[7]=6.4;
209 17 8:1 128 FULLRANGE[8]=8.0;
210 17 8:1 144 FULLRANGE[9]=12.0;
211 17 8:1 160 FULLRANGE[10]=16.0;
212 17 8:1 176
213 17 8:1 176 RANGE:=MAX-MIN;
214 17 8:1 189
215 17 8:1 189 (* CHECK FOR A CONDITION OF ZERO EXTENT *)
216 17 8:1 189 IF RANGE=0.0 THEN
217 17 8:2 204 BEGIN
218 17 8:3 204 MAX:=ABS(MAX*1.1);
219 17 8:3 220 MIN:=-ABS(MIN*1.1);
220 17 8:2 237 END;
221 17 8:2 237

```



```

298 17 3:1 105 FOR I:=7 DOWNTD 0 DO
299 17 3:2 118 BEGIN
300 17 3:3 118 MOVETO(0,I*23+9);
301 17 3:3 128 IF XNOR(ODD(I),ODDLINES) THEN
302 17 3:4 137 BEGIN
303 17 3:5 137 LINELABEL:=ROUND(LINEVALUE[I]
304 17 3:5 146 /EXP(EXPLABEL*2.30259));
305 17 3:5 168 STR(LINELABEL,LABELSTR);
306 17 3:5 181 WSTRING(LABELSTR);
307 17 3:5 186 WRITELN(LINEVALUE[I], ' ',LINELABEL);
308 17 3:5 240 (*CHECK FOR ZERO AXIS*)
309 17 3:5 240 IF ABS(LINEVALUE[I]/(LINEVALUE[7]-LINEVALUE[0])) < 0.01 THEN
310 17 3:6 284 BEGIN
311 17 3:7 284 TURNTO(0);
312 17 3:7 288 FOR J:=0 TO 9 DO
313 17 3:8 301 BEGIN
314 17 3:9 301 MOVETO(21+J*32,9+I*23);
315 17 3:9 316 TURN(90);
316 17 3:9 320 PENCOLOR(BLACK);
317 17 3:9 324 MOVE(3);
318 17 3:9 328 TURN(180);
319 17 3:9 334 MOVE(6);
320 17 3:9 338 MOVETO(21+J*32,9+I*23);
321 17 3:9 353 PENCOLOR(WHITE);
322 17 3:9 357 TURNTO(0);
323 17 3:9 361 MOVE(1);
324 17 3:9 365 PENCOLOR(BLACK);
325 17 3:8 369 END;
326 17 3:7 377 TURNTO(180);
327 17 3:7 383 MOVE(40);
328 17 3:6 387 END
329 17 3:5 387 ELSE
330 17 3:6 389 BEGIN
331 17 3:7 389 TURNTO(0);
332 17 3:7 393 MOVETO(21,9+I*23);
333 17 3:7 403 PENCOLOR(BLACK);
334 17 3:7 407 MOVE(3);
335 17 3:7 411 IF DOTTEDLINES THEN
336 17 3:8 414 BEGIN
337 17 3:9 414 FOR J:=0 TO 64 DO
338 17 3:0 427 BEGIN
339 17 3:1 427 PENCOLOR(WHITE);
340 17 3:1 431 MOVE(1);
341 17 3:1 435 PENCOLOR(BLACK);
342 17 3:1 439 MOVE(1);
343 17 3:1 443 PENCOLOR(WHITE);
344 17 3:1 447 MOVE(1);
345 17 3:1 451 PENCOLOR(BLACK);
346 17 3:1 455 MOVE(1);
347 17 3:0 459 END;
348 17 3:8 467 END
349 17 3:7 467 ELSE
350 17 3:8 469 BEGIN
351 17 3:9 469 PENCOLOR(WHITE);
352 17 3:9 473 MOVE(260);
353 17 3:8 479 END;
354 17 3:7 479 TURN(180);
355 17 3:7 485 PENCOLOR(BLACK);
356 17 3:7 489 MOVE(11);
357 17 3:6 493 END;
358 17 3:4 493 END;
359 17 3:3 493 PENCOLOR(NONE);
360 17 3:2 497 END;
361 17 3:1 505 YBOTTOMLINE:=LINEVALUE[0];
362 17 3:1 518 YDIVSIZE:=LINEVALUE[1]-YBOTTOMLINE;
363 17 3:1 535
364 17 3:1 535 (***** DO X-LINES *****)
365 17 3:1 535 LINEARAXIS(LINEVALUE,XMAX,XMIN);
366 17 3:1 547
367 17 3:1 547 (* PRINT X-AXIS EXPONENT *)
368 17 3:1 547 MOVETO(252,0);
369 17 3:1 554 WSTRING('E');
370 17 3:1 558 EXPLABEL:=EXPD(LINEVALUE[1]-LINEVALUE[0]);
371 17 3:1 585 STR(EXPLABEL,LABELSTR);
372 17 3:1 598 WSTRING(LABELSTR);
373 17 3:1 603

```

```

374 17 3:1 603 (* CHECK LINES TO BE LABELED *)
375 17 3:1 603 ODDLINES:=LABLEODDS(LINEVALUE);
376 17 3:1 611
377 17 3:1 611 (* WRITE LABEL & GRID LINE *)
378 17 3:1 611
379 17 3:1 611 FOR I:=7 DOWNTD 0 DO
380 17 3:2 624 BEGIN
381 17 3:3 624 MOVETO(8+I*32,0);
382 17 3:3 634 IF XNOR(ODD(I),ODDLINES) THEN
383 17 3:4 643 BEGIN
384 17 3:5 643 LINELABEL:=ROUND(LINEVALUE[I]
385 17 3:5 652 /EXP(EXPLABEL*2.30259));
386 17 3:5 674 STR(LINELABEL,LABELSTR);
387 17 3:5 687 WSTRING(LABELSTR);
388 17 3:5 692 WRITELN(LINEVALUE[I],', ',LINELABEL);
389 17 3:5 746 (*CHECK FOR AXIS*)
390 17 3:5 746 IF ABS(LINEVALUE[I]/(LINEVALUE[7]-LINEVALUE[0])) < 0.01 THEN
391 17 3:6 790 BEGIN
392 17 3:7 790 TURNTD(90);
393 17 3:7 794 FOR J:=0 TO 9 DO
394 17 3:8 807 BEGIN
395 17 3:9 807 MOVETO(21+I*32,9+J*23);
396 17 3:9 822 TURN(90);
397 17 3:9 826 PENCOLOR(BLACK);
398 17 3:9 830 MOVE(3);
399 17 3:9 834 TURN(180);
400 17 3:9 840 MOVE(6);
401 17 3:9 844 MOVETO(21+I*32,9+J*23);
402 17 3:9 859 PENCOLOR(WHITE);
403 17 3:9 863 TURNTD(90);
404 17 3:9 867 MOVE(1);
405 17 3:9 871 PENCOLOR(BLACK);
406 17 3:8 875 END;
407 17 3:7 883 TURNTD(270);
408 17 3:7 889 MOVE(40);
409 17 3:6 893 END
410 17 3:5 893 ELSE
411 17 3:6 895 BEGIN
412 17 3:7 895 TURNTD(90);
413 17 3:7 899 MOVETO(21+I*32,9);
414 17 3:7 909 PENCOLOR(BLACK);
415 17 3:7 913 MOVE(3);
416 17 3:7 917 IF DOTTEDLINES THEN
417 17 3:8 920 BEGIN
418 17 3:9 920 FOR J:=0 TO 45 DO
419 17 3:0 933 BEGIN
420 17 3:1 933 PENCOLOR(WHITE);
421 17 3:1 937 MOVE(1);
422 17 3:1 941 PENCOLOR(BLACK);
423 17 3:1 945 MOVE(1);
424 17 3:1 949 PENCOLOR(WHITE);
425 17 3:1 953 MOVE(1);
426 17 3:1 957 PENCOLOR(BLACK);
427 17 3:1 961 MOVE(1);
428 17 3:0 965 END;
429 17 3:8 973 END
430 17 3:7 973 ELSE
431 17 3:8 975 BEGIN
432 17 3:9 975 PENCOLOR(WHITE);
433 17 3:9 979 MOVE(184);
434 17 3:8 985 END;
435 17 3:7 985 TURN(180);
436 17 3:7 991 PENCOLOR(BLACK);
437 17 3:7 995 MOVE(6);
438 17 3:6 999 END;
439 17 3:4 999 END;
440 17 3:3 999 PENCOLOR(NONE);
441 17 3:2 1003 END;
442 17 3:1 1011 XBOTTOMLINE:=LINEVALUE[0];
443 17 3:1 1024 XDIVSIZE:=LINEVALUE[1]-XBOTTOMLINE;
444 17 3:0 1041 END;
445 17 3:0 1074
446 17 3:0 1074
447 1 1:0 0 END.

```

```

1 1 1:D 1 (**L #8:*)
2 1 1:D 1 (**S+*)
3 1 1:D 1
4 18 1:D 1 UNIT PLOTTERGRAPHICS;INTRINSIC CODE 18 DATA 19;
5 18 1:D 1
6 18 1:D 1 (***** PLOTTERGRAPHICS *****)
7 18 1:D 1 (*)
8 18 1:D 1 (*) WRITTEN BY G.C. MCGONIGAL (*)
9 18 1:D 1 (*)
10 18 1:D 1 (*) MATERIALS & DEVICES RESEARCH LAB (*)
11 18 1:D 1 (*) DEPT. OF ELECTRICAL ENGINEERING (*)
12 18 1:D 1 (*) UNIVERSITY OF MANITOBA (*)
13 18 1:D 1 (*)
14 18 1:D 1 (*) VER 1.0/1982 (*)
15 18 1:D 1 (*)
16 18 1:D 1 (******)
17 18 1:D 1 (*)
18 18 1:D 1 (*) PLOTTERGRAPHICS IS A GRAPHICS PACKAGE DESIGNED AS THE PLOTTER (*)
19 18 1:D 1 (*) IMPLEMENTATION OF UCSD TURTLEGRAPHICS. MOST TURTLEGRAPHICS (*)
20 18 1:D 1 (*) SUBROUTINES ARE SUPPORTED. (*)
21 18 1:D 1 (*)
22 18 1:D 1 (*) PROGRAMS ARE CONVERTED FROM TURTLEGRAPHICS TO PLOTTERGRAPHICS (*)
23 18 1:D 1 (*) BY PREFIXING THE SUBROUTINES WITH 'H'. (*)
24 18 1:D 1 (*)
25 18 1:D 1 (*) NOTE THAT THE PLOT DIMENSIONS REMAIN 192 X 282 BUT ALL (*)
26 18 1:D 1 (*) POSITIONAL & ANGULAR PARAMETERS ARE NOW OF TYPE REAL. ALSO, (*)
27 18 1:D 1 (*) THE HPENCOLOR PARAMETERS HAVE BEEN MODIFIED. (*)
28 18 1:D 1 (*)
29 18 1:D 1 (*) SUMMARY OF AVAILABLE PROCEDURES: (*)
30 18 1:D 1 (*)
31 18 1:D 1 (*) HINITTURTLE (*)
32 18 1:D 1 (*) HTURN (*)
33 18 1:D 1 (*) HTURNTO (*)
34 18 1:D 1 (*) HMOVE (*)
35 18 1:D 1 (*) HMOVETO (*)
36 18 1:D 1 (*) HPENCOLOR (*)
37 18 1:D 1 (*) HVIEWPORT (*)
38 18 1:D 1 (*) HWSTRING (*)
39 18 1:D 1 (*)
40 18 1:D 1 (******)
41 18 1:D 1
42 18 1:D 1 INTERFACE
43 18 1:D 1
44 29 1:D 1
45 29 2:D 3 FUNCTION SIN(X:REAL):REAL;
46 29 3:D 3 FUNCTION COS(X:REAL):REAL;
47 29 4:D 3 FUNCTION EXP(X:REAL):REAL;
48 29 5:D 3 FUNCTION ATAN(X:REAL):REAL;
49 29 6:D 3 FUNCTION LN(X:REAL):REAL;
50 29 7:D 3 FUNCTION LOG(X:REAL):REAL;
51 29 8:D 3 FUNCTION SORT(X:REAL):REAL;
52 29 8:D 5
53 18 1:D 5 USES TRANSCEND;
54 18 1:D 1
55 18 1:D 1 TYPE HSCREENCOLOR=(NO,YES,ONE,TWO,AWAY);
56 18 1:D 1
57 18 1:D 1 VAR PLOTTER:TEXT;
58 18 1:D 302
59 18 2:D 1 PROCEDURE HINITTURTLE;
60 18 2:D 1
61 18 3:D 1 PROCEDURE HTURN(ANGLE:REAL);
62 18 3:D 3
63 18 4:D 1 PROCEDURE HTURNTO(ANGLE:REAL);
64 18 4:D 3
65 18 5:D 1 PROCEDURE HMOVE(DIST:REAL);
66 18 5:D 3
67 18 6:D 1 PROCEDURE HMOVETO(X,Y:REAL);
68 18 6:D 5
69 18 7:D 1 PROCEDURE HPENCOLOR(PENMODE:HSCREENCOLOR);
70 18 7:D 2
71 18 8:D 1 PROCEDURE HVIEWPORT(LEFT,RIGHT,BOTTOM,TOP:REAL);
72 18 8:D 9
73 18 9:D 1 PROCEDURE HWSTRING(S:STRING);
74 18 9:D 43

```

```

75 18 9:D 43
76 18 1:D 43 IMPLEMENTATION
77 18 1:D 302
78 18 1:D 302 VAR CURRENTANGLE:REAL;
79 18 1:D 304
80 18 2:D 1 PROCEDURE HINITTURTLE;
81 18 2:0 0 BEGIN
82 18 2:1 0 REWRITE(PLOTTER,'REMOU:');
83 18 2:1 20 (* SET SCALING SAME AS SCREEN *)
84 18 2:1 20 WRITE(PLOTTER,'IN;IP;SCO,282,0,192;');
85 18 2:1 52 (* FENCOLOR=NO,PEN:=LLH CORNER *)
86 18 2:1 52 WRITE(PLOTTER,'PU;SPO;FA0.0,0.0;');
87 18 2:1 81 CURRENTANGLE:=0.0;
88 18 2:0 94 END;
89 18 2:0 106
90 18 2:0 106
91 18 3:D 1 PROCEDURE HTURN;
92 18 3:0 0 BEGIN
93 18 3:1 0 CURRENTANGLE:=CURRENTANGLE+ANGLE;
94 18 3:0 17 END;
95 18 3:0 30
96 18 3:0 30
97 18 4:D 1 PROCEDURE HTURNTO;
98 18 4:0 0 BEGIN
99 18 4:1 0 CURRENTANGLE:=ANGLE;
100 18 4:0 10 END;
101 18 4:0 22
102 18 4:0 22
103 18 5:D 1 PROCEDURE HMOVE;
104 18 5:D 3 VAR XMOVE,YMOVE:REAL;
105 18 5:0 0 BEGIN
106 18 5:1 0 XMOVE:=DIST*COS(CURRENTANGLE*1.74533E-2);
107 18 5:1 27 YMOVE:=DIST*SIN(CURRENTANGLE*1.74533E-2);
108 18 5:1 55 WRITE(PLOTTER,'FR',XMOVE:9:4,',',YMOVE:9:4,',');
109 18 5:0 117 END;
110 18 5:0 130
111 18 5:0 130
112 18 6:D 1 PROCEDURE HMOVETO;
113 18 6:0 0 BEGIN
114 18 6:1 0 WRITE(PLOTTER,'PA',X:9:4,',',Y:9:4,',');
115 18 6:0 62 END;
116 18 6:0 74
117 18 6:0 74
118 18 7:D 1 PROCEDURE HFENCOLOR;
119 18 7:0 0 BEGIN
120 18 7:1 0 CASE PENMODE OF
121 18 7:1 3 NO: WRITE(PLOTTER,'PU;');
122 18 7:1 20 ONE: WRITE(PLOTTER,'SP1;');
123 18 7:1 38 TWO: WRITE(PLOTTER,'SP2;');
124 18 7:1 56 YES: WRITE(PLOTTER,'PD;');
125 18 7:1 73 AWAY: WRITE(PLOTTER,'SPO;');
126 18 7:1 91 END;
127 18 7:0 108 END;
128 18 7:0 120
129 18 7:0 120
130 18 8:D 1 PROCEDURE HVIEWPORT;
131 18 8:0 0 BEGIN
132 18 8:0 0 (* IW USES ONLY PLOTTER UNITS *)
133 18 8:1 0 WRITE(PLOTTER,'IW',250+ROUND(LEFT*36.5248):6,',',279+ROUND(BOTTOM*39.375):6,',',
134 18 8:1 86 250+ROUND(RIGHT*36.5248):6,',',279+ROUND(TOP*39.375):6,',');
135 18 8:0 158 END;
136 18 8:0 170
137 18 9:D 1 PROCEDURE HWSTRING;
138 18 9:0 0 BEGIN
139 18 9:1 0 WRITE(PLOTTER,'DT',CHR(3),',',LB',S,CHR(3));
140 18 9:0 65 END;
141 18 9:0 78
142 1 1:0 0 END.

```

```

1 1 1:D 1 (*$L #B:*)
2 1 1:D 1 (*$S+*)
3 1 1:D 1
4 23 1:D 1 UNIT PENPLOT AIDS;INTRINSIC CODE 23;
5 23 1:D 1
6 23 1:D 1 (***** PENPLOT AIDS *****)
7 23 1:D 1 (* *)
8 23 1:D 1 (* WRITTEN BY G.C. MCGONIGAL *)
9 23 1:D 1 (* *)
10 23 1:D 1 (* MATERIALS & DEVICES RESEARCH LAB *)
11 23 1:D 1 (* DEPT. OF ELECTRICAL ENGINEERING *)
12 23 1:D 1 (* UNIVERSITY OF MANITOBA *)
13 23 1:D 1 (* *)
14 23 1:D 1 (* VER I.0/1982 *)
15 23 1:D 1 (* *)
16 23 1:D 1 (*****)
17 23 1:D 1 (* *)
18 23 1:D 1 (* PENPLOT AIDS IS A PACKAGE OF PASCAL SUBROUTINES DESIGNED*)
19 23 1:D 1 (* TO REDUCE THE COMPLEXITY OF PROGRAMS THAT CONSTRUCT *)
20 23 1:D 1 (* GRAPHICAL DISPLAYS ON THE HP7470A PLOTTER. *)
21 23 1:D 1 (* *)
22 23 1:D 1 (* PENPLOT AIDS IS ACCESSED FROM SYSTEM.LIBRARY BY THE DECL*)
23 23 1:D 1 (* USES TRANSCEND,TURTLEGRAPHICS,PENPLOT AIDS; *)
24 23 1:D 1 (* *)
25 23 1:D 1 (* SUMMARY OF PROC. & FUNC. PROVIDED: *)
26 23 1:D 1 (* NAME: TYPE/FUNCTION: *)
27 23 1:D 1 (* *)
28 23 1:D 1 (* HPLOTPOINT PROC WRITES A SYMBOL AT THE SPECIFIED PT. *)
29 23 1:D 1 (* HDRAWGRID PROC GENERATES AND LABELS THE GRIDLINES. *)
30 23 1:D 1 (* HAXISLABEL PROC WRITES TITLES FOR THE X- & Y-AXIS. *)
31 23 1:D 1 (* *)
32 23 1:D 1 (*****)
33 23 1:D 1
34 23 1:D 1 INTERFACE
35 23 1:D 1
36 29 1:D 1
37 29 2:D 3 FUNCTION SIN(X:REAL):REAL;
38 29 3:D 3 FUNCTION COS(X:REAL):REAL;
39 29 4:D 3 FUNCTION EXP(X:REAL):REAL;
40 29 5:D 3 FUNCTION ATAN(X:REAL):REAL;
41 29 6:D 3 FUNCTION LN(X:REAL):REAL;
42 29 7:D 3 FUNCTION LOG(X:REAL):REAL;
43 29 8:D 3 FUNCTION SQRT(X:REAL):REAL;
44 29 8:D 5
45 18 1:D 5
46 18 1:D 1
47 18 1:D 1 USES TRANSCEND;
48 18 1:D 1
49 18 1:D 1 TYPE HSCREENCOLOR=(NO,YES,ONE,TWO,AWAY);
50 18 1:D 1
51 18 1:D 1 VAR PLOTTER:TEXT;
52 18 1:D 302
53 18 2:D 1 PROCEDURE HINITTURTLE;
54 18 2:D 1
55 18 3:D 1 PROCEDURE HTURN(ANGLE:REAL);
56 18 3:D 3
57 18 4:D 1 PROCEDURE HTURNTO(ANGLE:REAL);
58 18 4:D 3
59 18 5:D 1 PROCEDURE HMOVE(DIST:REAL);
60 18 5:D 3
61 18 6:D 1 PROCEDURE HMOVETO(X,Y:REAL);
62 18 6:D 5
63 18 7:D 1 PROCEDURE HPENCOLOR(PENMODE:HSCREENCOLOR);
64 18 7:D 2
65 18 8:D 1 PROCEDURE HVIEWPORT(LEFT,RIGHT,BOTTOM,TOP:REAL);
66 18 8:D 9
67 18 9:D 1 PROCEDURE HWSTRING(S:STRING);
68 18 9:D 43
69 18 9:D 43
70 23 1:D 43 USES TRANSCEND,PLOTTERGRAPHICS;
71 23 1:D 1
72 23 1:D 1 TYPE HPDINTMARKER=(HPOINT,HDOT,HCROSS,HSQUARE);
73 23 1:D 1
74 23 1:D 1 HVECTOR= ARRAY[0..73] OF REAL;

```

```

75 23 1:D 1
76 23 2:D 1 PROCEDURE HPLOTPPOINT(XNUM, YNUM,
77 23 2:D 1 XBOTDMLINE, YBOTDMLINE, XDIVSIZE, YDIVSIZE:REAL;
78 23 2:D 13 CONNECTPOINTS:BOOLEAN; POINTSYMBOL:HPOINTMARKER);
79 23 2:D 15
80 23 3:D 1 PROCEDURE HDRAWGRID(XMAX, XMIN, YMAX, YMIN:REAL;
81 23 3:D 9 VAR XBOTDMLINE, YBOTDMLINE,
82 23 3:D 9 XDIVSIZE, YDIVSIZE:REAL; DOTTEDLINES:BOOLEAN);
83 23 3:D 14
84 23 4:D 1 PROCEDURE HAXISLABEL(XLABEL, YLABEL:STRING);
85 23 4:D 85
86 23 4:D 85
87 23 1:D 85 IMPLEMENTATION
88 23 1:D 1
89 23 1:D 1
90 23 5:D 3 FUNCTION HEXPO(X:REAL):INTEGER;
91 23 5:D 5 (* RETURNS THE EXPONENTIAL PART OF X *)
92 23 5:0 0 BEGIN
93 23 5:1 0 IF X=0.0 THEN
94 23 5:2 14 HEXPO:=0
95 23 5:1 14 ELSE
96 23 5:2 19 HEXPO:=TRUNC(LOG(ABS(X))+100)-100;
97 23 5:0 38 END;
98 23 5:0 50
99 23 5:0 50
100 23 6:D 3 FUNCTION HMANTISSA(X:REAL):REAL;
101 23 6:D 5 (* RETURNS THE MANTISSA OF X *)
102 23 6:0 0 BEGIN
103 23 6:1 0 HMANTISSA:=X/EXP(HEXPO(X)*2.30259);
104 23 6:0 30 END;
105 23 6:0 42
106 23 6:0 42
107 23 7:D 1 PROCEDURE HDRAWDARK;
108 23 7:D 1 (* DRAWS GRIDLINES*)
109 23 7:D 1 VAR I:INTEGER;
110 23 7:0 0 BEGIN
111 23 7:1 0 HPENCOLOR(NO);
112 23 7:1 4 FOR I:=1 TO 7 DO
113 23 7:2 15 BEGIN
114 23 7:3 15 HMOVE(21.0, 9+I*23.0);
115 23 7:3 37 HPENCOLOR(YES);
116 23 7:3 41 HMOVE(276.0, 9+I*23.0);
117 23 7:3 63 HPENCOLOR(NO);
118 23 7:3 67 HMOVE(21+I*32.0, 9.0);
119 23 7:3 89 HPENCOLOR(YES);
120 23 7:3 93 HMOVE(21+I*32.0, 192.0);
121 23 7:3 115 HPENCOLOR(NO);
122 23 7:2 119 END;
123 23 7:0 126 END;
124 23 7:0 140
125 23 7:0 140
126 23 8:D 1 PROCEDURE HLINEARAXIS(VAR LINEVALUE:HVECTOR; MAX, MIN:REAL);
127 23 8:D 6 (* USED BY HDRAWGRID TO ESTABLISH AXIS SCALING*)
128 23 8:D 6 VAR I, RGPTR: INTEGER;
129 23 8:D 8 DIVSIZE, RANGE, RGMANTISSA: REAL;
130 23 8:D 14 FULLRANGE:ARRAY[0..10] OF REAL;
131 23 8:D 36
132 23 8:0 0 BEGIN
133 23 8:0 0 (* SET-UP RANGE POSSIBILITIES *)
134 23 8:1 0 FULLRANGE[0]:=1.2;
135 23 8:1 16 FULLRANGE[1]:=1.6;
136 23 8:1 32 FULLRANGE[2]:=2.0;
137 23 8:1 48 FULLRANGE[3]:=2.4;
138 23 8:1 64 FULLRANGE[4]:=3.2;
139 23 8:1 80 FULLRANGE[5]:=4.0;
140 23 8:1 96 FULLRANGE[6]:=4.8;
141 23 8:1 112 FULLRANGE[7]:=6.4;
142 23 8:1 128 FULLRANGE[8]:=8.0;
143 23 8:1 144 FULLRANGE[9]:=12.0;
144 23 8:1 160 FULLRANGE[10]:=16.0;
145 23 8:1 176
146 23 8:1 176 RANGE:=MAX-MIN;
147 23 8:1 189
148 23 8:1 189 (* CHECK FOR A CONDITION OF ZERO EXTENT *)
149 23 8:1 189 IF RANGE=0.0 THEN
150 23 8:2 204 BEGIN
151 23 8:3 204 MAX:=ABS(MAX*1.1);
152 23 8:3 220 MIN:=-ABS(MIN*1.1);
153 23 8:2 237 END;

```

```

154 23      8:2  237
155 23      8:1  237 REPEAT
156 23      8:2  237 BEGIN
157 23      8:2  237 (* FIND A SUITABLE RANGE *)
158 23      8:3  237 RGMANTISSA:=HMANTISSA(RANGE);
159 23      8:3  249 RGFTR:=-1;
160 23      8:3  253 REPEAT
161 23      8:4  253 RGFTR:=RGFTR+1;
162 23      8:3  258 UNTIL RGMANTISSA <= FULLRANGE[RGFTR];
163 23      8:3  276
164 23      8:3  276 (* MAKE EACH DIV 1/8 OF FULLRANGE *)
165 23      8:3  276 DIVSIZE:=FULLRANGE[RGFTR]/8.0
166 23      8:3  288 *EXP(HEXPO(RANGE)*2.30259);
167 23      8:3  320
168 23      8:3  320 (* DETERMINE SUITABLE BOTTOMLINE *)
169 23      8:3  320 IF MIN >= 0.0 THEN
170 23      8:4  334 BEGIN
171 23      8:5  334 LINEVALUE[0]:=0.0;
172 23      8:5  350 WHILE MIN > LINEVALUE[0]+DIVSIZE DO
173 23      8:6  372 LINEVALUE[0]:=LINEVALUE[0]+DIVSIZE;
174 23      8:4  397 END
175 23      8:3  397 ELSE
176 23      8:4  399 BEGIN
177 23      8:5  399 LINEVALUE[0]:=0.0;
178 23      8:5  414 WHILE LINEVALUE[0]*1.001 > MIN DO
179 23      8:6  439 LINEVALUE[0]:=LINEVALUE[0]-DIVSIZE;
180 23      8:4  464 END;
181 23      8:4  464
182 23      8:4  464 (* DERIVE 8 GRIDLINES *)
183 23      8:3  464 FOR I:=1 TO 7 DO
184 23      8:4  476 BEGIN
185 23      8:5  476 LINEVALUE[I]:=LINEVALUE[I-1]+DIVSIZE;
186 23      8:4  501 END;
187 23      8:2  508 END
188 23      8:2  508 (* CHECK THAT THIS RESULT WILL BE SUITABLE *)
189 23      8:1  508 UNTIL LINEVALUE[7]-LINEVALUE[0]+DIVSIZE >= RANGE;
190 23      8:0  540 END;
191 23      8:0  562
192 23      8:0  562
193 23      4:D  1 PROCEDURE HAXISLABEL;
194 23      4:D  85 (* STRING XPRE IS PRINTED BEFORE THE EXPONENT,
195 23      4:D  85 XPOST AFTER EXP *)
196 23      4:D  85
197 23      4:0  0 BEGIN
198 23      4:1  0 HPENCOLOR(ND);
199 23      4:1  14 HMOVETO(120.0,-1.0);
200 23      4:1  30 HWSTRING(XLABEL);
201 23      4:1  35 HMOVETO(2.0,74.0);
202 23      4:1  51 WRITE(PLOTTER,'DIO.0,1.0;');
203 23      4:1  73 HWSTRING(YLABEL);
204 23      4:1  78 WRITE(PLOTTER,'DI;');
205 23      4:0  93 END;
206 23      4:0  106
207 23      4:0  106
208 23      2:D  1 PROCEDURE HPLOTPPOINT;
209 23      2:D  15 (* WRITES A SYMBOL AT THE REAL # CO-ORD. (XNUM,YNUM)
210 23      2:D  15 XBOTTOMLINE,YBOTTOMLINE,XDIVSIZE,YDIVSIZE ARE REAL PARMS GENERATED
211 23      2:D  15 BY DRAWGRID. THE POINT WILL BE CONNECTED BY A STRAIGHT LINE TO THE
212 23      2:D  15 PREVIOUS POINT IF CONNECTPOINTS=TRUE. POINTSYMBOL IS OF TYPE
213 23      2:D  15 POINTMARKER (EITHER CROSS,SQUARE,OR POINT). *)
214 23      2:D  15
215 23      2:D  15 VAR C:INTEGER;
216 23      2:D  16
217 23      2:0  0 BEGIN
218 23      2:1  0 IF NOT CONNECTPOINTS THEN
219 23      2:2  4 HPENCOLOR(ND)
220 23      2:1  5 ELSE
221 23      2:2  10 HPENCOLOR(YES);
222 23      2:2  14 (* CALC POSITION ON SCREEN *)
223 23      2:1  14 HMOVETO(21.0+(XNUM-XBOTTOMLINE)/XDIVSIZE*32.0,
224 23      2:1  42 9.0+(YNUM-YBOTTOMLINE)/YDIVSIZE*23.0);
225 23      2:1  73 HPENCOLOR(YES);
226 23      2:1  77 IF POINTSYMBOL = HCROSS THEN
227 23      2:2  82 WRITE(PLOTTER,'PRO.0,1.3,0.0,-2.6,0.0,1.3,1.3,0.0,-2.6,0.0,1.3,0.0;');
228 23      2:1  146 IF POINTSYMBOL = HSQUARE THEN
229 23      2:2  151 BEGIN
230 23      2:3  151 WRITE(PLOTTER,'PRO.0,1.0,-1.0,0.0,0.0,-2.0,2.0,0.0;');
231 23      2:3  199 WRITE(PLOTTER,'O.0,2.0,-1.0,0.0,0.0,-1.0;');
232 23      2:2  237 END;

```



```

312 23 3:3 171 WRITE(PLOTTER,'DI;');
313 23 3:2 186 END
314 23 3:1 186 ELSE
315 23 3:2 188 EXPLABEL:=0;
316 23 3:2 191
317 23 3:2 191 (* WRITE LABEL & GRID LINE *)
318 23 3:1 191 FOR I:=7 DOWNT0 0 DO
319 23 3:2 204 BEGIN
320 23 3:3 204 HMOVE TO(0.0,I*23.0+8);
321 23 3:3 226 LINELABEL:=LINEVALUE[I]/EXP(EXPLABEL*2.30259);
322 23 3:3 258 WRITE(PLOTTER,'SRO.6,1.2;LB',LINELABEL:8:2,CHR(3),'SR;');
323 23 3:3 321 (*CHECK FOR ZERO AXIS*)
324 23 3:3 321 IF (ABS(LINEVALUE[I]/(LINEVALUE[7]-LINEVALUE[0])) < 0.01) AND
325 23 3:3 364 (I<>0) THEN
326 23 3:4 371 BEGIN
327 23 3:5 371 HTURN TO(0.0);
328 23 3:5 381 FOR J:=0 TO 8 DO
329 23 3:6 394 BEGIN
330 23 3:7 394 HVIEWPORT(21.0,290.0,9.0,192.0);
331 23 3:7 421 DRAWAXIS(J,I);
332 23 3:7 427 HVIEWPORT(0.0,292.0,0.0,192.0);
333 23 3:6 455 END;
334 23 3:4 463 END;
335 23 3:3 463 HPENCOLOR(NO);
336 23 3:2 467 END;
337 23 3:1 475 YBOTTOMLINE:=LINEVALUE[0];
338 23 3:1 488 YDIVSIZE:=LINEVALUE[I]-YBOTTOMLINE;
339 23 3:1 505
340 23 3:1 505 (***** DO X-LINES *****)
341 23 3:1 505 HLINEARAXIS(LINEVALUE,XMAX,XMIN);
342 23 3:1 517
343 23 3:1 517 (* PRINT X-AXIS EXPONENT *)
344 23 3:1 517 EXPLABEL:=HEXPD(LINEVALUE[I]-LINEVALUE[0]);
345 23 3:1 544 IF (EXPLABEL > 2) OR (EXPLABEL < -1) THEN
346 23 3:2 556 BEGIN
347 23 3:3 556 HMOVE TO(185.0,-1.0);
348 23 3:3 572 WRITE(PLOTTER,'SRO.5,1.0;');
349 23 3:3 594 HWSTRING('X');
350 23 3:3 598 WRITE(PLOTTER,'SR;');
351 23 3:3 613 HWSTRING('10');
352 23 3:3 621 WRITE(PLOTTER,'PRO.0,2.0;');
353 23 3:3 643 STR(EXPLABEL,LABELSTR);
354 23 3:3 656 HWSTRING(LABELSTR);
355 23 3:3 661 WRITE(PLOTTER,'DI;');
356 23 3:2 676 END
357 23 3:1 676 ELSE
358 23 3:2 678 EXPLABEL:=0;
359 23 3:2 681
360 23 3:2 681 (* WRITE LABEL & GRID LINE *)
361 23 3:2 681
362 23 3:1 681 FOR I:=7 DOWNT0 0 DO
363 23 3:2 694 BEGIN
364 23 3:3 694 HMOVE TO(13+I*32.0,5.0);
365 23 3:3 717 LINELABEL:=LINEVALUE[I]/EXP(EXPLABEL*2.30259);
366 23 3:3 748 WRITE(PLOTTER,'SRO.6,1.2;LB',LINELABEL:6:2,CHR(3),'SR;');
367 23 3:3 811 (*CHECK FOR AXIS*)
368 23 3:3 811 IF (ABS(LINEVALUE[I]/(LINEVALUE[7]-LINEVALUE[0])) < 0.01) AND
369 23 3:3 854 (I<>0) THEN
370 23 3:4 861 BEGIN
371 23 3:5 861 HVIEWPORT(21.0,290.0,8.0,192.0);
372 23 3:5 889 HTURN TO(90.0);
373 23 3:5 899 FOR J:=0 TO 8 DO
374 23 3:6 912 BEGIN
375 23 3:7 912 HMOVE TO(21+I*32.0,9+J*23.0);
376 23 3:7 943 HPENCOLOR(YES);
377 23 3:7 947 WRITE(PLOTTER,'PR3.0,0.0,-6.0,0.0,3.0,0.0;');
378 23 3:6 986 END;
379 23 3:5 994 HVIEWPORT(0.0,292.0,0.0,192.0);
380 23 3:4 1021 END;
381 23 3:3 1021 HPENCOLOR(NO);
382 23 3:2 1025 END;
383 23 3:1 1033 IF DOTTEDLINES THEN HDRAWDARK;
384 23 3:1 1038 XBOTTOMLINE:=LINEVALUE[0];
385 23 3:1 1051 XDIVSIZE:=LINEVALUE[I]-XBOTTOMLINE;
386 23 3:0 1068 END;
387 23 3:0 1096
388 23 3:0 1096
389 1 1:0 0 END.

```